

NanoThailand 2016

Sunday 27 November 2016 - Tuesday 29 November 2016

THE GREENERY RESORT KHAO YAI



Book of Abstracts

Contents

Identification of Defects in Materials: A Combination of First-principles Calculations and Experiments 5	1
Magnetic Capture Hybridization –Polymerase Chain Reaction (MCH-Pcr) for Detection of Salmonella Typhimurium Artificially Contaminated in Drinking Water and Food 7 . .	1
Synthesis and Fabrication of Silicon Nitride Nanopore Device for Biomolecule Detection 8	1
AgNPs mechanism, AgNP-CAZ synergism, and anisotropic AgNPs activity against Burkholderia pseudomallei 9	2
Preparation of Hollow Co/Au/Pt Nanocatalysts for Methanol Oxidation 10	2
Enhanced sensitivity of lateral flow immunoassay for double-antigen detection of influenza A using dual-layered gold nanoparticles 11	3
Oriented antibody conjugation on dye-doped silica nanoparticles for targeted in vivo fluorescent imaging 12	3
Application of amine-functionalized magnesium ferrite nanoparticles in wastewater treatment 13	4
Turn-On Fluorescent Sensor from Indolium Salt for Cyanide Detection 14	5
8-Amidoquinoline Containing Glycinyl Group as Turn-on Fluorescent Sensors for Zn(II). 15	5
New 8-Aminoquinoline Derivatives as “Turn-On” Fluorescent Sensor for Cd(II) ion Detection 16	5
ELECTROWETTING ON DIELECTRIC (EWOD) OF SESSILE MICRODROPLETS CONTAINING POLYDISPERSE GOLD NANOPARTICLES 17	6
Effects of halogen on the properties of CH ₃ NH ₃ PbI ₃ –yXy layers for perovskite solar cells 18	7
Preparation of Copolymer from Recycle Plastic Bottle and Study of Its Applications in the Electrochromic Devices 19	7
2Mechanism of ferromagnetism occurring in CVD-adamantane films 20	8
Electrochemical aptasensor for glycated albumin in Diabetes mellitus diagnosis and monitoring 21	8

Enhancement of drug bioavailability of quaternized chitosan by dual synergistic mechanism through transcellular and paracellular transport in the intestinal cell monolayer using Caco-2 cell model 22	9
Effect of ZnO and TiO ₂ on Properties of Polystyrene/Nitrile Rubber Electrospun Fiber Mats 23	9
Efficient visible light-induced photocatalytic degradation of Rhodamine B over chlorophyll and Mg co-modified P25 nanoparticles 24	10
The observation of strain-induced valence band splitting on HfSe ₂ by Alkali metal intercalation 25	10
Enhanced activity and stability of CuO-ZnO-ZrO ₂ catalyst by addition of colloidal SiO ₂ nanoparticles for CO ₂ hydrogenation 26	11
Carbon Anode from Cassava for Lithium-ion Battery 27	11
Electron transporting material for Perovskite and Organic hybrid solar cell 28	12
Heterogeneous Suzuki cross-coupling reaction in water catalyzed by palladium nanoparticles supported on individual calcium carbonate plates derived from mussel shell particle. 29	12
Improvement of catalytic stability in Carbon Dioxide Reforming of Methane over Ni-carbon Composite Catalyst: Effect of Carbon Structure 30	13
Micrometers to nanometers conversion process in perovskite BaTiO ₃ particles 31	13
Styryl-Functionalized BODIPY as Fluorescent Probe For Metal Ions Detection in Aqueous Media 32	14
Imaging of cellular localization of nanoparticles using STED technology 33	14
Fabrication of Porous Gold-Silver Alloy Nanowires Array via Controlled Dealloying Process: a Simple Approach for Highly Stable and Sensitive SERS Substrate 34	14
Magneto and electro-optical study of Bismuth ferrite (BiFeO ₃) thin films 35	15
The electrochemical properties of NiO/NFs electrode induced by UV light irradiation 36	15
Effects of Brønsted acid on the Selective Catalytic Reduction of NO with NH ₃ on Ru-doped Ceria Catalyst 37	16
Analysis of electronic spectral weight of two-dimensional electron gases at the surfaces of ferroelectric KNb _x Ta _(1-x) O ₃ across T _c 38	16
Magneticfield-promoted cleaner production of small alcohols and hydrocarbons from CO ₂ over Cu-ZnO/ZrO ₂ and Fe/MCM-41 catalysts 39	17
Preparation of controlled release nanocapsule for mosquito repellent application 40	18
Novel of quinoline derivatives containing 5-membered heterocycles for Zinc ions detection 41	18
BODIPY Derivatives as Photocatalyst for Oxidative Coupling 42	19

Synthesis and Development of fluorescent sensor based on julolidine linked di-(2-picoly)amine derivatives 43	19
A novel fluorescent turn-on sensor from 8-hydroxyquinoline derivative for mercury detection in aqueous solution 44	20
Absorption spectra and activity of s-tetrazine derivatives on [4+2] Diels-Alder cycloaddition reaction 45	20
A Density Functional Theory Study of Formic Acid Formation from CO ₂ Hydrogenation over Au-exchanged MCM-22 Zeolite 46	21
Theoretical Investigation on the Electroreduction of CO ₂ to Methanol on Stepped Cu-based Alloy (211) Surfaces 47	21
Reaction mechanism for NO decomposition on oxotitanium porphyrin with NH ₃ selective catalytic reduction: A DFT study 48	22
Mechanisms of AgNPs-mediated antibiotic resistance in bacteria 49	23
Investigation on the effect of nanoparticles to ammonium salt based gel electrolytes 50	23
Protective effect of silk extracts on drug-induced phototoxicity 51	23
One-Dimensional Carbon Nanomaterials and Their Application for Oxygen Reduction Reaction 52	24
Salicylideneaniline-Functionalized Poly(m-phenyleneethynylene)s as Fluorescent Turn-On Chemosensors for Cations 53	25
Zinc stannate nanoparticles synthesized at room temperature: Effect of annealing on size, morphology and photocatalytic activity 54	25
Synthesis of novel benzyldipicolylamine linked 1,8-naphthalimide derivatives as new fluorescent chemosensors 55	26
Nanoencapsulation of tetrahydrocurcumin in CTS by rapid expansion of subcritical solutions coupled with ionic gelation 56	27
Enhanced piezoelectric properties and fatigue-free behavior of lead-free piezoelectric xBaZrO ₃ -(0.85-x)BaTiO ₃ -0.15CaTiO ₃ ceramics 57	27
Fabrication of silver nano-protrusion based on silver sulfide solid electrolyte for surface-enhanced Raman spectroscopy 58	28
Effect of Al Concentration on Al-doped ZnO Thin Films deposited by Magnetron Co-Sputtering Technique 59	28
DIAMONDOID COUNTER ELECTRODES FOR DYE-SENSITIZED SOLAR CELLS 60	29
Cassava root materials composited with PEDOT:PSS used as low cost counter electrodes in dye-sensitized solar cells 61	29
Effect of cylindrical length and regression model of Euler number of hydrocyclone 62	30
Silver nanoparticles induce cardiovascular toxicity in human endothelial cells and zebrafish embryos 63	30

Synthesis of poly (p-Phenylene ethynylene)s using Palladium Supported on Calcium Carbonate as Heterogeneous Catalyst 64	31
Fabrication of Perovskite Solar Cell via Rapid Convective Deposition Technique 65	31
Fabrication of Gold Disc Arrays on ITO glass: an Inverted Pattern Generated from Plasma Etching of Nanosphere Lithographic Mask 66	31
Penetration of Fluorescent Nanoparticles into the Cornea 67	32
3.5D printed soft actuator for novel robotic application 69	33
Mercury oxidation reaction mechanisms on halogenated activated carbon: a density functional theory study 70	33
Sol-gel Synthesis of Nanoparticulate Titanium Dioxide: Effects of Initial Reagents 71 . . .	33
Water disinfection using silver nanoparticles impregnated coffee grounds: Escherichia coli and Staphylococcus aureus killing in batch-mode 72	34
Modification of zeolite supporting diamine silver complex for antibacterial activity 73 . .	35
Preparation of nanocellulose from Jute fiber waste 74	35
Current-Induced Cleaning of Graphene and Graphene-Metal Contacts 75	35
Development of novel silica-coated superparamagnetic iron oxide nanoparticles for highly efficient magnetofection and molecular imaging. 76	36
Comparative study of local structure for sputter deposited nitrogen doped zinc oxide thin films 77	36
Preparation and characterization of cement 12CaO•7Al ₂ O ₃ /reduced graphene oxide hybrid composites and their electrical properties 78	37
Spectroscopy system using two dimensional detectors for undergraduate student laboratory 79	38
Colorimetric determination of Silver Nanoparticles with Dithizone-based in Aqueous Media 80	38
Sustained delivery scaffold loaded by cisplatin and curcumin 81	39
A Numerical Investigation of Enhanced Second-Harmonic Generation in One-Dimensional PIM/NIM Structure 82	39
Investigation of using carbon nanotube mixed with several metal phthalocyanine compounds for electronic tongue applications 83	40
The Increased Durability of Natural Dye on the SiO ₂ -Modified Paper 84	40
Binding mode prediction of 8-hydroxyquinoline derivatives as inhibitors against Dengue Virus NS3 Protease using molecular dynamics simulations 85	41
Investigation on the interactions between glucomannans and Bifidobacterium enzyme by using molecular dynamics simulations 86	41

Development of cellular platform for enhancing neuron differentiation 87	42
Magnetic Capture Hybridization –Polymerase Chain Reaction (MCH-Pcr) for Detection of Salmonella Typhimurium Artificially Contaminated in Drinking Water and Food 88 .	42
Development of Physicochemical Properties of Pomegranate Extract using “Liponiosome” Encapsulation Technique 89	43
Preparation of high surface area binary-CeCoOx for VOCs catalytic oxidation 90	43
Deoxygenation of oleic acid to produce bio-hydrogenated diesel over molybdenum oxide catalysts on supported alumina under inert atmosphere 91	44
Characteristics of a Nanocrystalline-based, UVA-activated, ‘Consume within’Indicator for Intelligent Packaging 92	44
Gas adsorption on MXene surfaces: Density Functional Theory calculations 93	45
Nano Roughening of Polyethylene Surface with Acrylic acid/Benzophenone via UV irradiation for Intelligent Packaging Application 94	45
Antioxidant Activities and Properties of Quercetin Nanoparticles-Incorporated Cellulose-based Packaging Films 95	46
Effect of Ammonia and Acid Concentrations on the Response of Fish Spoilage Indicator Solution Based on Coordination Compound of Transition Metal 96	46
An innovative application of magnetic field for CO ₂ hydrogenation reaction on Fe and Cu supported MCM-41 catalyst 97	47
Impact of an integrated in vivo-in vitro approach for evaluating the hazardous pulmonary effects of nanomaterials and the underlying mechanisms 98	47
Antimicrobial and Antioxidant Activity of Caffeic Acid Phenethyl Ester Nanoparticles 99	48
Magnetic properties and chemical state of nickel doped CuFeO ₂ delafossite oxide powders prepared by sol-gel method 100	48
TiO ₂ -doped WO ₃ coated on charcoal activated with increases photocatalytic and antibacterial properties synthesized by microwave-assisted sol-gel method 101	49
THALIDOMIDE IMPRINTED NANOPARTICLES ON THE THIN-FILM LAYERS OF INTER-DIGITATED CAPACITIVE ELECTRODE FOR SENSOR APPLICATIONS 102	49
Metal Phthalocyanine and Metal Oxide Modifying Multiwall Carbonnano Tube Paste Sensors for Classification of Sweet Taste 103	50
Observing Chitooligosaccharide Traveling through a Biological Nanopore of Escheriachia coli 104	50
Silica Nanoparticle Synthesis and Characterization with Dynamic Light Scattering Method: Solution Stability 105	51
Quantitative analysis of aqueous methanol solution using hyperspectral imaging 106 . .	52
Rapid VOC sensors based on electrolytically exfoliated graphene-loaded flame-made La-doped SnO ₂ composite films 107	52

Colloidal properties of montelukast sodium nasal spray 108	53
Selective Permeability of Antimicrobial Agents through the Protein Nanopore of the Highly-Drug Resistant Melioidosis Bacterium <i>Burkholderia pseudomallei</i> 109	54
Structural and electronic properties of the organic semiconductor ZnPc 110	54
Investigation the role of Co^{2+} in LiFePO_4 cathode material during batteries operation by In-situ XANES technique 111	55
The novel preparation of encapsulated Thai herbal extract-Alginate complex against bacteria caused periodontal diseases 112	55
Preparation and Evaluation of Nanosuspension-based Sildenafil Pressurized Metered-dose Inhalers for Treatment of Pulmonary Arterial Hypertension Using Poloxamer 188 as a Stabilizer 113	56
Biosensing with allosteric nano-biocatalysts: A reductase subunit of a bacterial hydroxylase as molecular example 114	57
Colloidal chitin-soaked nanoporous carbon nanotube thin films as biocompatible immobilization matrix of amperometric enzyme biosensors with long life-time 115	58
Electrospun nanofibers of polylactide (PLLA)/ polyglutamic acid (γ -PGA) blends and their use as ammonia detecting kits in intelligent meat packaging 116	59
Characterization of carbon fibers from Thai horse manure via hydrothermal carbonization 117	59
Effect of F incorporation on physical, electrical and optical properties of hydrothermally grown ZnO nanorods 118	59
Nanoparticulate Copper Oxide, Manganese Oxide, and Cobalt Oxide Synthesized by Solution Combustion Technique for Glucose Detection 119	60
Ultra-sensitive and highly selective H_2 sensors based on FSP-made Rh-substituted SnO_2 sensing films 120	60
Characterization of bacterial cellulose produced from agricultural by-product by <i>Gluconacetobacter</i> strains 121	61
Nanotechnology and Health 122	61
Electrical Properties of Co-Doped LiFePO_4 Nanomaterial by Impedance Spectroscopy Technique 123	62
Synthesis and identification of silica and activated carbon nanocomposite from rice husks for energy storage 124	63
Electrical properties of semi-conductive yarns based polyaniline for wearable ammonia detection 125	63
Production of Nanocellulose from Lime Residues Using Chemical-free Technology 126	64
Simulation of single quantum well solar cells 127	64

Comparative Study on the Catalytic Activity and Stability between Pt-Decorated Ru surfaces and Ru-Decorated Pt Surfaces Catalysts for Methanol Electrooxidation 128 . . .	65
Highly sensitive room-temperature acetone gas sensor based Ag-loaded ZnO nanoflowers 129	65
A Controlled Release Formulation of Medicinal Plant Extract Decrease Inflammation in Human Vascular Endothelial Cells: A Preliminary for Diabetic Adjunctive Treatment 130	66
Hydrophilic and Photocatalytic properties of Dip-coated Synthetic Rutile-based Thin Films Derived from Minerals Ores 131	66
Anatase/Rutile composite thin films prepared via dip coating technique and their hydrophilicity, stability and photocatalytic activity 132	67
DFT+U Study of CuO Surfaces and Vacancy Formation for CuO Nanowires-CNTs Hybrid Electrode in Supercapacitors 133	67
Preparation of ZnO Nanorods by Hydrothermal Method 134	67
Fabrication and preparation of Mg-reducing $12\text{CaO} \cdot 7\text{Al}_2\text{O}_3$ cement for enhancing of electrical and optical properties 135	68
I-V, C-V-f and G-V-f Characteristics of Nanocrystalline n-Type FeSi ₂ /p-Type Si Heterojunctions Fabricated Using Pulsed Laser Deposition 136	68
Fabrication and Nanostructure study of Hydroxyapatite Bioceramic from Cockle shells 137	69
Optical Extinction Spectra of Pure Noble Metal Nanorod and Silica Shell Coated Gold Nanorod Embedded in Organic Medium 138	69
Theoretical Calculation of Optical and Magneto Optical Properties of Magnetite Nanorods 139	70
Characterization of Junction Parameters in n-Type Nanocrystalline Iron Disilicide/Intrinsic Ultrananocrystalline Diamond/Amorphous Carbon Composite/p-Type Silicon Heterojunctions 140	70
The porous carbon derived from the KOH activation of agro-waste char for supercapacitor electrode 141	71
Gas Response of Tin Oxide Film Sensor to Varying Methane Gas Concentration 142 . . .	71
Colorimetric Determination of Arsenic in Natural Waters by Nanomaterial-Based Test Strips 143	72
Low Cost and Reliable Surface Plasmon Resonance-Based Detection System for Liquid Propane Gas 144	72
Highly dispersed Ni and Cu nanoparticles supported SBA-15 for hydrogenation of methyl levulinate to γ -valerolactone 145	73
Influence of adhesive rheology for various dispensing systems to achieve very small dot size 146	73

Thermal analysis of dual cure epoxy adhesive with very small dot size at extremely low and high heating temperature 147	74
Atomic structures of graphene like nanomaterials including SiC and BP 148	74
Coating of molybdenum oxide on anodized aluminium plate apply for ultracapacitor electrodes 149	75
Optical and Luminescence from Ln ³⁺ doped glasses and their applications 150	75
Optical and Luminescence from Ln ³⁺ doped glasses and their applications 151	76
Optical diffraction of binary-nanoparticle film prepared by convective deposition with vibration assistance 152	76
Fabrication and Electrochemical properties of CNF/MFe ₂ O ₄ : (M = Mn, CuMn) Composite Nanofiber for Electrochemical capacitors 153	76
The effect of green synthesized gold nanoparticles on rice germination and roots 154	77
Evaluation of immunochromatographic-gold nanoparticle based assay efficacy in the detection of protease inhibitor in HIV-1 infected patient's plasma 155	77
Effect of dc bias effect on the dielectric properties and nonlinear electrical behaviors of Bi _{1-x} BaxFeO ₃ ceramics 156	78
Fabrication, structure and magnetic properties of Ce _{1-x} FexO ₂ nanostructures 157	78
The Dc bias voltage effect on dielectric properties of Ni-doped TNTs prepared by hydrothermal route 158	79
Fabrication, Characterization, and Electrochemical Properties of Electrospun MnCo ₂ O ₄ Nanofibers 159	79
Synthesis, characterization and electrochemical properties of KFeO ₂ nanoparticles prepared by sol-gel method 160	80
Improved Electrochemical Properties of Activated Biomass/FeO _x /MnO _x Composite Prepared by Hydrothermal method for Supercapacitor Electrode Materials 161	80
Hydrothermal synthesis in egg white solution and magnetic properties of magnetite (Fe ₃ O ₄) nanoparticles 162	81
Titanate nanotubes-AgO nanocomposites: Synthesis, characterization, and dielectric properties 163	81
Magnetic properties of Co-doped BiFeO ₃ nanoparticles 164	82
A simple electrospinning system for fabrication of core-shell nanofibers 165	82
Molecular Structure and Formation of Melatonin in the Bulk Water and at the Water–Air Interface: A Molecular Dynamics Simulation Study 166	83
Theoretical Study of Ethanol Interaction with Pristine and P-doped Single-Walled Carbon Nanotubes 167	83

Fabrication, Structure, Electrochemical, Ferromagnetic and Ferroelectric Properties of Cu Doped bismuth ferrite Thin Film 168	84
Structure and magnetic properties of Mn-doped CeO ₂ nanostructures prepared by egg-white solution route 169	84
Nanocatalysts for Biorefinery and Advanced Biofuel Applications 170	85
DESIGNING MOLECULAR STRUCTURES OF D- π -A TYPE ORGANIC DYES FOR HIGH EFFICIENCY DYE-SENSITIZED SOLAR CELLS 171	85
Nanotechnology based delivery systems for peptides and vaccines 172	86
Classic Perovskite Ferroelectric BaTiO ₃ Ceramics Modified with Nanogold 173	86
Photocatalytic Activity of the Binary Composite CeO ₂ /SiO ₂ for Degradation of Dye 174 .	87
The mystery of high temperature superconductivity at the FeSe/STO interface 175	87
Effect of boron addition on the structure and magnetic properties of CoPt nanoparticles 176	88
How to Predict New Nano-structured Materials with Confidence? -Theoretical Study on Task Specific Ionic Liquid for Metal Extraction from Garbage Caused by Tsunami- 177	88
The effects of hydroxyapatite nanoparticle on germination and seedlings of rice 178 . . .	89
The effect of hydroxyapatite nanoparticles on rice (<i>Oryza sativa</i> L.) callus 179	90
Anticandidal Activity of the Spinel Ferrite CoFe ₂ O ₄ Nanospheres 180	90
Green synthesis of silver chloride nanoparticles: a comparison study in three different species of Curcuma 181	91
Synthesis of PLGA-based nanoparticles loaded with lupinifolin extracted from <i>Derris reticulata</i> 182	91
Toxicity Test of Nano-Encapsulated Eugenol Containing Biopesticide by Brine Shrimp Lethality Test 183	92
Rapid and portable aflatoxin sensor using screen printed graphene electrode 184	92
Risk mapping and Risk management by control of release –strategies to design better materials and products 185	93
Microfluidic device integrated with screen printed graphene based-electrochemical sensor for glutathione sensing 186	93
Prof. Ruengpung Sutthent, Director, COE MU 189	94
Fabrication of Highly Aligned CNT and P(VDF/TrFE) Nanofiber Sheets 229	94
Asst. Prof. Toemsak Sriksirin 230	95
Natural Materials for Dye Sensitized Solar Cells: Experimental and Theoretical Study 233	95

Nondestructive 3D Characterization of Materials Using Optical Coherence Tomography 235	95
Electrical properties and dielectric responses in rutile-TiO ₂ -based ceramics 240	96
Synthesis and fabrication of nanomaterials for applications in food and agriculture 241	97
Limitation of Rheology and Curing Processes for Tiny Adhesive Dot with Various Dispensing Systems in Hard Disk Assembly Process 243	97
Highly Sensitive Nucleic Acid and Antibody Based Electrochemical Detection by Using of Nanomaterials as Signal Amplification Elements 245	98
Nanomedicine-based drug delivery systems for anti-cancer targeting and treatment. 246	98
Chitosan-metal nanohybrids for microbial detection and extraction 247	99
Effects of Electric and Magnetic Fields on Nanoparticle Thin Films Prepared by Sparking-off Metal Tips 248	99
Smart Farm System : Case Studies in Thailand 249	100
Nano-materials Engineering and Manufacturing in Hard Disk Drives for Cloud Storage 250	100
Domain-Exchanged Antibody with Potentiated Effector Functions 251	100
Tailoring Nanocapsules for Self-Healing Materials 252	101
Use of nanobodies in developing a bacterial antibody production platform 253	102
Bionanomaterials for Diagnostics, Image and Drug delivery 254	102
Material, Device and Interfacial Engineering for High efficiency Solution Processable Organic Light Emitting Diode 255	102
Prof. Nguyen Van Hieu 256	103
Nanomaterials for analytical detection 257	103
Metal-oxide Semiconducting Nanostructures by Microwave-assisted Thermal Oxidation Technique for Sensor and Solar Cell Applications 258	104
Cosmeceutical based nanotechnology: the beauty from nature 259	105
Biodegradable nanocomposite blown films based on PLA and PBAT containing silver-loaded kaolinite: Formulation and property testing for use as smart packaging for dried longan 260	105
X-ray Absorption Investigation on Cation Distribution and Magnetic Behavior of Zinc Ferrite Nanoparticles 261	106
Printed Graphene Electronics 262	106
Molecular Dynamics Simulations and Gaussian Network Model in Improving Protein-Protein Binding Affinity: HIV and Dengue Cases 263	107
Chemical syntheses of functional nanostructures and their SERS applications 264	107

Possible electric field induced indirect to direct band gap transition in MoSe ₂	265	108
First-principles study on two dimensional dichalcogenides for hydrogen production	266	109
Sustainable Innovation of Magnetic Field Application in Catalytic Co ₂ Conversion	268	109
Polymer/Metal Nanoparticle/Nanocarbon Hybrid Materials for Highly Sensitive and Selective Volatile Organic compound Detection	269	109
Photoemission Electron Spectroscopy (PES) at the Siam Photon Laboratory, SLRI	276	110
Classification and Application of Diamond-Like Carbon Films Using SR-Based Spectromicroscopy	277	110
Synchrotron SAXS/WAXS for nano structural investigation	278	111
An Application of Synchrotron-based X-ray Absorption Spectroscopy Study on Advanced Functional Materials	279	111
Nano-needles, nano-conduits, nano-biocatalysts and nano-biopores On powerful tiny tools for atomic/molecular resolution surface inspections and effective nanoscopic facilitators of electroanalysis, bacterial cell survival and antibiotic design	280	112
The progress of Taiwan nano-EHS regulations and researches	282	112
Enhanced Production and Selected Use of Nanocellulose from Fruit and Vegetable Residues: A Brief Review	283	113
High throughput screening method for nanoparticles toxicity using 3D cells	284	113
Teaching and Learning on Nano Safety in School	285	114
Malaysia National Nanosafety Initiative.	286	114
Characterization of nanoparticles in photocatalytic and regular cement using an aerosolizing nanoparticle generator system	287	114
Perception and Attitudes about Nanotechnology and Nano-Safety in Thailand's University Community	288	115
Comparison of nano perception between Asia and Europe and its influence on nano regulation	289	115
Alternatives to animal testing in Nanotoxicology	290	116
Human studies and experimental studies for nanosafety	291	116
What Can We Learn from the Nanotoxicology Publications?	292	117
A recent development of mixed metal oxides/polymer nanocomposites as energy storage catalysts	293	118
Computational Studies of Transition-Metal Decorated Graphene Adsorbent for Air Pollutants Removal	294	118
Charge storage mechanisms of manganese oxide nanosheets and N-doped reduced graphene oxide aerogel for high-performance asymmetric supercapacitors	295	119

Functional and responsive core-shell nanoparticle assembly at oil and lipid interfaces 296	119
Welcome Remarks 299	120
The industrial-academic network for nanoscience research in cementitious materials 300	120
SCG Speaker 301	120
Development of Theranostic Nanoparticles for Cancers 303	121
Discovery of biological self-assembling systems that have potential for incorporation into nanodevices and sensors 306	121

Heron 1 / 5

Identification of Defects in Materials: A Combination of First-principles Calculations and Experiments

Author: Jiraroj T-Thienprasert¹

¹ *Department of Physics, Faculty of Science, Kasetsart University*

Corresponding Author: chorawut@gmail.com

It is well known that many physical properties of materials can be determined by the existence of point defects, which might be intentionally or accidentally added to the materials. For example, the electrical conductivity of Al-doped ZnO sample can be decreased by the presence of Zn vacancy (V_{Zn}) defect, which might be unintentionally created under O-rich growth conditions. In addition, the hydrogen defect is also reported to be a major obstacle for achieving *p*-type ZnO. Therefore, understanding the role of defects in materials can help us improving the material properties in a desired way. By combining the first-principles calculations with proper characterization techniques, such as x-ray absorption, infrared absorption, and photoluminescence, defects in materials can be understood in a great detail. A few examples, including Al-doped ZnO, SO-doped CdTe and N-doped Cu_2O , will be presented.

Poster session / 7

Magnetic Capture Hybridization –Polymerase Chain Reaction (MCH-PCR) for Detection of Salmonella Typhimurium Artificially Contaminated in Drinking Water and Food

Author: Goragot Supanakorn¹

¹ *Research Assistant*

Corresponding Author: goragot.sup@nanothailand.or.th

Magnetic polymeric nanoparticle (MPNP) has been used widely as a solid support for biomolecules in biomedical applications. Because it is convenient to control by applying external magnetic field and easy to surface functionalize. In this work, magnetic capture hybridization –polymerase chain reaction (MCH-PCR) was developed for detection of *S. Typhimurium* contaminated in drinking water and raw chicken meat artificially. Carboxylated MPNP was covalently bound to oligonucleotide probe specific to *invA* gene of *S. Typhimurium*, which is one of the most causative agents of food poisoning syndrome in Thailand. The probes were designed and synthesized to possess amino modification and five different spacers at the 5' end of sequence to compare their sensitivity and specificity of the assay. The probe bound MPNP was allowed to hybridize with target DNA in MCH reaction and magnetically separated to use as a template in PCR amplification. The amplified products were separated in agarose gel, stained and visualized under UV light. The advantage of this method contributes to high specific of probe-DNA hybrids leading to specificity enhancement of PCR assay. In addition, the MPNP facilitate separation of the target DNA easily from the food matrix.

Heron 2 / 8

Synthesis and Fabrication of Silicon Nitride Nanopore Device for Biomolecule Detection

Author: Thitikorn Boonkoom¹

¹ *NANOTEC*

Corresponding Author: thitikornboonkoom@gmail.com

Diabetes has been one of the major health issues worldwide and also in Thailand. More importantly, almost half of those with diabetes are undiagnosed. Although various test methods have been developed, the existence of anemia and thalassemia may cause inaccuracy in the diabetes mellitus testing from blood. An alternative biomarker molecule is glycated albumin which directly corresponds to the diabetes mellitus. Aim of this work is to utilise nanopore technology to detect level of the glycated albumin. The nanopore was fabricated by Focus Ion Beam technique on a 70 nm thick silicon nitride membrane. The testing system composes of 2 solution chambers separated by the silicon nitride nanopore. Electrochemical technique was performed for 2 purposes, 1) to identify the existence of the nanopore and 2) to determine the analyte shape, charge, and concentration from the ionic current profile during the analysis. Preliminary results suggested that the glycated albumin could be detected by the 100 nm nanopore with electrochemical measurement.

Poster session / 9

AgNPs mechanism, AgNP-CAZ synergism, and anisotropic Ag-NPs activity against *Burkholderia pseudomallei*

Co-author: Seangrawee Thammawithan ¹

¹ Student

Corresponding Author: sunshine.sc.bc19@gmail.com

Burkholderia pseudomallei is the causative agent of melioidosis, an endemic infectious disease primarily found in northern Australia and Southeast Asia. *B. pseudomallei* (BP) is intrinsically resistant to most common antibiotics. Our research interest is to find alternative in treatment of melioidosis. We observed the activity of AgNPs against several strains of BP and mechanism behind. Firstly, we studied the mechanism of AgNPs. AgNPs exhibited two-phase mechanism: cell death induction and ROS induction. The first phase was a rapid killing step within 5 min causing direct damage of the cytoplasmic membrane of the bacterial cells. The second phase, the ROS induction, occurred 1-4 h after AgNPs treatment where the Ag⁺ interacted with biomolecules resulting in ROS formation. This is the direct kinetic evidence of AgNPs killing mechanism by which cell death is separable from ROS induction. Secondly, we determined FIC index of AgNPs-CAZ combined activity, giving FIC index = 0.5 and 0.258 for *B. pseudomallei* H777 (wild type) and *B. pseudomallei* 316c (ceftazidime-resistance), respectively, indicating the synergistic effect. Combined AgNPs-CAZ induced increasing uptake of AgNPs in cell when compare with AgNPs or CAZ alone. Thirdly, we examined the anti-BP activity of the anisotropic AgNPs (asymmetrical shape). MIC of anisotropic AgNPs is lower than normal AgNPs, giving 8 µg/mL for *B. pseudomallei* H777. AgNPs and AgNPs-CAZ may be considered as a potential candidate to develop a novel alternative agent for melioidosis with fast action.

10

Preparation of Hollow Co/Au/Pt Nanocatalysts for Methanol Oxidation

Author: Kontee Thongthai¹

¹ Department of Chemistry, Faculty of Science, Chiang Mai University, Chiang Mai, Thailand

Corresponding Author: kontee.thongthai@gmail.com

Improvement of Pt-based catalysts for direct methanol fuel cell applications based on increasing surface area and changing chemical composition of the catalysts have been studied intensively [1,2]. Moreover, there are few studies [3,4], which use hollow trimetallic Co/Au/Pt nanoparticles (Co/Au/Pt NPs) to catalyze methanol oxidation. A comparison of the catalytic performances for the

methanol oxidation of monometallic Pt nanoparticles (Pt NPs) and the Co/Au/Pt NPs still has not been investigated. Thus, this work aim to investigate the catalytic activity of the Co/Au/Pt NPs supported on multi-walled carbon nanotubes (MWCNTs) for the methanol oxidation. In this study, an attention of synthesis of the Co/Au/Pt NPs and catalytic activity investigation of the synthesized Co/Au/Pt NPs supported on the MWCNTs for the methanol oxidation has been introduced and paid on. The Co/Au/Pt NPs were produced successfully via a simple successive reduction method. The transmission electron microscopy (TEM) is used to investigate structure of the Co/Au/Pt NPs and the TEM images show that the Co/Au/Pt NPs compose of hollow structure. The ultraviolet-visible spectroscopy (UV-vis) is used to investigate optical properties of the Co/Au/Pt NPs. The UV-vis results reveal that the Co/Au/Pt NPs show no absorption peak in the UV-vis region which is similar to the absorption behavior of the Pt NPs. These results can confirm deposition of Pt. The wavelength-dispersive X-ray spectroscopy (WDX) is used to investigate chemical compositions of the Co/Au/Pt NPs. The WDX data confirm the existence of Co, Au and Pt in the obtained Co/Au/Pt NPs samples. Cyclic voltammetry is used to investigate the catalytic properties of the Co/Au/Pt NPs supported on the MWCNTs for methanol oxidation. All samples of the Co/Au/Pt NPs, with different molar ratio of elemental composition, exhibit higher current density than that of the Pt NPs supported on the MWCNTs. The results show that combination of these three elements in the form of the hollow structure is promising choice for achieving good catalytic activity for the methanol oxidation.

References

- [1] H.P. Liang, H.M. Zhang, J.S. Hu, Y.G. Guo, L.J. Wan, C.L. Bai, "Pt hollow nanospheres: facile synthesis and enhanced electrocatalysts", *Angew. Chem. Int. Ed.*, 43 (2004), 1540-1543.
- [2] K.R. Lee, M.K. Jeon, S.I. Woo, "Composition optimization of PtRuM/C (M = Fe and Mo) catalysts for methanol electro-oxidation via combinatorial method", *Appl. Catal., B*, 91 (2009), 428-433.
- [3] Y. Chen, L. Hu, Y. Min, Y. Zhang, "Facile synthesis of noble metal (Au,Pt)/Co₃O₄ nanocomposite microspheres and their catalytic activity", *Mater. Chem. Phys.*, 124 (2010), 1166-1171.
- [4] S. Guo, Y. Fang, S. Dong, E. Wang, "High-efficiency and low-cost hybrid nanomaterial as enhancing electrocatalyst: spongelike Au/Pt core/shell nanomaterial with hollow cavity", *J. Phys. Chem. C* 2007, 111, 17104-17109.

11

Enhanced sensitivity of lateral flow immunoassay for double-antigen detection of influenza A using dual-layered gold nanoparticles

Author: Chayachon Apiwat¹

¹ *National Nanotechnology Center*

Corresponding Author: chayachon.api@nanotec.or.th

We designed and developed a highly sensitive lateral flow immunoassay (LFIA) for double-antigen detection of influenza A. The sensitivity enhancement of the assay was achieved by using two-layered gold nanoparticles in combination with double-target detection format. First, gold nanoparticles were conjugated to monoclonal antibodies (mAb) specific to the two most abundant influenza A proteins, nucleoprotein (NP) and matrix protein (M) and used as detector probes to detect two target antigens simultaneously. Then, the detection signal was enhanced via a signal amplification strategy of two-layered gold nanoparticles. Gold nanoparticles with the size of 15 nm and 40 nm were used to form a complex for signal amplification. Under optimum conditions, the system is capable to detect influenza A antigens in infected cells at levels as low as 47 TCID₅₀•mL⁻¹, which was lower than the conventional LFIA based on single-target detection. This proof-of-principle of dual-layered and double-targeted gold nanoparticles based LFIA is promising for further development of single-step, rapid, and sensitive tests for screening and diagnosis of various diseases.

Heron 2 / 12

Oriented antibody conjugation on dye-doped silica nanoparticles for targeted *in vivo* fluorescent imaging

Author: Kiatnida Treerattrakoon¹

¹ National Nanotechnology Center, NSTDA

Corresponding Author: kiatnida@nanotec.or.th

Here we developed a fluorescent probe for *in vivo* colorectal cancer detection using Cy5-doped silica nanoparticles (Cy5-SiNPs) conjugated to monoclonal antibody (mAb) with controlled orientation. Monoclonal antibody specific to anti-epithelial cell adhesion molecule (EpCAM), a cell surface protein overexpressed in colorectal carcinoma, was conjugated on the Cy5-SiNPs coated with protein G layer. The site specific interaction between protein G and constant domains (Fc) of the antibody allowed for oriented immobilization of the antibody with binding sites (Fab) facing outward. As a result, the target binding affinity of the antibodies is maintained. The targeting efficiency of the Cy5-SiNPs with oriented mAb conjugation demonstrated 8 times higher sensitivity than Cy5-SiNPs with randomly conjugated mAb for *in vitro* detection of HT-29 cells using confocal fluorescence imaging and flow cytometry. *In vivo* targeting efficiency of the Cy5-SiNPs with oriented mAb conjugation was further investigated on HT-29 tumor xenograft model. Fluorescent signal was only observed at the tumor site of the mouse injected with Cy5-SiNPs with oriented conjugation of anti-EpCAM mAb and the fluorescent signal remained up to 14 days post injection. Whereas the mouse injected with control probe demonstrated weak fluorescent signal at all timepoints. In conclusion, this study demonstrated that the Cy5-SiNPs with oriented antibody conjugation has enhanced tumor targeting efficiency *in vitro*, and is applicable for targeted *in vivo* imaging. This make them a promising candidate to be developed into a new class of effective fluorescence contrast agents for cancer diagnostics.

Falcon 1 / 13

Application of amine-functionalized magnesium ferrite nanoparticles in wastewater treatment

Author: Jeeranan Nonkumwong¹

¹ Department of Chemistry, Faculty of Science, Chiang Mai University, Chiang Mai, Thailand

Corresponding Author: nonkumwongjb@gmail.com

Magnesium ferrite ($MgFe_2O_4$) is one of the magnetic materials in spinel ferrite group which could be utilized for using in adsorbent applications due to their removability from medium solution by applying external magnetic field [1,2]. The capability of functionalization by grafting specific functional groups on their surfaces provide the possibility to synthesize the different types of magnetic nanoparticles for removing a large number of both organic and inorganic contaminants in wastewater [3]. Amongst many pollutants, heavy metal ions and dyes are considered as the crucial problems in wastewater. Thus, this present work focuses on using the synthesized magnesium ferrite nanoparticles as the effective heavy metal and dye nanoadsorbents. Mesoporous amine-functionalized $MgFe_2O_4$ nanoparticles ($MgFe_2O_4-NH_2$ NPs), with maximum magnetization of around 35 emu·g⁻¹, were successfully synthesized and simultaneously functionalized under a refluxing condition by using ethanolamine as a surface modifier. The grafting of amine groups onto the $MgFe_2O_4$ NPs was clearly confirmed by the Fourier transform infrared spectrum. Adopting the $MgFe_2O_4-NH_2$ NPs as magnetic nanoadsorbents to remove heavy metal and dye from simulated wastewater is reported. Related to this aspect, the optimal adsorption conditions were carefully examined. It was found that the obtained materials exhibited excellent removal efficiency together with rapid adsorption [4].

References

- [1] B. Y. Yu and S. Y. Kwak: Dalton Trans. 40, 9989 (2011).
- [2] S. Mohapatra, S. R. Rout and A. B. Panda: Colloids Surf. A 384, 453 (2011).
- [3] J. Gómez-Pastora, E. Bringas and I. Ortiz: Chem. Eng. J. 256, 187 (2014).
- [4] J. Nonkumwong, S. Ananta and L. Srisombat: RSC Adv. 6, 47382 (2016).

Heron 2 / 14

Turn-On Fluorescent Sensor from Indolium Salt for Cyanide Detection

Authors: Apiwat Promchat¹; Mongkol Sukwattanasinitt¹

Co-author: Paitoon Rashatasakhon¹

¹ Organic Synthesis Unit, Department of Chemistry, Faculty of Science and Nanotec-CU Center of Excellence on Food and Agriculture, Chulalongkorn University, Bangkok 10330, Thailand.

Corresponding Authors: paitoon.r@chula.ac.th, smongkol@chula.ac.th, joejoja@hotmail.com

A highly sensitive turn-on fluorescent sensor for cyanide was developed based on benzylidenes containing methylindolium group. Three benzylidene derivatives were synthesized from the condensation reactions between benzaldehyde derivatives and methyleneindoline. Only one of these three derivatives shows strong visible blue fluorescence selectively to cyanide which was clearly observed in submicromolar range. The detection of cyanide with this compound was optimized in aqueous media using a non-ionic surfactant, Triton X-100 and sonication technique to give very low limit of detection in subnanomolar range. The compound was also developed into a paper-based and gel-based sensing kits for on-site naked eye detection of cyanide in micromolar range under black light illumination (360 nm).

15

8-Amidoquinoline Containing GlycinyI Group as Turn-on Fluorescent Sensors for Zn(II).

Author: Mongkol Sukwattanasinitt¹

¹ a. Department of Chemistry, Faculty of Science, d. Nanotec-CU Center of Excellence on Food and Agriculture, Department of Chemistry, Faculty of Science, Chulalongkorn University, Bangkok 10330, Thailand.

Corresponding Author: msukwatt@gmail.com

Fluorescent chemosensors for Zn(II) are attractive for microscopy and imaging for studying the role of Zn(II) biological in biological system. In this work, we discovered that 8-aminoquinoline containing amino group at alpha-position of the amino acid (**1**) pendant was effective for Zn(II) fluorescence imaging in plant tissue. In the presence of Zn(II) in aqueous media, ligand **1** exhibits selective fluorescence enhancement at 504 nm with a remarkable 24-fold increase of the fluorescence quantum yield. To tune the emission color and test for the generality of the core ligand, 5-arylethynyl-8-aminoquinoline derivatives were synthesized to study the effect of the electronic effects on the fluorescence responses of the ligands upon the complexation with Zn(II).

Falcon 1 / 16

New 8-Aminoquinoline Derivatives as “Turn-On” Fluorescent Sensor for Cd(II) ion Detection

Authors: Jutawat Hojitsiriyant¹; Mongkol Sukwattanasinit²

¹ *Department of Chemistry, Faculty of Science, Chulalongkorn University, Bangkok 10330, Thailand.*

² *Department of Chemistry, Faculty of Science, Chulalongkorn University, Bangkok 10330, Thailand, Nanotec-CU Center of Excellence on Food and Agriculture, Department of Chemistry, Faculty of Science, Chulalongkorn University, Bangkok 10330, Thailand.*

Corresponding Authors: msukwatt@gmail.com, jutawat.h@gmail.com

Two 8-aminoquinoline derivatives, **Q1** and **Q2**, containing one and two quinoline groups, respectively, are synthesized. In water, **Q1** and **Q2** showed strong electronic absorption peaks at 340 nm and 350 nm, with molar extinction coefficients of 3605 and 2475 M⁻¹cm⁻¹, respectively. The solutions are weakly fluorescent having quantum efficiency below 10%. In the presence of metal ions, the strong fluorescence signal at 480 nm is observed exclusively with Cd(II) ion. The fluorescence enhancement was probably the result of the restriction of photo-induced electron transfer (PET) process. In aqueous Tris solution pH 7.4, **Q2** shows significantly greater fluorescence enhancement ratio (I/I₀) of 30-fold comparing with 7-fold observed for **Q1**. The fluorescence detection of Cd(II) ion in water is possible in a wide pH range of 4 to 9 with the detection limit as low as 25 nM.

Heron 1 / 17

ELECTROWETTING ON DIELECTRIC (EWOD) OF SESSILE MICRODROPLETS CONTAINING POLYDISPERSE GOLD NANOPARTICLES

Author: Crismar Patacsil¹

¹ *University of the Philippines Baguio and Ateneo de Manila University (Philippines)*

Corresponding Author: cppatacsil@gmail.com

The wetting property of materials continues to be studied due to its important applications in many natural and industrial processes. Applying an external voltage affects the contact angle and offers a way to manipulate wettability without changing the chemical composition of the contacting phases. The use of external electric fields to control wettability has promising new applications in microfluidics which include laboratory-on-a-chip platforms for various biological sample preparation and analysis processes, fluid lens systems, electrowetting displays, and control of fluids in multichannel structures. Among various droplet manipulating mechanisms, electrowetting-on-dielectric (EWOD) is widely used because of its relatively simple device structure and fabrication. In this study, we investigate enhanced wetting effects of metal nanoparticles at very low concentrations in fluids in an electrowetting on dielectric (EWOD) experiment.

Nanoparticles manifest completely different properties (physical, chemical, electronic, magnetic and optical) from their bulk material. We explore the interaction of gold nanoparticle (AuNP) suspensions in a liquid droplet with applied electric field which cannot be observed with bulk gold. A basic planar electrowetting set-up is employed consisting of a bottom copper electrode coated with a thin insulating layer of uncured PDMS (Silicon oil) mounted on an adjustable stage and a platinum wire upper electrode injected in contact with the sessile electrowetting gold nanofluid microdroplet sitting over the dielectric layer. A voltage source is connected across the top and bottom electrodes and changes in the contact angle of the droplet, as voltage is varied, is captured using a USB microscope camera. The contact angles of the images are determined using a free software Image J.

We first tested our experimental set up with pure fluid (deionized water) microdroplets as the reference fluid. We found the uncured PDMS (Silicon oil) dielectric layer to have high hydrophobicity where the sessile water droplet is observed to have an average initial contact angle of 102.6 degrees

(no applied voltage). As voltage is applied at increasing increments of 1 volt, we observe electrowetting actuation (decrease in contact angle). The data for electrowetting of the reference fluid fits well with the Young-Lippmann equation for EWOD with an effective dielectric constant of about 18 and a saturation or breakdown voltage of 35V corresponding to decrease in contact angle to 67.2 degrees. Very low concentrations of gold nanofluid (deionized water containing gold nanoparticles with an average size of 10 nm) were prepared with the following concentrations (μM): 0.5, 0.25 and 0.05. Following the same procedure with the reference fluid microdroplets, we found that the presence of nanoparticles enhanced the electrowetting actuation of the sessile microdroplets in the described EWOD configuration. All concentrations containing gold nanoparticles showed enhanced electrowetting response (greater decrease in contact angle as voltage is increased) compared to the reference fluid (deionized water). The higher concentration, the more sensitive the electrowetting response. The 0.5 μM gold nanofluid concentration showed sensitivity to very low applied voltage (0-10V) with voltage breakdown (V_x) at 10V corresponding to a saturation contact angle (θ_x) of 68 degrees and a corresponding effective dielectric constant of 160. The 0.25 μM gold nanofluid concentration showed voltage breakdown $V_x = 20\text{V}$, $\theta_x = 64.5$ degrees and $k = 50$ while for the 0.05 μM gold nanofluid concentration, $V_x = 30\text{V}$, $\theta_x = 59.5$ degrees and $k = 30$.

Finally, to further verify that the gold nanoparticles are really the reason for the enhanced electrowetting actuation in the microdroplets, an ultra low concentration (0.005 μM) of the gold nanofluid is prepared. The ultra low gold nanoparticle concentration showed identical response to the electrowetting of the reference fluid verifying our claim of the enhanced electrowetting effect due to the gold nanoparticles. These results with sessile microdroplets in EWOD may pave the way to introducing metal nanoparticles towards better and more sensitive microdroplet for electronic and optical manipulation and other applications.

18

Effects of halogen on the properties of $\text{CH}_3\text{NH}_3\text{PbI}_3\text{-yXy}$ layers for perovskite solar cells

Author: Vorrada Loryuenyong^{None}

Corresponding Author: vorrada@gmail.com

Nowadays, solar cells based on $\text{CH}_3\text{NH}_3\text{PbX}_3$ (when X is halogen) perovskite materials have been intensively studied due to their broad absorption spectrum, long charge carrier lifetime and long carrier diffusion length. However, from previous reports, halogen in perovskite structure typically affects the properties of $\text{CH}_3\text{NH}_3\text{PbI}_3\text{-yXy}$ active layers in perovskite solar cells. In this study, we then investigated the effects of halogen on the properties of $\text{CH}_3\text{NH}_3\text{PbI}_3\text{-yXy}$ layers. Perovskite films were prepared by sequential deposition 2-step technique. PbI_2 or $\text{PbI}_2\text{-PbCl}_2$ solution was first spin-coated on FTO glasses and subsequently 30 mg/ml of $\text{CH}_3\text{NH}_3(\text{IxBry})$ solution, with different ratio of I and Br (1:0, 2:1, 4:1, 1:4, 1:2 and 0:1), was coated on top. Then, they were annealed at 90 °C for 1 hour and 100 °C for 25 minutes to transform into perovskite structure. The characterization of perovskite films included X-ray diffraction, UV-Vis spectroscopy, photoluminescence spectroscopy (PL) and Scanning Electron Microscopy. The results indicated that $\text{CH}_3\text{NH}_3\text{PbI}_3$ have the widest visible light absorption analysis. Having Br and Cl in $\text{CH}_3\text{NH}_3\text{PbI}_3\text{-xBrx}$ and $\text{CH}_3\text{NH}_3\text{PbI}_3\text{-x-yBrxCly}$, respectively, would decrease the absorption in visible light region. However, it could reduce electron and hole recombination as well as increase cell stability, which leads to higher DSSCs' efficiency.

19

Preparation of Copolymer from Recycle Plastic Bottle and Study of Its Applications in the Electrochromic Devices

Author: Achanai Buasri¹

Co-author: Vorrada Loryuenyong¹

¹ *Silpakorn University***Corresponding Authors:** achanai130@gmail.com, vorrada@gmail.com

In this study, waste poly(ethylene terephthalate) (PET) bottle was depolymerized using excess ethylene glycol (EG) in the presence of zinc acetate as a catalyst. It was found that the reacted products consist mainly of bis-2-hydroxy ethylene terephthalate (BHET) monomer. Poly(ethylene terephthalate)-poly(lactic acid) (PET-PLA) copolymers were synthesized by the reaction of BHET with L-lactic acid monomers (LLA) using the catalytic system. The samples were analyzed by nuclear magnetic resonance (NMR) and differential scanning calorimetry (DSC). The ¹H and ¹³C NMR studies confirm the incorporation of lactate units in PET chains after reaction. Further, we report the use of graphene conductive ink and PET-PLA as the electrochromic device. Copolymer film was coated with graphene ink by spin coating method. Our results primarily indicate that the configuration presents an easy and expeditious way of preparing the electrochromic device.

Falcon 1 / 20

2Mechanism of ferromagnetism occurring in CVD-adamantane films

Author: Suppanut Sangphet¹¹ *Suranaree University of Technology***Corresponding Author:** suppanut.tone@gmail.com

Recently there have been reports of room-temperature ferromagnetism induced in carbon compounds, including “Teflon” sheets and “Q-carbon”. In this work, we would like to create room-temperature ferromagnetism with the 1-cage from adamantane; the smallest member of the material called “diamondoid” series (nano-diamond structures). By using chemical vapor deposition (CVD), we prepared the films on various substrates, e.g. Si, quartz and sapphire. Intriguingly, we found the signature of moderately strong ferromagnetism with saturated magnetization up to 120 emu/cm³. By using XPS and EDS, we have found no trace of any magnetic elements, e.g. Fe, Co, and Ni. The Raman spectra display forms of carbon bondings occurring in the film surface, including sp², sp³ and C-H. Furthermore, NMR spectra show that chemical bonding of the substrate have changed during the CVD process. These suggest that carbon atoms of adamantane molecules are largely decomposed to other forms with non-sp³ bondings. The origin of this ferromagnetism, including dangling bond (which is suggested to be the cause of ferromagnetism in Teflon sheets) and a single π -state coupling (which is reported to be cause of ferromagnetism in isolated hydrogen atom absorbed on graphene), will be discussed.

Heron 2 / 21

Electrochemical aptasensor for glycated albumin in Diabetes mellitus diagnosis and monitoring

Author: Sasinee Bunyarataphan¹¹ *National Nanotechnology Center (NANOTEC), National Science and Technology Development Agency***Corresponding Author:** bsasinee@hotmail.com

A simple electrochemical aptasensor was developed for the detection of glycated albumin (GHSa) using ssDNA aptamer that selectively binds to GHSa as a recognition element. The biotinylated ssDNA aptamer was immobilized on a streptavidin-modified screen-printed carbon electrode (SPCE). The changes of interfacial features of the electrode surface, which were based on the aptamer-GHSa

interaction, were probed in the presence of the reversible redox $\text{Fe}(\text{CN})_6^{3-}$ using square wave voltammetry (SWV) measurements. Our results showed that the minimum detection limit of this sensor was $10 \mu\text{g/ml}$ with a calibration curve to the range of 16 mg/ml . The aptasensor showed high selectivity for GHSA over other molecules that is usually available in the blood. Importantly, our aptasensor was successfully applied to detect GHSA in blood serum samples, which demonstrated the higher levels of GHSA concentrations in diabetes than normal persons. These indicate that our electrochemical aptasensor has a potential for diagnosis and monitoring of diabetes mellitus.

22

Enhancement of drug bioavailability of quaternized chitosan by dual synergistic mechanism through transcellular and paracellular transport in the intestinal cell monolayer using Caco-2 cell model

Co-author: Pattarapond Gonil¹

¹ Nanoengineered Soft Materials for Green Environment Laboratory, National Nanotechnology Center (NANOTEC), National Science and Technology Development Agency (NSTDA), Thailand Science Park, Pathumthani 12120, Thailand

Corresponding Author: pattarapond@nanotec.or.th

Development of poorly soluble and unstable peptide drugs using drug delivery system has been introduced to improve drug bioavailability via oral administration. Among the novel oral drug carriers interested in nanotechnology, chitosan Quat-188, is the modified chitosan with quaternization process to improve solubility without any effect on the mucoadhesive property of core chitosan. In our previous study, chitosan Quat-188 showed well biocompatibility on human intestine in the non-toxic dose without significant effect on intestinal proliferation and differentiation [1]. However, the drug absorption enhancement of chitosan Quat-188 on human intestine remained to be unknown. Therefore, aim of this study was to further examine the potential effects of chitosan Quat-188 on improvement of drug bioavailability through transcellular and paracellular pathway in intestinal cells by using Caco-2 cells as an in vitro model.

In transcellular pathway focusing on P-glycoprotein (P-gp), the bidirectional transport and intracellular accumulation in Caco-2 cells were measured by radiolabeled digoxin (Digoxin[H3]) and calcein AM uptake, respectively. The results indicated that chitosan Quat-188 was able to inhibit the P-gp function by decreasing the efflux of P-gp substrate (Digoxin[H3]) and increasing the intracellular accumulation of calcein. In addition, in paracellular pathway, trans-epithelial electrical resistance (TEER), transport of FITC labeled dextran (FD4) and immunofluorescence of tight junction protein were investigated. Our results demonstrated that chitosan Quat-188 enhanced the paracellular permeability by decreasing the TEER value and increasing the FD4 transport in a dose-manner response. Moreover, chitosan Quat-188 acts as the reversible opener of tight junction protein since the removal of chitosan Quat-188 could attenuate the TEER value and reverse the structure of tight junction protein.

Taken together, these findings indicated that chitosan Quat-188 has the dual synergistic effects to enhance drug bioavailability on both transcellular and paracellular transport by decreasing the drug efflux via impairing the P-gp function and by increasing drug absorption via reversible opening the tight junction protein. Our results suggested the usefulness of chitosan quat-188 as the safely and controllably drug carrier in development of the oral drug delivery system.

23

Effect of ZnO and TiO₂ on Properties of Polystyrene/Nitrile Rubber Electrospun Fiber Mats

Author: Poonsub threepopnatkul¹

¹ *Department of Materials Science and Engineering, Faculty of Engineering and Industrial Technology, Silpakorn University, Nakhon Pathom 7300, Thailand*

Corresponding Author: poonsubt@yahoo.com

This research is aimed to study the effect of zinc oxide (ZnO) and titanium dioxide (TiO₂) on mechanical and antibacterial properties of PS/NBR electrospun fibers. 15 wt% of polystyrene (PS) blended with nitrile rubber (NBR) at 50:50 w/w is dissolved in tetrahydrofuran prepared PS and NBR solution. ZnO and TiO₂ are added into PS/NBR solution at 1.0, 2.0 and 3.0 wt%. The addition of 2.0 wt% of ZnO into PS/NBR electrospun fibers maximized Young's modulus and tensile strength. For the effect of TiO₂, increasing content of TiO₂ up to 1.0 wt% increased Young's modulus and tensile strength of PS/NBR electrospun fibers while addition of TiO₂ beyond 1.0 wt% decreased the Young's modulus and tensile strength. The percentage strain at break is also decreased as the content of ZnO and TiO₂ increased. Moreover the anti-bacterial properties, it found that the addition of 2.0 wt% ZnO the fibers inhibited the growth of *E. coli* and *S. aureus*.

Heron 2 / 24

Efficient visible light-induced photocatalytic degradation of Rhodamine B over chlorophyll and Mg co-modified P25 nanoparticles

Author: Thanaree Phongamwong¹

¹ *KU-Green Catalysts Group, Department of Chemical Engineering, Faculty of Engineering, Kasetsart University*

Corresponding Author: thanaree.ph@gmail.com

The new composite materials of TiO₂ nanoparticles and biomolecules are promising to provide the potential alternative for improving the photocatalytic activity by merging the ability and features of both material types. In this research, the unique visible light-responsive chlorophyll and magnesium (Mg) co-modified P25 catalyst (Chl-Mg/P25) was successfully synthesized by using a simple incipient wetness impregnation method. Chlorophyll and Mg were loaded on P25 nanoparticles with an attempt to enhance photocatalytic efficiency and inhibit the recombination of photo-induced electron-hole pair. The existences of chlorophyll and Mg on P25 were verified by Fourier transform infrared spectroscopy (FT-IR) and X-ray photoelectron spectroscopy (XPS). The synthesized catalysts were tested for photocatalytic degradation under visible light by using Rhodamine B (RhB) as a probe molecule and the effect of chlorophyll and magnesium on photocatalytic degradation were investigated. It was found that the activities of catalysts were in the order of: P25 < Mg/P25 < Chl/P25 < Chl-Mg/P25. The addition of chlorophyll, Mg, and chlorophyll-Mg in the catalyst could promote the photocatalytic efficiency for approximately 1.9, 1.1, and 2.3 times of P25, respectively. These outstanding photocatalytic activities could be attributed to the enhancement in visible light harvesting from chlorophyll, the higher charge separation efficiency from Mg, and the synergistic effect between chlorophyll-Mg and P25 nanoparticles. Moreover, Chl-Mg/P25 catalyst also showed a good recyclability and high stability after seven repeated experiments.

Heron 1 / 25

The observation of strain-induced valence band splitting on HfSe₂ by Alkali metal intercalation

Author: Tanachat Eknapakul¹

¹ *Suranaree University of Technology*

Corresponding Author: atomic_e_spirit@hotmail.com

Alkali metal intercalation in layered-transition metal dichalcogenides (LTMDs) has been intensively studied due to a wide range of attractive properties such as enhancement of superconductivity, quasi-freestanding, and negative electron compressibility which lead to many potential nanoelectronic applications. Essentially, many researchers study the correlation between electron doping and strain (and vice versa) in order to manipulate their electronic structure, band gap, and carrier mobility. In this work, we have measured the electronic structure of 1T-HfSe₂ by using angle resolved photoemission spectroscopy (ARPES) together with *in situ* alkali metal evaporation. Our ARPES data as a function of electron doping show the monotonic increase of in-plane p-orbital valence band splitting (VBS) reaching as high as 350 meV and the band gap reduction up to 250 meV for a carrier density around $5 \times 10^{14} \text{ cm}^{-2}$ (corresponding to ~20% of Brillouin zone). These VBS values are very similar over various alkali metal dopants (including Na, Cs, and Rb) suggesting that the in-plane lattice reduction is dominated while the out-of-plane lattice expansion is neglected at the valence band maximum. The density functional theory calculation (DFT) has been used to understand the electronic structure of HfSe₂ under the condition of alkali metal intercalation and strain. At 25% of Na doping, the out-of-plane lattice constant (c) increases up to 11% while the in-plane lattice constant (a) decreases around 3% which can be described by the different coulomb interaction over Se atoms. The calculation of electronic structure under uniaxial tensile strain is very well in agreement of our ARPES data in both of VBS and band gap shrinkage indicating that uniaxial strain can be induced by alkali metal intercalation. Finally, our finding should help to simplify the study in strain physics as well as for large-scale strain engineered devices.

Keyword: alkali metal intercalation, layered-transition metal dichalcogenides, strain, angle resolved photoemission spectroscopy, density functional theory.

26

Enhanced activity and stability of CuO-ZnO-ZrO₂ catalyst by addition of colloidal SiO₂ nanoparticles for CO₂ hydrogenation

Author: Thongthai Wittoon¹

¹ Department of Chemical Engineering, Faculty of Engineering, Kasetsart university

Corresponding Author: onglovely@gmail.com

In this study, a series of CuO-ZnO-ZrO₂-SiO₂ catalysts were prepared by co-precipitation of Cu, Zn and Zr precursors with dispersed colloidal silica nanoparticles. The effect of silica content (0–5 wt%) on the physicochemical properties of the resulting catalysts as well as their catalytic activity in CO₂ hydrogenation were investigated. The catalysts were characterized by thermal gravimetric analysis (TG), X-ray diffraction (XRD), H₂-temperature programmed reduction (H₂-TPR), transmission electron microscope (TEM), time-resolved x-ray absorption spectroscopy (TRXAS), CO₂ and H₂ temperature-programmed desorption (CO₂ and H₂-TPD). The promotional effect was most effective for low amounts of SiO₂ (<1.5 wt%). An increase in methanol synthesis activity of 25% compared to the ternary SiO₂ free system was observed. Promotion was characterized by a geometric modification which was expressed by a higher inter-dispersion of metal oxides. Moreover the presence of SiO₂ nanoparticles in the CuO,ZnO,ZrO₂ system enhanced the stability of the catalyst.

27

Carbon Anode from Cassava for Lithium-ion Battery

Author: Pakwan Chanprakhon^{None}

Corresponding Author: pakwan.rondine@gmail.com

Recently, carbon prepared from cassava was used as counter electrodes for dye-sensitized solar cell and the efficiency of the solar cell was found to be very high. In this research, carbon from cassava is

used as anode electrode in Li-ion battery. The carbon was prepared by carbonizing the dry cassava at various temperatures. The morphology was studied by scanning electron microscopy (SEM). The structure of carbon from cassava was studied by Raman spectroscopy. Cyclic voltammetry was for understanding its electrochemical property. The charge-discharge profile was studied by galvanostatic test. The results will be discussed.

28

Electron transporting material for Perovskite and Organic hybrid solar cell

Author: Pisist Kumnorkaew¹

¹ *National Nanotechnology Center*

Corresponding Author: pow0521@yahoo.com

We introduce a new electron transporting material (ETM) made of zinc cadmium sulfide and titanium oxides. This new material has shown significant enhancement in efficiency of photovoltaic device such as Perovskite, Organic, and Dye Sensitized Solar Cell. In this study, zinc cadmium sulfide suspension was added to titanium oxide sol-gel. The addition of zinc cadmium sulfide helps reduce energy level and increase electron transfer in electron transporting layer compared to that in the pristine titanium dioxide film. At the optimum addition of ZnCdS, at least 20% percent improvement of photovoltaic devices were observed. The mixture was prepared at room temperature and deposited to each photovoltaic device via rapid convective deposition, in which one-fifth of materials were consumed compared with traditional spin coating technique. With the new ETM and convective deposition technique, high efficiency and low cost Perovskite (> 10%PCE) or Organic hybrid solar cell (>5% PCE) can be fabricated.

Falcon 1 / 29

Heterogeneous Suzuki cross-coupling reaction in water catalyzed by palladium nanoparticles supported on individual calcium carbonate plates derived from mussel shell particle.

Author: Sukumaporn Chotnitikornkun¹

Co-author: Mongkol SUKWATTANASINITT²

¹ *Department of Chemistry, Faculty of Science, Chulalongkorn University, Bangkok 10330, Thailand.*

² *Nanotec-CU Center of Excellence on Food and Agriculture, Department of Chemistry, Faculty of Science, Chulalongkorn University, Bangkok 10330, Thailand.*

Corresponding Authors: smongkol@chula.ac.th, pucca_so-cute@hotmail.com

A new palladium nanoparticles catalyst supported on individual calcium carbonate plates (Pd/ICCP) is prepared from Asian green mussel shells and used as heterogeneous catalyst in Suzuki cross coupling reaction. The reduction of palladium (II) generates palladium (0) nanoparticles which can embed on individual calcium carbonate plates (ICCP) to give Pd/ICCP. The prepared Pd/ICCP catalyst is characterized by scanning electron microscopy (SEM) and energy-dispersive X-ray spectroscopy (EDX), indicating an entire dispersion of palladium onto the surface of individual calcium carbonate plates. Furthermore, palladium content in the prepared Pd/ICCP catalyst is determined by inductively coupled plasma optical emission spectroscopy (ICP-OES). The optimized study is investigated in Suzuki cross-coupling reaction between 4-iodoanisole and phenylboronic acid. It reveals that using potassium carbonate in mixed solvent of EtOH: H₂O (3:2) in the presence of 2 mol% of Pd/ICCP

give 4-methoxybiphenyl in 90% isolated yield at 40 °C. Moreover, in the presence of cetyltrimethylammonium bromide (CTAB) as phase transfer agent, the reaction can preform in water as a sole solvent to give the product in excellent yield under the same condition.

30

Improvement of catalytic stability in Carbon Dioxide Reforming of Methane over Ni-carbon Composite Catalyst: Effect of Carbon Structure

Author: Waleeporn Donphai¹

¹ *Department of Chemical Engineering, Faculty of Engineering,*

Corresponding Author: waleepornd@gmail.com

Carbon dioxide and methane have been utilized as reactant gases to produce hydrogen and carbon monoxide through dry reforming reaction. However, the main problem is catalyst deactivation by coke formation. In order to solve this problem, nickel-carbon nanotubes (Ni-CNTs) composite material with a unique structure of Ni on the tips of CNTs used as catalyst could prolong the catalyst lifetime during the reaction. In this research, the effects of carbon structures of Ni-CNTs composites over mesocellular silica (MS) support on catalytic activity and stability in dry reforming reaction were investigated. Ni-CNTs composite catalysts (Ni-CNTs(x)/MS) were synthesized via the catalytic chemical vapor deposition (CCVD) technique at 650, 700, and 750°C, and were then used in dry reforming reaction at temperatures of 550, 650, and 750°C. With increasing the CCVD temperature, the relative amounts of highly stable CNTs and less stable CNTs significantly increased. Among these composite catalysts, Ni-CNTs(750)/MS catalyst showed better catalytic stability than those of Ni-CNTs(650)/MS and Ni-CNTs(700)/MS catalysts because of its composite structure contained the highest relative amount of highly stable CNTs. . In addition, Ni-CNTs(750)/MS composite catalyst gave the highest turnover frequency (TOF) values of 2.62 and 3.63 times higher than those of the conventional Ni/MS catalysts at the reaction temperatures of 650 and 750°C, respectively. This outstanding performance could be attributed to the existence of highly stable CNTs could significantly enhance the catalytic performance and stability of this Ni-CNTs composite catalyst in dry reforming reaction.

Falcon 1 / 31

Micrometers to nanometers conversion process in perovskite Ba-TiO₃ particles

Author: Thitirat Charoonsuk^{None}

Co-author: Wanwilai Vittayakorn¹

¹ *Collage of Nanotechnology, King Mongkut's Institute of Technology Ladkrabang*

Corresponding Author: wanwilai.vi@kmitl.ac.th

A one-step “top-down” process was proposed in this work to obtain nanoparticle products of tetragonal barium titanate (BaTiO₃; BT) with highly accurate stoichiometry and morphological control. A micrometer-sized BT precursor significantly decreases to nanometer-sized product particles and its irregular shape changes to nearly spherical with narrow size distribution via surface active etching. Both XRD and Raman results of BaTiO₃ nanoparticles indicated a tetragonal crystal structure. The 77.5 ± 2.5 nm sized BaTiO₃ powder product still polarized spontaneously at room temperature and the ferroelectric phase transition was confirmed at around 127 °C. Dielectric permittivity was found to be ~ 166.42 by Landauer-Bruggeman effective medium approximation (LB-RMA). Experimental procedures revealed a possible process mechanism observed within the etched surface and

Oriented-attachment growth models, and this demonstrated approach could be used as an excellent platform for preparing advanced ceramic nanoparticles.

Heron 2 / 32

Styryl-Functionalized BODIPY as Fluorescent Probe For Metal Ions Detection in Aqueous Media

Author: Suthikorn Jantra¹

Co-author: Mongkol Sukwattanasinitt¹

¹ *Department of Chemistry, Faculty of Science, Chulalongkorn University, Bangkok Thailand*

Corresponding Authors: smongkol@chula.ac.th, sudd_y2j@yahoo.co.th

Fluorescent-based sensors have received extensive attention due to its highly sensitive and rapid sensing ability to detect metal ions. In this study, we have developed a new BODIPY derivative, **mTBODdiSalic** for detection of metal ions in aqueous media. The probe has been synthesized from 2,4-dimethylpyrrole and 5-formylsalicylic acid in 4 steps and fully characterized with NMR and Mass spectrometry. **mTBODdiSalic** displays a maximum absorption and emission at wavelength 642 and 662 nm which appear as blue color in daylight and pink under fluorescent black light, respectively. Among 19 various metal ions, **mTBODdiSalic**'s emission was selectively quenched by the addition of Cu^{2+} and Al^{3+} ions. Moreover, **mTBODdiSalic** could react with Au^{3+} to afford maximum absorption wavelength shift from 642 into 573 nm (purple color) along with maximum emission wavelength shift from 662 into 596 nm (orange fluorescence). Therefore, **mTBODdiSalic** could be used to visually discriminate between Au^{3+} over other cations in aqueous solution under a UV-vis lamp.

33

Imaging of cellular localization of nanoparticles using STED technology

Author: Paninee Chetprayoon¹

¹ *Nano Safety and Risk Assessment Laboratory, National Nanotechnology Center*

Corresponding Author: paninee@nanotec.or.th

Visualization of subcellular levels is always difficult to be achieved by conventional fluorescence microscopy due to the diffraction limit of light. Stimulated Emission Depletion (STED) is a super-resolution microscopy that can improve the spatial resolution to below 70 nm. Herein, we demonstrated cellular localization of nanoparticles in A549, human lung epithelial cell line by using a STED super-resolution microscope. This Imaging technique will be useful for toxicological studies on cell-nanoparticles interaction, as well as pharmacological studies on effects of nano-drug carrier at the target tissues.

34

Fabrication of Porous Gold-Silver Alloy Nanowires Array via Controlled Dealloying Process: a Simple Approach for Highly Stable and Sensitive SERS Substrate

Author: Natta Wiriyakun¹

¹ *National Nanotechnology Center (NANOTEC), National Science and Technology Development Agency (NSTDA), Pathum Thani 12120, Thailand*

Corresponding Author: n.wiriyakun@gmail.com

Surface enhance Raman scattering (SERS) has received a great interest as a powerful tool for enhancing the Raman characteristic peaks of molecules. For commercial purpose, SERS substrate is practically required to accomplish all four features, which are high sensitivity, reproducibility, uniformity and ability to provide stable Raman signal. There are a few works of developed SERS substrates that meet all the requirements. However, an approach for fabrication of SERS substrate for the long-term stability without reduction of sensitivity has not yet been reported.

This work presents a simple approach for fabrication of porous gold-silver alloy nanowires array as SERS substrate. The highly ordered two-dimensional (2D) array of gold-silver alloy nanowires (AuAg NWs) was first created via template-based electrochemical deposition, followed by the controlled dealloying process. Systematic study of the controlled dealloying process revealed that the porous nanowires array maintaining their rigid nanostructures was successfully obtained when using mild acid etching. SERS performance of the fabricated substrates was fully evaluated using 4-mercaptobenzoic acid (4-MBA) as a probe molecule. Exceedingly, a 150-fold Raman signal with respect to typical gold film substrate was obtained. Additionally, uniformity in Raman signal in both macroscopic and microscopic area was obtained. For the large-area uniformity, SERS signal within a circular area of 2-cm diameter was examined and given the acceptable relative standard deviation (RSD) less than 12.16% (n =12). While, the uniformity of Raman signal in a microscopic area was investigated by Raman mapping in the square area (100x100 μm^2). The result shows the exceptional RSD less than 3% for 16,384 individual spectra. Moreover, an excellent stability of our SERS substrate was also continuously monitored, with 100% of the initial Raman signal over a month and the detectable signal over 3 months of storage at room temperature. According to the result of SERS performance testing, it is obviously seen that our proposed route by simple controlling of dealloying process can provide an excellent SERS substrate for further applications in bio- and chemical sensors.

Hornbill 1 / 35

Magneto and electro-optical study of Bismuth ferrite (BiFeO₃) thin films

Author: Siwat Polin¹

¹ *School of physics, Institute of science, Suranaree university of technology, Nakhon Ratchasima, Thailand 30000*

Corresponding Author: siwat.polin@gmail.com

Multiferroic materials, which exhibit both electrical and magnetic ferroic orders, have attracted much attention due to its potential application in electronics. Normally, the relation of both phenomena have to be analysed by several instruments. Here, optical-Kerr-effect properties of bismuth ferrite (100) thin film has been investigated. The Kerr rotation of light reflected from the BiFeO₃ surface was measured through reading from the photodiode while the magnetic field and electric field was applied. Our results shows the electrical-polarization and magnetization of films. Moreover, an ultraviolet-induced enhancement of polarization can be detected, imply magneto and electro-optical measurement may be a powerful method in multiferroic materials research.

Heron 2 / 36

The electrochemical properties of NiO/NFs electrode induced by UV light irradiation

Author: Supansa Musikajaroen¹

¹ School of Physics, Institute of Science, Suranaree University of Technology, Nakhon Ratchasima, Thailand 30000

Corresponding Author: supansa_j@outlook.com

A simple thermal oxidation has been used for fabricating nanostructured NiO/NFs electrodes at a temperature lower 1000°C in air. The results obtained from x-ray diffraction (XRD) and scanning electron microscope (SEM) have shown the structure and morphology of Ni foam (NFs) before and after oxidation. The electrochemical characterization measurements have shown that the NiO/NFs electrodes are sensitive to UV light, as observed from the increase in measured current. The effect of UV-irradiation will be discussed.

Keywords: NiO electrode, UV light, Electrochemical, Thermal oxidation

37

Effects of Brønsted acid on the Selective Catalytic Reduction of NO with NH₃ on Ru-doped Ceria Catalyst

Author: Chirawat Chitpakdee¹

¹ National Nanotechnology Center, National Science and Technology Development Agency, 111 Thailand Science Park, Paholyothin Rd., Klongluang, Pathumthani 12120, Thailand

Corresponding Author: chirawat@nanotec.or.th

Reaction mechanism of selective catalytic reduction (SCR) of NO by NH₃ on the clean and Brønsted acid surfaces of Ru-deoped CeO₂(111) were investigated using density functional theory calculation corrected by on-site Coulomb interactions (DFT+U). The calculations were performed by Vienna Ab initio Program Package (VASP). The proposed reaction mechanism on the clean surface consists of two competitive catalytic pathways (ABCD and AED pathways), while that on the Brønsted acid surface follows FC pathway. The activation energy barriers of all elementary steps as well as the corresponding relative energies of all intermediates, reactants, and products were calculated. On the clean surface, an NH₃ molecule is preferentially adsorbed on the Lewis acid Ru-dopant site. The dissociation of the first N-H bond is broken spontaneously after the NH₃ adsorption and forms the NH₂ species. Then this NH₂ species readily interacts with a NO gas and converts to the NONH intermediate (IM:4). Note that IM:4 could be decomposed to H₂O and N₂O via step B or decomposed to N₂ and H₂O via step E. The calculation results reveal that step B is more feasible in term of lower activation energy barrier; 34 kJ/mol for the former and 129 kJ/mol for the later. Therefore, the reaction on the clean surface is suggested to follow ABCD pathway. In addition, the NH₃-SCR of NO over Brønsted acid surface of Ru-deoped CeO₂(111) were considered to study the effect of the presence of Brønsted proton on the catalyst surface. The reaction follows FC pathway, which occurs easily because of the substantial small activation barriers. The calculations reveal that the presence of Brønsted acid on the surface catalyst accelerates the decomposition of NO by NH₃ over Ru-deoped CeO₂(111) catalyst.

Heron 1 / 38

Analysis of electronic spectral weight of two-dimensional electron gases at the surfaces of ferroelectric KNb_xTa_(1-x)O₃ across T_c

Author: Sujinda Chaiyachad¹

Co-authors: Tanachat Eknapakul²; Worawat Meevasana³

¹ School of Physics, Institute of Science, Suranaree University of Technology

² Suranaree University of Technology

³ School of Physics, Suranaree University of Technology

Corresponding Authors: keng_462535@hotmail.com, worawat@gmail.com, atomic_e_spirit@hotmail.com

A two-dimensional electron gas (2DEG) (confined electron which is free to move in two dimensions at the interface/surface) was discovered at the LaAlO₃/SrTiO₃ interface; later on 2DEG was also observed at the bare surfaces of SrTiO₃ and KTaO₃. This system can enhance some physical properties (i.e. superconductivity and ferroelectric polarization) as well as the novel properties such as negative electron compressibility and unusual coexistence of ferromagnetism and superconductivity. In this work, by using angle-resolved photoemission spectroscopy, we have studied the temperature dependence (T=20-130K) of 2DEGs at bare surfaces of ferroelectric KNb_xTa_(1-x)O₃ (KTN) (x=0.02, 0.03 and 0.05) across their ferroelectric transition temperatures (T_c). We found that the 2DEG spectral weight gradually decreased at temperature below ferroelectric T_c. The possible reason can be described by the transition from paraelectric to the ferroelectric which broadens the quantum well state due to electrical polarization. The number of electrons, which are initially confined at the surfaces, will be delocalized and hence the electronic spectral weight of 2DEG nature is changed. Our finding may help mediate the fundamental study of 2DEGs and phase transition as well as for functional oxide devices.

39

Magneticfield-promoted cleaner production of small alcohols and hydrocarbons from CO₂ over Cu-ZnO/ZrO₂and Fe/MCM-41 catalysts

Author: Metta Chareonpanich¹

¹ Kasetsart University

Corresponding Author: iamannmetta@gmail.com

Magneticfield-promoted cleaner production of small alcohols and hydrocarbons from CO₂ over Cu-ZnO/ZrO₂and Fe/MCM-41 catalysts

Metta Chareonpanich^{1,2,*}, Waleeporn Donphai^{1,2}, Sirapassorn Kiatphuengporn³, Jumras Limtrakul^{2,4}

¹KU-Green Catalysts Group, Department of Chemical Engineering, Faculty of Engineering, Kasetsart University, Bangkok 10900, Thailand

²NANOTEC Center for Nanoscale Materials Design for Green Nanotechnology, and Center for Advanced Studies in Nanotechnology and its Applications in Chemical, Food and Agricultural Industries, Kasetsart University, Bangkok 10900, Thailand

³Nanomaterials for the Energy and Catalysis Lab, National Nanotechnology Center, National Science and Technology Development Agency, Pathumthani12120, Thailand

⁴ Department of Materials Science and Engineering, School of Molecular Science and Engineering, Vidyasirimedhi Institute of Science and Technology, Rayong 21210, Thailand

*Corresponding author: +66 25792083, fengmtc@ku.ac.th

ABSTRACT

Based on green and sustainable application for the enhancement of catalyst performance and energy conservation, an external magnetic field has been applied in CO₂ hydrogenation reaction to improve the catalytic activity and reduce the energy consumption. In this research, the performances of Cu-ZnO/ZrO₂ and xFe/MCM-41 catalysts with ferro/ferrimagnetic property under magnetic field with different magnetic flux intensities (0-27.7 mT) and orientations (north-south and south-north) were

investigated. It was found that both Cu-ZnO/ZrO₂ and xFe/MCM-41 catalysts operated under magnetic field gave higher CO₂ conversions, compared to that of without magnetic field at all reaction temperatures. The highest CO₂ conversions under magnetic field condition were 1.8–3.0 times, and 1.5–1.8 times higher than that of without magnetic field for Cu-ZnO/ZrO₂ and xFe/MCM-41, respectively. These outstanding catalytic activities could be attributed to the fact that magnetic field help facilitate the reactant adsorption and surface reaction over magnetized catalysts, leading to the decrease of apparent activation energy, and the increase of selectivities to hydrocarbons and CH₃OH. Moreover, this challenge in application of magnetic field in CO₂ hydrogenation process help reduce CO₂ emission into the atmosphere compared to the convention reactor, and therefore led to the carbon-neutral CO₂ conversion process.

Falcon 1 / 40

Preparation of controlled release nanocapsule for mosquito repellent application

Author: Jaruwan Joothamongkhon¹

¹ *National Nanotechnology Center, National Science and Technology Development Agency*

Corresponding Author: jaruwan@nanotec.or.th

Mosquito repellents can help to protect against mosquitoes which transmit many disease such as Zika, malaria, dengue and other viral diseases [1,2]. Recently, people have used the products which made of both chemical and natural mosquito repellent agents [3]. However, the fast evaporation of active ingredients in mosquito repellents limits the time protection against mosquitoes [3,4]. To prolong the release time of mosquito repellent agent, the encapsulation technique can be applied. In this study, polymeric nanocapsules containing mosquito repellent agents, i.e. N,N-diethyl-m-toluamide (DEET) and eucalyptus oil were prepared by oil-in-water precipitation method. The hydrodynamic diameter and particle size distribution of prepared nanocapsules were characterized using dynamic light scattering method (DLS). Protection time against mosquito bites was investigated at various storage time. Moreover, the primary skin irritation of the nanocapsules were studied in using rabbit model. DEET-based mosquito repellent and eucalyptus oil-based mosquito repellent nanocapsules provided up to 12 hours and 3 hours of protection against mosquitoes, respectively. The polymer encapsulation is one effective approach to reduce the risk of mosquito bite and consequently prevent from many mosquito-borne diseases.

41

Novel of quinoline derivatives containing 5-membered heterocycles for Zinc ions detection

Author: Anawat Ajavakom¹

Co-author: Mongkol Sukwattanasinitt¹

¹ *Organic Synthesis Unit, Department of Chemistry, Faculty of Science and Nanotec-CU Center of Excellence on Food and Agriculture, Chulalongkorn University, Bangkok 10330, Thailand.*

Corresponding Authors: smongkol@chula.ac.th, anawat77@hotmail.com

Fluorescent probes based on 8-aminoquinoline and 8-hydroxyquinoline containing 5-membered heterocyclic aromatic and nonaromatic rings are synthesized and evaluated as a chemosensor for metal ions. One of 8-aminoquinoline derivatives bearing L-proline exhibits a turn-on fluorescence response to Zn²⁺ in aqueous media by showing strong emission peak at 505 nm. The limit of detection for Zn²⁺ is in the 4.83 nM. On the other hand, the derivatives containing 5-membered aromatic ring show relatively low and less selective fluorescence responses to metal ions in aqueous media. The

lone pair electrons of the heteroatoms in the aromatic rings are weaker binder to the metal ion in comparison with the that in the non-aromatic proline ring.

42

BODIPY Derivatives as Photocatalyst for Oxidative Coupling

Author: Piyamaporn Tangkasemsamran¹

¹ *Department of Petrochemical and polymer science*

Corresponding Author: piyamaporn.ta@gmail.com

Photoredox catalytic organic reactions promoted with visible light have gained much attention recently, allowing to prepare various organic compounds in good yields and selectivity under mild reaction conditions. In this work, we synthesized three iodo-BODIPY derivatives, **I-GB**, **3I-GB** and **I-RB** as a photocatalysts for oxidative coupling of thiol to disulfide. **I-GB** and **I-RB** can be synthesized from the condensation of 4-iodobenzaldehyde with 2,4-dimethylpyrrole and 2-phenylpyrrole, respectively to obtain **I-GB** (20% yield) and **I-RB** (36% yield). Then, iodination of **I-GB** give rise to the formation of **3I-GB** in 58% yield. All BODIPYs are fully characterized with ¹H NMR, ¹³C NMR and mass spectrometry. The 4-chlorothiophenol is used as model to investigate the photocatalytic activity of iodo-BODIPYs and compare with the conventional photocatalyst, Rose Bengal. Under the irradiation with White LED in isopropanol at room temperature, in the presence of three BODIPYs the complete conversion of thiol into the corresponding disulfide are obtain in less than one hour while in Rose Bengal case, more than XX % of starting material remain the reaction mixture. Our finding will be useful for the design of robust organic photocatalyst for photooxidation reaction.

43

Synthesis and Development of fluorescent sensor based on julolidine linked di-(2-picoly)amine derivatives

Author: Anawat Ajavakom¹

Co-author: Thanaphong Lertpiriyasakulkit²

¹ *Nanotec-CU Center of Excellence on Food and Agriculture, Department of Chemistry, Faculty of Science, Chulalongkorn University, Bangkok 10330, Thailand*

² *Program of Petrochemistry and Polymer Science, Faculty of Science, Chulalongkorn University, Bangkok 10330, Thailand*

Corresponding Authors: anawat77@hotmail.com, thanaphong.le@gmail.com

A new series of fluorescent sensors JP (J2P, J3P and J4P) was successfully synthesized via a simple Schiff base reaction by linking a fluorophore using 8-hydroxyjulolidinyl aldehyde **1** with di-(2-picoly)amine (DPA) derivatives **2**. The aldehyde **1** has been prepared by two important steps which are substitution of *m*-Anisidine with 1-bromo-3-chloropropane and Vilsmeier-Haack formylation reaction. On the contrary, substrates **2** were also synthesized by substitution of DPA to the corresponding nitrobenzyl bromide followed by the reduction of nitro group into amine group. All target compounds were characterized by using ¹H NMR, ¹³C NMR, HRMS and UV-Vis spectroscopy. The maximum absorption wavelength (λ_{max}) of J2P, J3P and J4P in methanol were observed at 380, 415 and 420 nm, respectively. Based on the assumption that chelation-enhanced fluorescence (CHEF) may be involved in the sensing mechanism, the enhancement of the fluorescent signal(s) is expected to be investigated by fluorescence spectroscopy. And the sensing properties of JP(s) will be presented in details at the poster session.

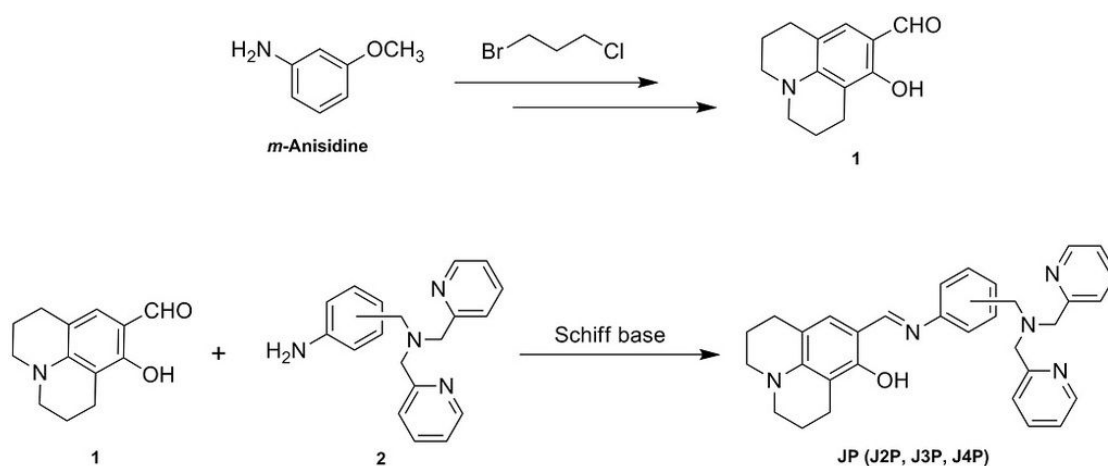


Figure 1: Synthesis of JP.

44

A novel fluorescent turn-on sensor from 8-hydroxyquinoline derivative for mercury detection in aqueous solution

Author: Mongkol Sukwattanasinitt¹

¹ Nanotec-CU Center of Excellence on Food and Agriculture, Department of Chemistry, Faculty of Science, Chulalongkorn University, Bangkok 10330, Thailand

Corresponding Author: smongkol@chula.ac.th

Nowadays, fluorescent chemosensors play an important role in analytical and environmental chemistry especially for detection of toxic metal ions. In this work, three new 8-hydroxyquinoline (8HQ) derivatives **Q1**, **Q2** and **Q3** are synthesized and were used as fluorescence turn-on sensors for metal ions. For **Q1**, 8HQ was O-substituted with acetate ester of diethylene glycol. The O-substitution of 8HQ with diethylene glycol followed by the extension of the pi-conjugation at 5-position with 4-ethynyl N,N-dimethyl aniline moiety gives **Q2** and the acetylation of **Q2** gives **Q3**. In acetonitrile, the absorption spectra of 8HQ and **Q1** were similar showing two absorption maxima around 240 and 300 nm, while those of **Q2** and **Q3** were around 300 and 370 nm. The emission maximum of 8HQ and **Q1** was observed at 400 nm whereas that of **Q2** and **Q3** was red-shifted to 560 nm. In polar aprotic solvent, the fluorescence of **Q2** and **Q3** are visible to naked-eye under black light that becomes invisible in protic solvents such as CH_3OH and H_2O . Therefore, 8HQ and its derivatives are investigated as turn-on fluorescent sensors for metal ions in mixed solvents. In $\text{CH}_3\text{CN}/\text{H}_2\text{O}$ (90/10 v/v), only **Q1** shows selective turn-on fluorescence with trivalent ions such as Al^{3+} , Cr^{3+} and Fe^{3+} , while 8HQ, **Q2** and **Q3** show non-selective and low fluorescence response to metal ions. In $\text{CH}_3\text{OH}/\text{H}_2\text{O}$ (30/70 v/v), 8HQ shows known green fluorescence enhancement with Al^{3+} while **Q3** shows interestingly strong green fluorescence (510 nm) enhancement selectively with Hg^{2+} . The detection limit of Hg^{2+} by **Q3** is 64 nM or 13 ppb. The Tyndall effect observed along with the increase of fluorescence intensity of **Q3** upon the addition of Hg^{2+} suggests that the fluorescence enhancement of **Q3** with Hg^{2+} is due to the aggregation induced emission (AIE). The AIE of **Q3** is also observed without Hg^{2+} at higher fraction of H_2O (80-90%).

45

Absorption spectra and activity of s-tetrazine derivatives on [4+2] Diels-Alder cycloaddition reaction

Author: Patipan Charoenwiangnuea¹

¹ NANOTEC-KU-Center of Excellence on Nanoscale Materials Design for Green Nanotechnology, Kasetsart University, Bangkok 10900, Thailand

Corresponding Author: aa1565@hotmail.com

Derivatives of s-tetrazine (R-T-R') are theoretical studied to examine the effect of the connected groups (R and R') to their absorption spectra and their reactivities on Diels-Alder cycloaddition. In case of absorption spectra, all s-tetrazine derivatives have absorption spectrum about 550nm which cause by $n \rightarrow \pi$ transition in the tetrazine ring. Another absorption peak around 300-450nm can only be observed when electron donating groups OH, NH₂ and phenyl were added to the tetrazine ring which correspond to the $\pi \rightarrow \pi$ transition and their aptitudes follow their strengths of the electron donating groups (except OH-T-H, OH-T-COOH and NH₂-T-COOH). In case of electron withdrawing groups attached to the tetrazine ring, it does not change a peak at 550 nm but cause the red shift and reduce adsorption strength of 300-450 nm region. For reaction activities of s-tetrazine derivatives when reacted with ethylene. The molecular electronic structures state that the reaction follows the inverse electron demand Diels-Alder addition fashion. The activation energies for this reaction increase when an electron donating groups is added but decrease when an electron withdrawing group is attached to the tetrazine ring.

46

A Density Functional Theory Study of Formic Acid Formation from CO₂ Hydrogenation over Au-exchanged MCM-22 Zeolite

Author: Winyoo Sangthong¹

¹ NANOTEC Center for Nanoscale Materials Design for Green Nanotechnology and Center for Advanced Studies in Nanotechnology for Chemical, Food and Agricultural Industries, Kasetsart University, Bangkok 10900, Thailand

Corresponding Author: w.sangthong@gmail.com

One of the important goals in energy and environmental research is to find novel materials to sequester and convert greenhouse gases to useful chemicals. In this study, the well calibrated Density Functional Theory (DFT) is used to study the adsorption of CO₂ and H₂ in order to investigate possible reaction pathways for CO₂ hydrogenation to formic acid over gold supported MCM-22 zeolite catalyst. The adsorption energies of CO₂ and H₂ on Au-MCM-22 catalyst are -15.2 and -30.4 kcal/mol, respectively. From the order of adsorption, two possible reaction mechanisms are proposed. The first mechanism, hydrogen molecule is first adsorbed on gold and zeolite, resulting in gold hydride and Brønsted acid site of zeolite. Formic acid is consecutively formed via the protonation of CO₂ over the Brønsted acid and simultaneous formation of the bond between CO₂ and the hydride group. The activation energy of the rate determining step of this pathway is 39.5 kcal/mol. In the second mechanism, CO₂ is primarily interacted over the active site. The hydrogen is co-adsorbed and reacted with CO₂ to produce intermediate adsorbing on Au. The activation energy of this step is 40.5 kcal/mol. The hydrogen transfer to HCOO intermediate to generate formic acid is proposed in the last step. Due to these comparable pathways at least at high temperature, both the reaction mechanisms could therefore be possible, depending on the order of adsorption. Accordingly, the gold-exchanged MCM-22 zeolite could be potentially used as the catalyst for producing formic acid from CO₂ and hydrogen molecules.

Heron 1 / 47

Theoretical Investigation on the Electroreduction of CO₂ to Methanol on Stepped Cu-based Alloy (211) Surfaces

Author: Pussana Hirunsit¹

¹ National Nanotechnology Center (NANOTEC), National Science and Technology Development Agency (NSTDA), 111 Thailand Science Park, Pathum Thani 12120, Thailand

Corresponding Author: pussana@nanotec.or.th

A systematic investigation of CO₂ electroreduction to CH₃OH on copper-based alloys stepped (211) surfaces was performed using density functional theory calculations associated with the standard hydrogen electrode model. The interaction of the key C_xH_yO_z intermediates is shown to be related to the CO adsorption energy due to the similar charge transfer characteristics of the C–O bond in CO and those intermediates. The overpotential, the limiting-potential elementary step, and selectivity to CH₄, CH₃OH, and HCOOH are determined. The competitive reaction of H₂ evolution is also investigated. The results demonstrate that the CO protonation is the limiting-potential step on most surfaces, with the exception on Cu₃Au and Cu₃Co surfaces. Methanol production is favorable on Cu₃Pd and Cu₃Pt surfaces, yet they show high overpotential (~0.7 V). In spite of the excessive strong CO interaction on some surfaces, the overpotential may be reduced on the surface which is able to decouple the CO adsorption energy and HCO/COH adsorption energy. The key of methanol selectivity is CH₂OH intermediate formation favorability associated with the preference of CH₂OH protonation at the C atom over the O atom. The calculations reveal that the electroreduction activity on Cu-based alloys catalysts do not show a volcano-type relation as was previously found on pure metal catalysts.

48

Reaction mechanism for NO decomposition on oxotitanium porphyrin with NH₃ selective catalytic reduction: A DFT study

Author: Rathawat Daengngern¹

¹ National Nanotechnology Center, NSTDA, 111 Thailand Science Park, Phahonyothin Road, Khlong Nueng, Khlong Luang, Pathum Thani 12120 Thailand

Corresponding Author: rathawat@gmail.com

Nitric oxide (NO), one of the pollutant gases released from exhaust and industrial process, plays a major role in undesired effects such as greenhouse effect. Commercial catalysts for NH₃-selective catalytic reduction (SCR) of NO are extensively used in removal of NO. However, these catalysts may give some drawbacks including toxicity at high temperature range. An alternative catalyst for NH₃-SCR is paid attention on metal-porphyrins for NO conversion to N₂. The reaction mechanism of NO decomposition with NH₃-SCR to environmental friendly products (e.g. N₂, H₂O) of oxotitanium-porphyrin catalyst (TiO-Por) has been systematically investigated by means of density functional theory (DFT) calculations with M06L functional to explore the potential use of this catalyst. In this study, the mechanistic cycle of NO decomposition with NH₃-SCR is proposed in four steps: 1) NO adsorption, 2) oxidation of NH₃, 3) formation of NHNOH via NH₂NO intermediate and 4) NHNOH decomposition. From our calculations, the N–H bond cleavage in the formation of the NHNOH intermediate is the rate determining step with the energy barrier (E_a) of about 32 kcal/mol. The NO decomposition releases N₂ and H₂O as the products, implying that the catalyst has high selectivity toward N₂ with a small desorption energy of about 3 kcal/mol. In addition, the activation energy for NH₃-SCR of NO decomposition is lower than the reduction of NO over the commercial catalysts. The results suggest that TiO-Por is a potential catalyst for NO decomposition with NH₃-SCR.

References

1. P. Maitarad, et al. Environ. Sci. Technol. (2014) 48, 7101.
2. A. Yamamoto, et al. Catal. Sci. Technol. (2015) 5, 556.

3. P. Maitarad, *et al.* Catal. Sci. Technol. (2016) 6, 3878.

49

Mechanisms of AgNPs-mediated antibiotic resistance in bacteria

Author: Chitrada Kaweeteerawat¹

¹ National Nanotechnology Center

Corresponding Author: namjajaja@gmail.com

Silver nanoparticles (AgNPs) are an important class of nanomaterials, largely due to their outstanding antibacterial properties. However, little is known about their toxicity and environmental impacts. In this study, we report that AgNPs lead to growth inhibition and oxidative stress in gram negative bacteria; *Escherichia coli* and gram positive bacteria; *Staphylococcus aureus*. Interestingly, bacteria pre-exposed to AgNPs exhibit increased minimal inhibitory concentration (MIC) and minimal biocidal concentration (MBC) when treated with diverse antibiotics (ampicillin, penicillin, chloramphenicol and kanamycin). The bacterial resistance to antibiotics is accompanied with less permeable membranes, lower levels of oxidative stress, decreased membrane potential and elevated levels of intracellular ATP found in AgNP-treated bacteria compared to their untreated counterparts. These results underscore a potential consequence of the inadvertent exposure of AgNPs to bacteria in the environment, and highlight the need to regulate the disposal and use of silver nanoparticles in consumer products and industry.

Falcon 1 / 50

Investigation on the effect of nanoparticles to ammonium salt based gel electrolytes

Author: Chuleekorn Chotsuwan¹

¹ National Nanotechnology Centre, NSTDA, Thailand

Corresponding Author: chuleekorn@nanotec.or.th

Gel electrolytes (GEs) are used in electrochemical devices replacing liquid electrolytes in order to avoid the evaporation of solvent and to increase the stability of devices. Many additives such as polymers, carbon fillers, and inorganic fillers have been used as a matrix in gel electrolytes to increase the viscosity and the ionic conductivity of gel electrolytes. In this work, silica nanoparticles were added to tetraalkyl ammonium based liquid electrolyte with propylene carbonate as a solvent to prepare GE. We selected N(Bu)₄PF₆ as a supporting solid electrolyte due to its stability at high temperature and under atmosphere as comparison to traditional lithium based electrolyte salt. Silica nanoparticles has been selected as a matrix due to its low cost and solidified properties in electrolytes. The conductivity measurements of GEs with varying nanoparticle contents were performed to determine the effectiveness of ion transport in the GE matrix. The conductivity of gel electrolyte was in a range of 1.0-6.0 mS/cm at room temperature. An operative potential window of the GE in contact with a Pt electrode were determined by cyclic voltammetry was -2.5 - +2.5 V vs. Ag(s). We also evaluated the diffusion coefficient of ferrocenium ions in prepared gel electrolyte to determine the effectiveness of gel electrolyte as a comparison to liquid electrolyte. The cyclic voltammograms of both gel and liquid electrolyte showed that the nanoparticles increased the viscosity of liquid electrolyte while maintained the effectiveness of ferrocenium ions transport in the prepared electrolytes. These novel gel electrolytes are a good candidate for electrochemical based gel electrolytes.

Protective effect of silk extracts on drug-induced phototoxicity

Co-author: Waleewan Eaknai¹

¹ *National Nanotechnology Center, National Science and Technology Development Agency*

Corresponding Author: waleewan@nanotec.or.th

Silk extracts, considered as a waste material in the textile industry, is mainly composed of sericin protein. Sericin has recently been shown various bioactivities and therefore has the high potential uses for skin anti-aging, skin moisturizer and wound healing¹. To value added to the extracts of Thai silks, our colleagues have recently developed the purifying process² and applied the purified silk extracts in nano-cosmeceutical products and nano-delivery system. In the present study, we further evaluated the usefulness of silk extracts by focusing on the protective effect of silk extracts on drug-induced phototoxicity. Chlorpromazine (CPZ), common used antipsychotic drug, was selected as a representative drug causing drug-induced phototoxicity. The skin epidermal cell, A431 cell line, was used as in vitro skin model of this study. Our results demonstrated that UVA treatment decreased the viability of A431 cells in UVA dose-dependent manner and treatment with CPZ following with UVA exposure dramatically decreased cell viability as shown by significant increasing of IC₅₀ value, suggesting the CPZ-induced phototoxicity in A431 cells. These results were consistent with previous report showing that CPZ could be activated by UV irradiation to generate the free radicals and led to phototoxicity and photo-allergic reaction³. Interestingly, our results showed that pre- and post-treatment with silk extracts at concentration of 25 µg/mL attenuated cell viability after treatment with CPZ and UVA when compared to the cells non-treated with silk extracts. Furthermore, pre- and post-treatment with silk extracts and CPZ treatment following with UVA exposure improved the level of intracellular glutathione comparing to the cells non-treated with silk extracts. The underlying mechanism related to the protective effect of silk extracts on CPZ-induced phototoxicity will also be discussed in this study. In conclusion, our results indicated that silk extracts can attenuate the skin damage causing by drug-induced phototoxicity. These findings support the usefulness of silk extracts in novel applications especially in the protection of drug-induced phototoxicity simultaneously with using nanotechnology to improve their efficacy.

Falcon 1 / 52

One-Dimensional Carbon Nanomaterials and Their Application for Oxygen Reduction Reaction

Author: Malinee Niamlaem¹

Co-author: Winyoo Sangthong²

¹ *Department of Chemistry, Faculty of Science, NANOTEC Center for Nanoscale Materials Design for Green Nanotechnology, and Center for Advanced Studies in Nanotechnology and its Applications in Chemical, Food and Agricultural Industries, Kasetsart University, Bangkok 10900, Thailand*

² *NANOTEC Center for Nanoscale Materials Design for Green Nanotechnology and Center for Advanced Studies in Nanotechnology and its Applications in Chemical, Food and Agricultural Industries, Kasetsart University, Bangkok 10900, Thailand*

Corresponding Authors: w.sangthong@gmail.com, malinee.niaml@gmail.com

We report here the production of one-dimensional carbon nanomaterials (1D-CNMs) including carbon nanotubes (CNTs) and carbon nanofibers (CNFs) via the use of the oxidative dehydrogenation (C₂H₂-CO₂) and the acetylene (C₂H₂) decomposition using a catalytic chemical vapor deposition (CCVD) method. Ni was selected as the catalyst for the synthesis due to its ability to produce different types of 1D-CNMs (CNFs and CNTs) by simple variation of the synthesis temperature. The successful synthesis was obtained via the currently used technique. CNFs were obtained at a relatively low temperature (400°C) via both reactions whereas at relatively higher temperatures

(>500°C), CNTs were obtained. The electrocatalytic activity of the obtained products was investigated for oxygen reduction reaction (ORR), which is one of key reactions for the development of many technological devices including oxygen sensors, fuel cells and batteries. It was found that the carbon products exhibit good electrocatalytic activity (with the current density ranging from 1.22-5.04 mA/cm²), although they have not been incorporated with any metal catalyst and modified with any additional treatment. In addition, the products with different characteristics exhibit different catalytic behaviors. The insight obtained in this work is important for the development of non-metal electrocatalysts for ORR.

Heron 1 / 53

Salicylideneaniline-Functionalized Poly(*m*-phenyleneethynylene)s as Fluorescent Turn-On Chemosensors for Cations

Author: Nopparat Thavornsin¹

Co-author: Mongkol Sukwattanasinitt²

¹ Department of Chemistry, Faculty of Science, Chulalongkorn University, Bangkok 10330, Thailand.

² Nanotec-CU Center of Excellence on Food and Agriculture, Department of Chemistry, Faculty of Science, Chulalongkorn University, Bangkok 10330, Thailand.

Corresponding Authors: smongkol@chula.ac.th, nok_mawaw@hotmail.com

Two different series of conjugated polymer, poly(*m*-phenyleneethynylenes) (*m*-PPEs) containing different amounts of salicylideneaniline moieties (50% and 100%) have been synthesized via a post-functionalization of aniline group on *m*-PPEs backbone. PPEs are successfully prepared in excellent yield (90-99%) and spectroscopically characterized the structure by ¹H, ¹³C NMR and FTIR exhibited signals that reasonably correlate with the desired polymer. The resulting polymers displayed weak orange emission at 560 nm and undergo remarkable turn-on bright blue fluorescent emission at 450 nm response to Fe²⁺, Fe³⁺, Al³⁺ and Cr³⁺ without any change with other cations.

Falcon 1 / 54

Zinc stannate nanoparticles synthesized at room temperature: Effect of annealing on size, morphology and photocatalytic activity

Author: Muhammad Najam Khan¹

¹ Baluchistan University of Information Technology, Engineering and Management Sciences (BUITEMS), Quetta Pakistan

Corresponding Author: najammalghani@gmail.com

Abstract

Photocatalytic activity of Zinc stannate (Zn₂SnO₄) ZTO described in our previous work [1, 2] depict that ZTO nanoparticles have comparable photocatalytic activity to other photocatalyst such as Zinc Oxide (ZnO) nanoparticles and Titanium dioxide (TiO₂) nanoparticles. The aim of this work is to explore the effect of annealing i.e. high temperature behavior on size, morphology and photocatalytic activity of room temperature synthesized nanoparticles.

It has been reported that annealing at high temperature results in alterations in surface states of semiconductor [3, 4]. These surface alterations can impact the dye adsorption on surface of catalyst. Room temperature synthesized samples were annealed to study the annealing effect at different temperatures on the photocatalytic efficiency of ZTO. Annealing was carried out at two different

temperatures i.e. at 250°C and 400°C.

Scanning electron micrograph (SEM) of annealed particles was carried out in order to observe morphological changes before and after annealing at two different temperatures. SEM micrographs obtained for above samples revealed that annealed samples did not result in any morphological changes in the length or diameter of ZTO nanoparticles.

Optical absorption spectra of Methylene Blue (MB) adsorption on surface of ZTO nanoparticles annealed at 250°C and 400°C for period of one hour was calculated which perceived that the amount of MB adsorbed is higher for the ZTO samples without annealing as compared to samples annealed at different temperatures i.e. at 250 °C and at 400 °C.

UV/Vis optical absorption spectra of annealed ZTO samples was used to study the effect of annealing on native defects. It was observed that the absorption peak is at about 270 nm in all the cases i.e. annealed and without annealed samples which illustrate that the ZTO nanoparticles preserve uniform size after annealing at different temperatures.

Photocatalytic activity of annealed samples and without annealing was observed for the degradation of methylene blue and corresponding reaction rate constant *k* values were calculated.

From reaction rate constant *k* values it is evident that annealing didn't result in improvement of photocatalytic activity as samples without annealing showed higher photocatalytic activity than sample annealed at 400°C.

This can be attributed to removal of surface defects due to annealing and subsequent reduction in photocatalytic activity.

References:

1. Najam Khan, M., et al., Visible light photocatalysis of mixed phase zinc stannate/zinc oxide nanostructures precipitated at room temperature in aqueous media. *Ceramics International*, 40(6):8743–8752.
2. Baruah, S., Dutta Zinc stannate nanostructures: Hydrothermal growth. *Science and Technology of Advanced Materials*, 2011. 12(1): p. 013004.
3. Sun, R.-D., et al., Photoinduced Surface Wettability Conversion of ZnO and TiO₂ Thin Films. *The Journal of Physical Chemistry B*, 2001. 105(10): p. 1984-1990.
4. Chung, J., J. Lee, and S. Lim, Annealing effects of ZnO nanorods on dye-sensitized solar cell efficiency. *Physica B: Condensed Matter*, 2010. 405(11): p. 2593-2598.

55

Synthesis of novel benzyldipicolylamine linked 1,8-naphthalimide derivatives as new fluorescent chemosensors

Author: Anawat Ajavakom¹

Co-author: Paitoon Rashatasakhon¹

¹ *Organic Synthesis Research Unit, Department of Chemistry, Faculty of Science, Chulalongkorn University, Bangkok, 10330, Thailand*

Corresponding Authors: anawat77@hotmail.com, paitoon.r@chula.ac.th

Water soluble fluorescent chemosensors are of interest for the metal ion detection in aqueous media such as industrial wastewater. This research involves the synthetic preparation of the series of 1,8-naphthalimide derivatives linked with *ortho*, *meta*, or *para* amino benzyldipicolylamine (N2D, N3D, and N4D). These target molecules of this research were designed to possess naphthalimide moiety as fluorophore and benzyldipicolylamine as a receptor and water soluble moiety. Firstly, benzyldipicolylamine can be easily obtained from the substitution of nitrobenzylbromide by dipicolylamine at room temperature. Then, the nitro group on benzyl ring was reduced by Pd/C under hydrogen gas in ethanol followed by the amidation with 1,8-naphthalic anhydride to gain the corresponding N2D, N3D, and in and N4D in 31%, 19%, and 30% yield, respectively. In order to add more binding site into the fluorescent sensor, 4-hydroxy-meta amine was used to produce another chemosensor

4HN3D, in 13% yield. According to the results of photophysical property investigation in milliQ water, these sensors exhibited the absorption maximum around at 345 nm. Also these compounds revealed the similar emission peak at around 400 nm. The sensing properties of target compounds will be investigated and the detailed results will be presented at the poster session.

56

Nanoencapsulation of tetrahydrocurcumin in CTS by rapid expansion of subcritical solutions coupled with ionic gelation

Author: Amporn Sane¹

¹ (1) Department of Packaging and Materials Technology, Faculty of Agro-Industry, Kasetsart University, Bangkok 10900, Thailand. (2) NANOTEC Center for Nanoscale Materials Design for Green Nanotechnology, Kasetsart University, Bangkok 10900, Thailand. (3) Center for Advanced Studies in Nanotechnology for Chemical, Food, and Agricultural Industries, Kasetsart University, Bangkok 10900, Thailand

Corresponding Author: amporn.sane.ku@gmail.com

Fabrication of tetrahydrocurcumin (THC) nanoparticles encapsulated in chitosan (CTS) was achieved by a two-step method. THC nanoparticles were produced by rapid expansion of subcritical solutions of THC in a mixture of carbon dioxide and ethanol (1:1, w/w) with pre-expansion temperature and pressure of 80 °C and 276 bar, respectively. The aim of this study was to investigate the encapsulation conditions, i.e. CTS concentration, volume of CTS solution, and sodium tripolyphosphate (TPP) concentration, on the size of encapsulated THC nanoparticles and loading capacity of THC. After coating with CTS crosslinked with TPP, the size range of THC nanoparticles increased from 10-120 nm to 15-140 nm, with more than 85% smaller than 100 nm. The obtained encapsulated THC nanoparticles exhibited a spherical shape with average sizes of 45-56 nm and THC loading capacity of 34-47%. Increasing TPP and CTS concentrations and CTS solution volume in encapsulation resulted in larger encapsulated nanoparticles with lower THC loading capacity. The antioxidant activity of encapsulated THC nanoparticles increased with THC loading capacity, and encapsulation of THC in crosslinked CTS prolonged the release and antioxidant activity of THC. Finally, our results indicate that a combination of rapid expansion of subcritical solutions and ionic gelation could be an alternative to produce uniform-sized nanocapsules containing relatively large content of active substances.

Falcon 1 / 57

Enhanced piezoelectric properties and fatigue-free behavior of lead-free piezoelectric xBaZrO₃-(0.85-x)BaTiO₃-0.15CaTiO₃ ceramics

Author: Rangson Muanghlua¹

¹ Faculty of Engineering, King Mongkut's Institute of Technology Ladkrabang

Corresponding Author: nopsiri.c@gmail.com

Lead-free xBaZrO₃-(0.85-x)BaTiO₃-0.15CaTiO₃; x = 0.00-0.20 (xBZ) ceramics were successfully prepared using the conventional solid-state reaction method. X-ray diffraction data showed a pure-phase perovskite structure for compositions up to x < 0.200. At room temperature, x-ray diffraction patterns of ceramics with the composition range of 0.00 ≤ x < 0.10 possess tetragonal structure. Mixed-phase coexistence of tetragonal and rhombohedral phases were found at 0.10 ≤ x ≤ 0.15 and transformed to cubic for x > 0.125 according to the lowered Curie temperature. Raman scattering showed mixed phases of tetragonal and orthorhombic phases. Temperature-dependent dielectric data shows anomaly phase transitions determined by composition changes. Phase diagram was provided according to temperature-dependent dielectric data. Compositions near composition-induced

phase transition provided enhanced ferroelectric and piezoelectric properties. Unipolar electric field induced strain of $x = 0.125$ ceramic shows surprisingly high longitudinal piezoelectric coefficient (d_{33}^*) of 2244 pm/V at relatively low electric field of 5 kV/cm. Fatigue measurement carried out on the morphotropic phase boundary composition showed a small degradation in maximum strain after 106 cycles using an applied field of 20 kV/cm at 10 Hz.

58

Fabrication of silver nano-protrusion based on silver sulfide solid electrolyte for surface-enhanced Raman spectroscopy

Co-author: Chaweewan Sapcharoenkun¹

¹ *National Nanotechnology Center (NANOTEC)*

Corresponding Author: chaweewan@nanotec.or.th

Silver (Ag) nanostructure surfaces are extensively used as substrates for surface-enhanced Raman spectroscopy (SERS) due to their characteristic surface plasmon resonance (SPR) throughout the visible, near-infrared, and infrared region. However, recent development for Ag-SERS substrates suffer from poor reproducibility, low performance, low stability and poor uniformity of SERS enhancement. Herein, a simple, low-cost and high-throughput synthesis method to construct the high-performance Ag nano-protrusion (NP) SERS substrate in a controllable manner has been developed. The SERS substrate derived from Ag nano-protrusions (NPs) is based on silver sulfide (Ag₂S) solid electrolytes which was synthesized via a wet chemical process. Ag NPs were fabricated by electron beam irradiation method. The highest density of Ag NPs as SERS substrate was found to be 2.2×10^8 rods/cm². The SERS effect of methylene blue (MB) adsorbed on Ag/Ag₂S substrate has been investigated and a maximum enhancement factor (EF) of 1.9×10^3 was achieved. This enhancement factor is 3-fold higher in magnitude than that of Ag film substrate without Ag NPs.

Falcon 1 / 59

Effect of Al Concentration on Al-doped ZnO Thin Films deposited by Magnetron Co-Sputtering Technique

Author: Kittipong Tantisantisom¹

¹ *NANOTEC*

Corresponding Author: kittipongnanotec@gmail.com

Al-doped ZnO (AZO) thin films were deposited on glass and silicon substrates by magnetron co-sputtering of two targets, a ZnO ceramic target and an Al metallic target. During the samples fabrication, ZnO was prepared by RF magnetron sputtering while Al pulses were added by DC magnetron sputtering with various shutter opening conditions. During the ZnO sputtering, the Al shutter was opened periodically with a fix duration time of 3 seconds. The amount of Al in the thin film was modulated by varying the number of Al pulses. In order to achieve the same film thickness for all samples, the total deposition time was then fixed. The properties of the AZO thin films were characterized by several techniques. From UV-Vis spectroscopy, all samples show more than 85% transmission in the visible range but reveal absorptions in the ultraviolet region, corresponding to the energy gap of ZnO. The results suggest an increase in the energy gap with higher Al concentration in the ZnO films. In addition, electrical properties of thin films were characterized by the Hall measurement. The film resistivity changes with Al pulsing. With increasing number of Al pulses, the film resistivity reduces and reaches the minimum at 105 pulses before bouncing up. The Al atomic concentrations in the films were also investigated by Auger electron spectroscopy. It was found that the Al atomic concentration at the minimum resistivity corresponds to 5.6%. Corresponding to the

XRD results, they express the highest peak intensity of the 002 plane at the same Al pulsing condition. Such agreement of both techniques suggests a relationship between the electrical resistivity and the film crystallinity and grain size. Furthermore, the results suggest that the Al doping and oxide formation might be occurred at every pulsing condition. At Al pulsing below 105 times, the Al doping is more effective, however for Al pulsing above 105 times, the amount of Al in this region could be over the solubility limit of Al in ZnO. The aluminum oxide cluster which is the electrical insulator might form and take the dominant role for blocking the charge transport in thin film. The formation of insulating cluster might be confirmed by the slightly shifting of signal peaks from the X-ray photoelectron spectroscopy technique. This study could lead to the growth mechanism realization of transparent conductive oxide thin film to obtain the desired properties for optoelectronic devices application.

Heron 1 / 60

DIAMONDROID COUNTER ELECTRODES FOR DYE-SENSITIZED SOLAR CELLS

Author: Sumeth Siriroj^{None}

Corresponding Author: sumeth.siriroj@gmail.com

Dye-sensitized solar cells (DSSCs) are a leading contender for low-cost solar energy generation. The highest efficiency of DSSC is from platinum(Pt) counter electrode (14.1%), however platinum is very expensive and there are other materials that can use as counter electrode such as conductive polymer, carbon nanotube and other carbon form. In this work we use diamondoids (nano powder of diamond) which exhibit negative electron affinity property, enabling the better transfer of electrons back to DSSC. We prepared counter electrodes by using diamondoids with –thiol function and applying the self-assembly monolayer technique on gold and platinum substrate. We fabricated working electrodes by using TiO₂ coated on FTO glass and immersing it in N719 dye. For electrolyte we used iodine electrolyte as media collector. The efficiency of the DSSC with adamantane (smallest molecule of diamondoids) film is close to one with the reference cell Pt film. The large enhancement comes from the DSSCs with tetramantane films which give efficiency as high as 10.95%, comparing to the reference Pt cell with efficiency of 8.55%; this increase is approximately 25%. However, we still have some problem with this technique. Iodine electrolyte destroys the gold substrates and shortens the cell lifetime greatly. Then we try to deposit diamondoids films on platinum substrate and found that diamondoids can enhance efficiency of platinum slightly with very high stability as platinum. Irrespective of the exact microscopic mechanism driving this, our results already reveal exciting, but hitherto unappreciated, possibilities for the use of diamondoids in dye-sensitized solar cells. We expect our findings to be of relevance to perovskite-based solar cells. More generally, our approach offers an attractive and low-cost route to exploit diamondoids in a range of applications in other catalytic processes.

Heron 2 / 61

Cassava root materials composited with PEDOT:PSS used as low cost counter electrodes in dye-sensitized solar cells

Author: Seksan Lowpa¹

Co-authors: Sumeth Siriroj¹; Worawat Meevasana²

¹ School of Physics, Suranaree University of Technology, Nakhon Ratchasima 30000, Thailand

² School of Physics, Suranaree University of Technology

Corresponding Authors: sumeth.siriroj@gmail.com, seksa96@hotmail.com, worawat@gmail.com

A composite film of Cassava root and Poly (3,4-ethylenedioxy thiophene):polystyrene sulfonate (C/PEDOT:PSS) was prepared as a high electrocatalytic material for the counter electrode (CE) of

a dye-sensitized solar cell (DSSC). The effect of sintered of Cassava root under Ar atmosphere at 1000 °C was intended for increasing the conductivity, and the PEDOT:PSS was used for a strong adhesion of the composite film to the FTO-Glass substrate. The DSSC with the C/PEDOT:PSS composite CE exhibited a high energy conversion efficiency (η) of 9.54% under full sunlight illumination condition of 100 mW/cm², comparable to that of the DSSC based on the Pt electrode (10.03%). The composite catalytic film of C/PEDOT:PSS is a low-cost alternative for replacing the conventional and expensive Pt film.

Hornbill 1 / 62

Effect of cylindrical length and regression model of Euler number of hydrocyclone

Author: Pakpoom Supachart¹

¹ *King Mongkut's University of Technology Thonburi*

Corresponding Author: pakpooms243@gmail.com

This research was focused in two parts, experimental results and regression model. First, the research was studied on the proportion of cylindrical length that affected to the separation efficiency using a 40 mm hydrocyclone. The effects of cylindrical lengths of 60, 80 and 100 mm were investigated. The tested suspension was the mixed of silica and water. The silica particles have an average size of 9-10 micrometer at the solid concentration of 0.5% w/v. The feed flow rate of 1 m³/hr was operated with the flow ratio of 0.1. From experimental result, it was found that the shorter cylindrical length, the higher separation efficiency. At the condition of the cylindrical length of 60 mm, the vortex finder length of 40 mm and the conical length of 200 mm revealed the best separation efficiency up to 84.06 percent. Second, regression model of Euler number of hydrocyclone was presented. In this work, data obtained from the experiments in the first part and data of earlier researches totally of 75 were used to make the relationship between the proportion of hydrocyclone and Euler number. By the multiple linear regression method, it was found that the constants, was 3,439 and the regression coefficient of n_2 , n_3 , n_4 and n_5 were 0.380, 0.486, 0.222 and 0.039, respectively.

Keywords: Cylindrical length, Regression model, Euler number, Hydrocyclone

63

Silver nanoparticles induce cardiovascular toxicity in human endothelial cells and zebrafish embryos

Author: Wittaya Pimtong¹

¹ *Nano Safety and Risk Assessment Laboratory, National Nanotechnology Center*

Corresponding Author: wittaya.pimtong@gmail.com

Silver nanoparticles (AgNPs) have distinctive physicochemical properties that make them attractive in a variety of applications. These uses are rapidly expanding. Thus, the exposure of human and other organisms, especially aquatic organisms, to AgNPs is obviously increased. In order to gain new insights into the toxicity of silver nanoparticles, the study of cardiovascular effects was investigated in vitro and in vivo. In vivo study, we found that AgNPs caused mortality, and malformations in zebrafish embryos. These malformations included pericardial edema, yolk sac edema, sluggish circulation, bent tail, and heart and head malformations. The investigation of AgNP exposure to human umbilical vein endothelial cells (HUVECs) showed that AgNPs induce some level of cell cytotoxicity, however, after alkaline phosphatase staining, we found no defect on sub-intestinal vessels (SIVs) in AgNP-exposed embryos. In addition, we also revealed a novel defect of AgNPs on erythropoiesis in zebrafish embryos.

64

Synthesis of poly(*p*-Phenylene ethynylene)s using Palladium Supported on Calcium Carbonate as Heterogeneous Catalyst

Author: Ryo Sakthanasait¹

¹ *Department of chemistry, Faculty of science, Chulalongkorn University*

Corresponding Author: mrryo37@gmail.com

Our research focuses on the development of the synthesis of poly(*p*-phenylene ethynylene)s, PPEs via the Sonogashira coupling reaction using palladium supported on calcium carbonate as heterogeneous catalyst. We screened different palladium catalysts, bases and solvent to determine the optimal condition. The optimized study reveals that the use of Pd/CaCO₃ in diisopropylamine as a base in dimethylformamide as a solvent at 80 °C give the PPE in good yield after precipitation with methanol. The Gel Permeation Chromatography (GPC) data indicates that an average molecular weight (Mw) is 24,185 while degree of polymerization (DP) and polydispersity index (PDI) are 53 and 2.7, respectively. Inductively coupled plasma optical emission spectrometer (ICP-OES) measurement reveals that leaching of palladium into PPEs are only 0.3% w/w. When compare these data with the conventional homogeneous catalyst, PdCl₂ (PPh₃)₂, it indicates that our PPEs show better properties in term of DP, PDI and contamination of palladium. This finding provides the new method to prepare the high purity PPE for the optoelectronic material.

Heron 1 / 65

Fabrication of Perovskite Solar Cell via Rapid Convective Deposition Technique

Author: Natpapon Saranrom¹

¹ *Mahidol University*

Corresponding Author: top.saranrom@gmail.com

Here, we introduce a new technique, called rapid convective deposition, to fabricate planar perovskite solar cells. This technique uses a reclining blade to draw a liquid droplet across a substrate thus advancing thin film can be deposited on a substrate. Thickness and morphology of the thin film can be controlled by deposition speed and blade angle as well as liquid volume and concentration. Unlike the conventional spin coating, the convective deposition consumes much less material in fabrication process. Recently, we have demonstrated high efficiency and low cost fabrication of perovskite solar cell with ITO/PEDOT:PSS/Perovskite/PCBM/TiO_x/Al structure. Except the ITO and Al metal electrode, all the solid films were deposited layer by layer via the convective deposition. In addition, the low temperature treatment less than 120 oC were conducted in this experiment. Recently, more than 10% solar cell efficiency has been achieved. Furthermore, this rapid and scalable deposition technique has been used in fabrication of electrochromic windows, polymer/hybrid solar cell and anti-reflective glass.

66

Fabrication of Gold Disc Arrays on ITO glass: an Inverted Pattern Generated from Plasma Etching of Nanosphere Lithographic Mask

Author: Aroonsri Ngamaroonchote^{None}

Corresponding Author: katinnoi23@gmail.com

We report a method to fabricate gold disc array pattern on indium tin oxide (ITO) glass by incorporation of nanosphere lithography and plasma etching technique. In the process, hexagonal close-packed polystyrene (PS) spheres were served as mask for blocking an interaction of oxygen plasma and indium tin oxide surface. Topographic images and C-AFM current mappings demonstrated different thicknesses and conductivities of plasma etched ITO surface, particularly in gap area between PS spheres and area under PS spheres. We found that exposed ITO surface exhibit significantly higher resistivity compare with the area protected by PS spheres. As a result, site-selective electrodeposition of gold was produced on patterned ITO glass. The microdiscs diameter and distance between microdiscs can be controlled by plasma etching condition. The gold disc diameter decreased linearly with an increase of plasma etching time in range of 1-8 min and no change was observed with longer etching time up to 20 min. The formation of this structure also depends on plasma etching power. Size and density of gold particles increased with electrodeposition charge. Finally, this novel fabrication suggests a simple and low-cost technique for design and development of specific structure of metal disc array towards electrochemical and optical sensing applications.

Hornbill 1 / 67

Penetration of Fluorescent Nanoparticles into the Cornea

Author: Sangly P Srinivas¹

¹ *Indiana University*

Corresponding Author: srinivas@indiana.edu

Nanoparticles-based drug/gene delivery have been reported for potential therapeutic management of various ocular surface and corneal disorders [Kompella UB, et al., *Nanomedicines for back of the eye drug delivery, gene delivery, and imaging*. *Prog Retin Eye Res.* 2013;36:172-98]. In this study, we have examined penetration of mono-dispersed silica nanoparticles stained with Rhodamine B (RhB) and FITC at the microscopic level. Specifically, we have employed a custom-built confocal scanning microfluorometer (CSMF).

Our custom-built CSMF is designed for recording depth-resolved fluorescence across the cornea repeatedly over long periods (several hours) [Srinivas SP, Maurice DM., *A microfluorometer for measuring diffusion of fluorophores across the cornea*. *IEEE Trans Biomed Eng.* 1992 Dec;39(12):1283-91]. Depth resolution of the CSMF is ~ 7 µm using a 40x water immersion objective of 1.2 mm working distance; Zeiss) at 2.66 µM of fluorescein. Excitation, obtained from blue/green LEDs, is < 2 µW at the focal plane. This limits the potential for photobleaching. Scanning speed > 40 µm/sec. Simultaneous trans-corneal fluorescence and scatter can be accomplished.

Mono-dispersed silica of 6 nm (Sigma Inc; Cat # S5130) were stained with RhB (Sigma Inc; Cat #83690) by overnight exposure of the nanoparticles to 0.1 mg/mL of the dye. The particles were washed in PBS 2-3x and then used next day. Excitation from a blue LED was filtered through an interference filter (470 + 10 nm). RhB fluorescence (> 530 nm) and scattered light collected through the exit slit, which is held parfocal to excitation slit, were detected by the PMTs (Fig. 1). Experiments were performed with excised porcine eye. As a lipophilic dye, RhB partitions into epithelium and accumulates over time and eventually diffuses into stroma as observed. We found significant uptake of the nanoparticles into the epithelium. But lack of significant fluorescence at anterior stroma following FITC-stained nanoparticles (Fig. 3C) indicates that although the nanoparticles are taken up by the epithelium, not much is released into the stroma. When RhB-Si or FITC stained chitosan-dextran sulphate (CDNs; 400 nm) nanosuspension were administered on bare stroma, the particles penetrated significantly.

Our data is insufficient to explain the penetration of the Si nanoparticles across the cornea with and without epithelium. The collagen fibrils in the stroma, which lie in the lamellae and are parallel to the surface of the tissue, can be expected to offer steric hindrance to the movement of the particles in conjunction with the charged glycosaminoglycans surrounding each fibril. Moreover, we recall that the fibrils in a given lamella are parallel to one another with each lamella oriented at a finite angle with respect to the neighboring lamellae. How this intricate ultrastructure permits movement of nanoparticles (6-50 nm), with and without an inwardly-directed water movement, remains to be explored.

69

3.5D printed soft actuator for novel robotic application

Author: preedee pinpradup¹

¹ Nanotec

Corresponding Author: preedee@nanotec.or.th

Recently, robotic technology can take place of humans in hazardous environments or manufacturing processes. However, conventional design is not suitable for home use because of rigidity, hardness, and electrical part. In comparison with such conventional robotics, soft robotics are non-rigid robots built from soft deformable materials. They can offer a new and safety approach for home use. To develop the soft robotics, soft actuator is an important part for the robotic movement. Generally, fabrication method of the soft actuator part is by plastic casting. However, the method is time consuming and complicated. 3D printing, in contrast, is another novel technique developed especially for building high complexity parts. Therefore, in this work, we designed an actuator and studied the formation of the actuator using the 3D printing technique (material jetting). Structure pattern, number of bulb, and active pressure in the actuator were varied to optimize the actuator performance. The printed materials were also characterized by optical microscope, scanning electron microscope, and dynamic mechanical analysis. Such active moving function of the 3D structure could be defined as the extra dimension of such actuator.

70

Mercury oxidation reaction mechanisms on halogenated activated carbon: a density functional theory study

Author: chompoonut rungnim^{None}

Corresponding Author: chompoon.r@gmail.com

The complete reaction mechanisms of elementary mercury (Hg) adsorption and oxidation on halogenated activated carbon (AC) models have been demonstrated for the first time using density functional theory (DFT) calculations. Two different halogenated AC models, namely X-AC and X-AC-X (X=Cl, Br, I), were used to compare the effect of degrees of halogenation on the reaction reactivity. The mechanism consists of (i) Hg adsorption, (ii) HgX formation, and (iii) HgX₂ formation. The calculated potential energy surfaces reveal that Hg can be found both in the forms of Hg physisorption and mercury halide (HgX) chemisorption on the AC edge. Through the Hg physisorption energies are independent to the halide types of the halogenated AC, the activation energies required for the HgX formations increase as the order of HgI < HgBr < HgCl. The HgX is found to be stable state on the AC edge and its further desorption from the AC as HgX form or further oxidation to mercury-dihalides (HgX₂) are energetically unfavorable. The trend of the calculated barriers for HgX formations are corresponded with the experimental observation. Therefore, the HgX formation is predicted as a crucial step in Hg oxidation of halogenated AC and in addition the halide concentration increases the reactivity of halogenated AC.

71

Sol-gel Synthesis of Nanoparticulate Titanium Dioxide: Effects of Initial Reagents

Author: Oratai Jongprateep¹

¹ Materials Innovation Center, Faculty of Engineering, Kasetsart University 50 Ngamwongwan Rd, Ladyao, Chatuchak Bangkok 10900, Thailand

Corresponding Author: oratai.j@ku.ac.th

Synthesis of pure anatase TiO₂ with particle sizes smaller than 100 nanometers has been one of the focuses in the area of photocatalysts. In order to achieve the desired chemical composition and particle size, appropriate initial reagents are required. This study aimed at examining effects of sol-gel initial reagents, specifically titanium (IV) isopropoxide (TTIP), sub-micrometer- sized titanium dioxide dissolved in sulfuric acid, and titanium dioxide dissolved in sulfuric acid with addition of polyacrylic acid, on chemical compositions and particle sizes of TiO₂ powders. Experimental results indicated that preparation of nano-particulate titanium dioxide, with the average size ranging from 48 to 85 nanometers, could be achieved when using TTIP and sub-micrometer- sized titanium dioxide dissolved in sulfuric acid with addition of polyacrylic acid as initial reagents. The results also revealed that the finest average particle size was attained in the powder prepared from TTIP. For the powder prepared from sub-micrometer- sized titanium dioxide dissolved in sulfuric acid without addition of polyacrylic acid, larger particle sizes with an average of 130 nanometers were present. In addition, formation of a secondary phase, identified as titanium oxide sulfate, was observed. Chemical compositions as well as particle sizes were discussed with respect to structures of the initial reagents and polymerization reactions potentially occurred during the sol-gel process. Antibacterial activity of the powder prepared from sub-micrometer-size titanium dioxide dissolved in sulfuric acid with addition of polyacrylic acid was evaluated. Reduction of *Staphylococcus aureus* by more than 99.9% was observed.

Heron 2 / 72

Water disinfection using silver nanoparticles impregnated coffee grounds: *Escherichia coli* and *Staphylococcus aureus* killing in batch-mode

Author: CHONLADA POKHUM¹

¹ *National Nanotechnology Center*

Corresponding Author: chonlada@nanotec.or.th

Silver nanoparticles (Ag-NPs) were impregnated on the surface of coffee grounds (CF) (referred to as Ag-CF hybrid, having 0.44 and 0.80 % weight of Ag), for achieving water disinfection in a batch set-up. First, Ag-CF was synthesized by coating with nature-inspired nanoparticles that containing Ag-NPs on their surface. Subsequently, *Escherichia coli* and *Staphylococcus aureus* cells-killing experiments were performed in a 1000 ml flask with Ag-CF hybrid (batch-mode) for 15 min. Experiment with *E. coli* using 50 mg Ag-CF hybrid having 0.80% weight of Ag per 1 ml cell suspension showed that, 10⁶ CFU/ml of cells was completely disinfected within 15 min contact time. The visible colony was zero. For *S. aureus*, water having 10⁶ CFU/ml *S. aureus* could not be completely killed in all treatments. A maximum inactivation of *S. aureus* was 98.75% for 50 mg Ag-CF hybrid having 0.80 % weight of Ag per 1 ml cell suspension at 15 min. Moreover, the pH and Ag concentration in the water after adding CF were 4.61 and 86 µg/L, respectively. Hence, water disinfection can be easily achieved in a batch manner within 15 min, with our Ag-CF addition.

Keywords: Silver nanoparticles, Antibacterial, *Escherichia coli*, *Staphylococcus aureus*

73

Modification of zeolite supporting diamine silver complex for antibacterial activity

Co-author: Wiyong Kangwansupamonkon¹

¹ *National Nanotechnology Center, National Science and Technology Development Agency*

Corresponding Author: wiyong@nanotec.or.th

The antibacterial zeolite powder prepared by replacing ion-exchangeable in zeolite with silver diamine complex. These composites showed improved discoloration with time and UV stability compared with conventional antibacterial zeolite (silver ions or silver nanoparticles incorporated into zeolite). They were characterized by Transmission electron microscopy (TEM), X-ray diffraction (XRD) and Atomic absorption spectroscopy (AAS). Zeolite supporting diamine silver complex showed strong antibacterial efficacy against the Gram-positive *Staphylococcus aureus* (S. aureus, ATCC 6538) and Gram-negative *Pseudomonas aeruginosa* (P. aeruginosa, ATCC 27853). Moreover, zeolite-Ag(NH₃)₂⁺ exhibited excellent color stability under UV irradiation. Therefore, they could be a beneficial tool for the development of coating application.

Falcon 1 / 74

Preparation of nanocellulose from Jute fiber waste

Author: Rehan Abbasi¹

¹ *Balochistan University of Information Technology, Engineering and Management Sciences*

Corresponding Author: rehan_abbaci@hotmail.com

The objective of this work was to use the spinning waste in form of short fibres for the preparation of nano size fillers in nanocomposite applications. The present paper concerns with the jute fibres as the source to produce nanocellulose by high energy planetary ball milling process and its potential applications as fillers in biodegradable nanocomposite plastics used in automotives, packaging and agriculture applications. Influence of various milling conditions like nature of milling (i.e. dry or wet), milling time and ball size are studied on the particle size distribution and morphology of jute nanoparticles obtained. Wet milling in the deionised water resulted into particle size refinement below 500 nm with narrow size distribution after 3 hours of milling at the cost of small amount of contaminations introduced from milling media.

75

Current-Induced Cleaning of Graphene and Graphene-Metal Contacts

Author: Ratchanok Somphonsane¹

¹ *King Mongkut's Institute of Technology Ladkrabang*

Corresponding Author: rsomphonsane@gmail.com

The issue of contact resistance between graphene and metal contacts is crucial in the development of high-speed graphene devices. However, fabrication-related contamination severely affects the contact resistance in graphene and hence an effective post-fabrication method is needed to resolve

this problem. Current-induced cleaning has previously been used successfully to clean the surface of graphene using the concepts of Joule heating. However, its effect on the graphene-metal contact resistance has not been well documented. By studying as many as 20 devices with varying sample sizes and geometry, we demonstrate that current-induced annealing may be used as an effective in-situ annealing procedure to improve the graphene-metal contact resistance which has long been an issue in characterizing graphene-based devices. With this technique, we are able to reduce the overall resistance systematically to around $1000 \Omega \mu\text{m}$, which is competitive with the best values obtained in the literature to treat this problem. We also demonstrate the effectiveness of current annealing in desorbing contaminants from the surface of the graphene layer, simultaneously shifting the charge-neutrality point to zero back-gate voltage, thus allowing the tuning of carrier density on both the electron and hole sides of the Dirac spectrum. Finally, we highlight certain high-bias effects such as electromigration that may prove to be detrimental to the operation of these devices.

Heron 2 / 76

Development of novel silica-coated superparamagnetic iron oxide nanoparticles for highly efficient magnetofection and molecular imaging.

Author: Jeerapond Leelawattanachai¹

¹ *National Nanotechnology Center*

Corresponding Author: jeerapond@nanotec.or.th

Magnetofection, a site-specific delivery of nucleic acids to cells guided by a magnetic field, has received increasing attention for its great potential on gene therapy. To promote its clinical therapeutic applications, development of safe and effective magnetic nanocarriers is in high demand. Superparamagnetic iron oxide (SPIO) nanoparticles have been clinically proven safe and used as a magnetic resonance imaging contrast agent approved by Food and Drug Administration. In this work we present an initial study of the development of novel silica-coated SPIO nanoparticles for efficient magnetofection. Our patented silica-coated SPIO nanoparticles have many features including 1) facile synthesis with a 2-hour reaction time (compared to a 24-hour standard Stöber process; 2) stability in biological fluids for a year with low degree of aggregation; 3) lack of degradation and oxidation due to polyvinyl alcohol coating layer; and 4) versatility for surface functionalization and drug loading of the silica shell. In this study, the silica-coated SPIO could efficiently condense plasmid DNA (pDNA) into nanoparticles (PSPIO), which exhibited several favourable properties for gene delivery. In vitro transfection efficiency of PSPIO was significantly enhanced under an external magnetic field in a variety of cancer cell lines and PSPIO were found advantageous over existing nonviral transfection methods with the additional benefit of maintaining high cell viability. The superiority of magnetofection could not be inhibited by serum, and fast accumulation of PSPIO on cancer cells was observed. In conclusion, our results demonstrate that the silica-coated SPIO is a technically simple and effective alternative to current methods for gene transfer as well as molecular imaging under the guidance of a magnetic field. Ongoing and future work includes pharmacokinetic study of PSPIO and tumor-directed gene therapy in vivo.

77

Comparative study of local structure for sputter deposited nitrogen doped zinc oxide thin films

Author: Jedsada Manyam¹

¹ *National Science and Technology Development Agency*

Corresponding Author: jedsada.nanotec@gmail.com

Incorporation of N anion into ZnO crystal has been known to induce structural distortion and can cause dramatic change in its electronic structure. It has been reported that thin films with great variance in crystallinity and electrical properties such as highly crystalline p-type or amorphous high carrier mobility n-type ZnO films can be achieved by particular growth control of N doped ZnO or zinc oxynitride thin films using reactive sputtering deposition. In this work, we measured x-ray absorption spectroscopy (XAS) near Zn K edge energy to probe local atomic environment around Zn atom for nitrogen doped ZnO thin films, aiming at examining structural profile for those films by fitting variable to their extended x-ray absorption fine structure (EXAFS). Thin film samples were prepared using variety of RF magnetron sputtering depositions in order to investigate an influence of preparation method on the local structure. ZnO target sputtered with either continuous or gas timing flow of Ar and N₂ reactive gases were utilized to coat thin films of undoped or nitrogen doped ZnO on a silicon substrate. The other samples were deposited on a glass substrate at high partial pressure of N₂ with Zn target. XRD results confirmed that the deposited films were in Wurtzite ZnO crystalline phase. For EXAFS analysis, variables for the Wurtzite ZnO model were found reasonably fitted to each EXAFS spectrum within a range covering 2 nearest neighbor atomic shells surrounding the Zn center atom, thus details on Zn-O (or Zn-N) and Zn-Zn bond lengths, variance of atomic position attributed from structural disorder, and amplitude factors relevant to the number of atom on each scattering shell were extracted. Typically, it was found that N doped samples posed high degree of structural disorder and similar anion to cation ratio in opposition to the undoped ZnO. The thin film prepared with high partial pressure N₂ gas tended to have relatively large bond lengths and low density of anion and cation in the Wurtzite structure which could be due to the presence of other zinc oxynitride phase mixed in the sample. With an assist of principal component analysis (PCA), samples could be classified into groups according to the fitting variables. For example, N doped samples deposited using ZnO target could be grouped together, where as an undoped sample and the others were well distinguished. This study quantified structural feature for selected N doped thin film and suggested a rough guide on applying reactive gas sputtering deposition for tailoring local structure of the deposited film.

78

Preparation and characterization of cement 12CaO•7Al₂O₃/reduced graphene oxide hybrid composites and their electrical properties

Author: Chaiwat Prohmpetch¹

¹ *Department of Physics, Faculty of Science, King Mongkut's Institute of Technology Ladkrabang, Chalokkrung Road, Ladkrabang, Bangkok, 10520, Thailand*

Corresponding Author: wat_tsu@hotmail.com

Chaiwat Phrompeta, Chaval Sriwongb, Chesta Ruttanapuna,*and Santi Maensiric

a Department of Physics, Faculty of Science, King Mongkut's Institute of Technology Ladkrabang, Chalokkrung Road, Ladkrabang, Bangkok, 10520, Thailand

bDepartment of Chemistry, Faculty of Science, King Mongkut's Institute of Technology Ladkrabang, Chalokkrung Road, Ladkrabang, Bangkok, 10520, Thailand

cSchool of Physics, Institute of Science, Suranaree University of Technology Nakhon Ratchasima, 30000, Thailand

*E-mail: chesta.ruttanapun@gmail.com

Abstract; The aim of this work is to study the preparation and characterization of cement 12CaO•7Al₂O₃/reduced graphene oxide hybrid composite, and the including electrical properties were also investigated. In the preparation, the hybrid composites were easily prepared by directly mixing method based on the use of fixed 12CaO•7Al₂O₃ (C12A7) suspension with different amounts of reduced graphene oxide (rGO) suspensions. The prepared hybrid samples were characterized by using X-ray diffraction (XRD), Fourier-transformed infrared spectroscopy (FT-IR), Raman spectroscopy, scanning electron microscopy (SEM) and transmission electron microscopy (TEM) techniques. The results showed that the crystalline phases and functional groups of these composites are corresponding to pristine

C12A7, whereas all of rGO characteristic peaks are not observed. Nevertheless, the characteristic peaks of rGO in the hybrid composites could be seen and confirmed by Raman spectroscopy technique. From the electrical test found that the electrical conductivities of C12A7/rGO composites were increased with increasing amounts of rGO nanosheets loading. This may be due to the fact that it corroborates the strong interfacial interaction between rGO and C12A7 particles.

Keywords: $12\text{CaO}\cdot 7\text{Al}_2\text{O}_3$ (C12A7), Reduced graphene oxide (rGO), Electrical conductivity

79

Spectroscopy system using two dimensional detectors for undergraduate student laboratory

Author: Suwan Plaipichit¹

Co-author: Surawut Wicharn¹

¹ *Department of physics, Faculty of Science, Srinakharinwirot University*

Corresponding Authors: surawutw@g.swu.ac.th, suwanp@g.swu.ac.th

In this paper, we propose spectroscopy system, which use Complementary metal–oxide–semiconductor (CMOS) image sensor as two dimensional detectors, for studying in undergraduate laboratory. The goal of this system is to make students understand internal structure of commercial spectrometer and characteristic of light spectrum. Light with various wavelengths propagated via variable slit, which is used to control width of spectrum, has been focus on reflective grating and then separated to various spectrum. After that, separated spectrum has been recorded by CMOS image sensor which consists of two dimensional array pixels. Each pixel can be determined as wavelength of light by calibrating with Mercury lamp which is standard light source that has exact spectrum value. By using CMOS image sensor, student can observe distribution of real light spectrum and spectrum graph together. The results show that characteristic spectrum obtained from our system is identical with commercial instrument. Moreover, our system not only be applied for undergraduate studying, but also might be applied with other optical spectroscopy method in future.

80

Colorimetric determination of Silver Nanoparticles with Dithizone-based in Aqueous Media

Author: Sujittra Srisung¹

¹ *Srinakharinwirot University*

Corresponding Author: ssrisung@yahoo.com

Silver nanoparticles (AgNPs) has been widely used for commercial products with many applications. An increasing number of commercial products cause risks and exposure of AgNPs effects for human and the environment. Therefore, the measurement of AgNPs in the aquatic environment is important. Dithizone ligand is evaluated as one of the most effective chelating reagents for metal ions because of its high sensitivity and selectivity. In this work, dithizone was carried out for AgNPs detection in the aquatic environment. Dithizone is focused on the geometry conformation and interaction of dithizone with silver using UV-Vis spectroscopy and FT-IR spectroscopy using density functional approaches B3LYP and the 6-31G(d,p) basis set. Moreover, the silver-dithizone complex was investigated using ¹H NMR spectra using B3LYP/6-311+G(2d,p) level of calculation compared with the experimental data. The results revealed the ion exchange interaction between hydrogen of dithizone and silver with the lowest of binding energies of silver-dithizone complex formation. When AgNPs was added to the dithizone solution, affected color change from colorless to orange was observed. While the metal ions such as Na⁺, K⁺, Cu²⁺, Mg²⁺, Ba²⁺, Mn²⁺, Fe³⁺, Co²⁺, Ni²⁺,

Cu²⁺, Ag⁺, Zn²⁺, Cd²⁺, Hg²⁺ and Pb²⁺ didn't interfere with the recognition process for AgNPs. Therefore, the results can be the useful information for the measurement of complex interaction using the analysis of computer simulations and the limit of detection for AgNPs were 0.071 mg/L. Finally, this method can be applied for determination of AgNPs in the aquatic environment.

81

Sustained delivery scaffold loaded by cisplatin and curcumin

Author: Nicha Thepsri¹

¹ *Department of Pharmaceutical Chemistry, Faculty of Pharmaceutical Sciences and Nanotec-PSU Center of Excellence on Drug Delivery System, Prince of Songkla University, Hat-yai, Songkhla, Thailand*

Corresponding Author: nicha.the@gmail.com

Cisplatin (CP) is an essential anticancer drug, according to the World Health Organization's List of Essential Medicines. The drug has a number of side-effects, such as nephrotoxicity, neurotoxicity, ototoxicity; and can be the causes of hemolytic anemia, electrolyte disturbance, nausea, and vomiting. Cisplatin resistance is problematic for treatment of many cancers.

Curcumin (CMN) is a diarylheptanoid, the principal curcuminoid of turmeric (*Curcuma longa*). It exerts potent anti-inflammatory effect, which is protective against some form of cancer progression. In fact, curcumin has additional anti-cancer effect that is independent of its anti-inflammatory activity.

In this research, scaffolds consisting of Zr-dropped hydroxyapatite (Zr-HA), CMN-entrapped β -cyclodextrin (CMN- β CD), and CP-encapsulated polycaprolactone (CP-PCL) were prepared by using the compression molding technique. CMN and β CD were physically mixed. The hydrophilicity of PCL was increased by alkaline hydrolysis. The hydrolyzed PCL was melted into which CP and Zr-HA were added. The mixture of CP/Zr-HA/PCL was set at room temperature. Then, it was ground to fine powder. These two solid phases, e.g., CMN- β CD and CP/Zr-HA/PCL, were mixed and pressed to form scaffolds.

By using FTIR technique, there are specific peaks of hydroxyl groups on the spectra of the hydrolyzed PCL. Upon pressing, there are films of the PCL covering the HA particles, but the films are not completely coated as indicated by XRD pattern. By using DSC technique, CMN is completely entrapped into the β CD structure, and CMN and β CD are compatible with each other. The charge property of the scaffolds was investigated by using toluidine blue (TB) as a drug model. The negative charges of the scaffolds are expected to interact with the positive charges of TB, resulting in its stable binding. The TB binding efficiency varies between 13 and 52%, depending on the degree of PCL hydrolysis. The release of TB is sustained without an initial burst release. The penetration of TB deeply inside the scaffolds was ascertained by using a confocal microscope, indicating that the depth is about 40 μ m. The releases of both CP and CMN from the scaffolds were sustained by at least 10 days and the released CP and CMN still exhibit cytotoxicity to cancer cells, according to the MTT assay. The addition of CMN can reduce the CP doses while keeping the constant cytotoxic effect. It seems that side effects of CP can be diminished by using in with CMN.

82

A Numerical Investigation of Enhanced Second-Harmonic Generation in One-Dimensional PIM/NIM Structure

Author: Surawut Wicharn^{None}

Corresponding Author: surawutw@g.swu.ac.th

In this paper, we demonstrate a numerical investigation of an enhanced second-harmonic generation (SHG) effect in a one-dimensional positive-index material/negative-index material (1D-PIM/NIM) structure with nonlinear deep grating. The 1D-PIM/NIM structure composed of common linear PIM layers and NIM layers, whose electric permittivity and magnetic permeability are described by Lorentz dispersion model for allowing negative refractive index behavior, doped with nonlinear $\chi(2)$ material in periodically arrangement. To model SHG phenomenon, we develop a completed set of nonlinear coupled-mode equations (NCMEs) by perturbing nonlinear wave equation by a small factor with appropriate scale following a way of multiple-scale analysis (MSA). Then, we solve the NCMEs to obtain the second-harmonic output fields and conversion efficiency. We also discuss a backward phase-matching (BPM) condition, which is satisfied by tuning a fundamental frequency (FF) in a negative refractive index region and second-harmonic (SH) frequency in a positive refractive index region, and band-edge field enhancement condition, which is created by rearranging PIM and NIM layers in optimal periodic fashion. By using both conditions, a conversion efficiency of SHG can be dramatically improved comparing with SHG conversion efficiency of an equivalent length generic nonlinear NIM structure.

Falcon 1 / 83

Investigation of using carbon nanotube mixed with several metal phthalcyanine compounds for electronic tongue applications

Author: Arthit Jityen^{None}

Corresponding Author: j.arthit89@gmail.com

Carbon nanotube (CNT) has an excellent property in high electrical conductivity and can be mixed with an active compound in order to use as a functional electrode. Due to variety of metal phthalcyanine (MPc) compound can be formed by different metal atom, the MPc with several metal spices was used as an array detection in electronic tongue classification for a number of coffee types. In this work, 100 mg of CNT and 100 mg of MPc including CoPc, FePc, ZnPc, and MnPc powders blended with 700 μ l of paraffin oil were used as working electrodes by embedding in a hollow Teflon rod. Electrochemical characteristics of the fabricated electrodes in Robusta, Arabica, blend coffee and cocoa were investigated by scanning cyclic voltammogram (CV) with scanning rate of 0.05V/s from -1.5 to 1.5V respectively to Ag/AgCl electrode for five scanning loops. The CV of blended CNT with some MPc indicated the effect of catalytic oxidation of saccharides and/or polyphenol on the sensor surface. This led to distinguish pattern of CV for successful classification in these four groups. The obtained main feature of electrochemical information was analyzed by using wavelet analysis and then the principal components analysis (PCA) was implemented to represent the distribution in the first few principle components. The PCA results indicated separate groups with total contribution more than 90% representing from the PC1 and PC2 and the major feature extraction can be described by components of wavelet analysis.

Heron 2 / 84

The Increased Durability of Natural Dye on the SiO₂-Modified Paper

Author: Radchada Buntam¹

¹ *Department of Chemistry, Faculty of Science, Silpakorn University*

Corresponding Author: radchadab@yahoo.com

Cellulose, extracted from plant, has been widely used in various purposes especially in paper industry. In industry, cellulose is modified by many organic and inorganic substances in order to improve the quality like smoothness, whiteness and mechanical strength. However the deterioration of the paper according to the degradation of cellulose has been found in many ancient documents and paintings. The causes of cellulose alteration are from biodegradation, photodegradation, acid hydrolysis

and oxidation. In this research, filter paper, a representative of cellulose fiber, was coated by SiO₂ to improve its stabilities. The surface of the cellulose was initially modified by various methods as follows:

1. esterification by polycarboxylic acids like tartaric acid (TA) and butanetetra-carboxylic acid (BTCA) to obtain FIL-TA and FIL-BTCA respectively
2. etherification by sodium monochloroacetate to obtain FIL-MCAA
3. coating by carboxymethylcellulose to obtain FIL-CMC

Then each of the modified filter papers was subsequently coated by SiO₂. All paper samples were characterized by SEM/EDS, XRD and TGA. The Smoothness (Bekk method), air resistance (Gurley method) and bursting test of paper were also performed. All coated papers were then placed in saturated curcumin solution for 20 min. The stability of this natural dye on the paper was tested against UV-A radiation ($\lambda = 315\text{--}400\text{ nm}$) for various time interval. The changes in the color parameters L, a, and b were measured; L index of color represents black-to-white color, a index represents green-to-red color, and b index represents blue-to-yellow color. The overall change in color indices of the coated papers can be calculated as the following equation:

$$\Delta E = ((\Delta L)^2 + (\Delta a)^2 + (\Delta b)^2)^{1/2}$$

where ΔL , Δa , and Δb are the differences between the values of the color indices before and after radiation. The TA-SiO₂ paper shows the lowest ΔE value.

85

Binding mode prediction of 8-hydroxyquinoline derivatives as inhibitors against Dengue Virus NS3 Protease using molecular dynamics simulations

Author: Patchreenart Saparpakorn¹

¹ NANOTEC Center for Nanoscale Materials Design for Green Nanotechnology, Kasetsart University and Center for Advanced Studies in Nanotechnology for Chemical, Food, and Agricultural Industries, Faculty of Science, Kasetsart University

Corresponding Author: p_saparpakorn@yahoo.com

NS3 protease (NS3pro) is an interesting target for discovering the new potent inhibitors of Dengue virus (DENV). The NS3pro is a serine protease consisting of catalytic triad (HIS51, ASP75, and SER135) and expresses role in the step for post-translational cleavage of substrate. Some derivatives of 8-hydroxyquinoline are found as potent NS3pro inhibitors. Molecular dynamics (MD) simulations were applied in order to investigate the structural information of these derivatives in NS3pro. From the results, MD simulations reveal key amino acids for the binding. H-bond interaction to catalytic amino acids (HIS51 and SER135) and H-bonds through other amino acids in NS3pro binding site are also found. Information from the study can indicate the structural effect of 8-hydroxyquinoline derivative during the binding and can use for further analysis in order to improve the activity of DENV inhibitor.

86

Investigation on the interactions between glucomannans and Bifidobacterium enzyme by using molecular dynamics simulations

Author: Napassorn Jensupakarn^{None}

Corresponding Author: orientalpearl_mook@hotmail.com

Konjac glucomannan is a polysaccharide extracted from the *Amorphophallus konjac* K.Koch plant. It is often used as food additives due to their low toxicity, biodegradability and low calories. The unique properties of konjac glucomannan is a prebiotic, a non-digestible food, which cannot be digested and absorbed in human stomachs and small intestines. Therefore, it is fermented in the large intestine

and becomes food for the beneficial bacteria or probiotics especially bifidobacteria and lactobacilli in human colons. This study examined the effect of the size of konjac glucomannan on the prebiotic property. The interactions between the different degrees of polymerization of konjac glucomannan and Bifidobacterium enzyme were investigated in 0.15 M sodium chloride solution at 310 K by using molecular dynamic simulation. The results have shown that water molecules dramatically affect the alignment of konjac glucomannan in the system. The active site of Bifidobacterium enzyme that determined by the calculations are composed of ASP154, ARG49, ASN206, and ASN401. The lowest flexibility of GM5 structure shows strong interactions with Bifidobacterium enzyme. The most suitable size of konjac glucomannan that can bind with the enzyme has the degree of polymerization between 5 to 8.

Heron 2 / 87

Development of cellular platform for enhancing neuron differentiation

Author: Suthiwan Udomrat¹

¹ *Materials Science and Engineering program, and Capability Unit for Nanoscience and Nanotechnology, Faculty of Science, Mahidol University, Bangkok, THAILAND*

Corresponding Author: taggi_e@hotmail.com

Material surface properties are considered as critical factor for the study of *in Vitro* cell growth pattern and activities. It provides advantages not only for study of cellular activity but also for biomedical technology such as tissue engineering. Neuron is a typical cell type widely used to examine cell communication, alignment and differentiations. In the present study, a simple pattern of indium tin oxide (ITO) for neuron culture is introduced. Circular inter-digitated design of ITO electrode was fabricated to capture a small amount of cell for cellular observations. In order to enhance cell attachment, the fabricated electrode surface was modified by poly-L-lysine, a type of extracellular matrix. SH-SY5Y cell, a human neuroblastoma cell line, was cultured on the modified surface and the cell growth was observed periodically. Small electrical field was applied to the culture for a period of time then cells were fixed for SEM imaging. It is clearly demonstrated that the amount of differentiated cell increased from 42% to 63.5% after subjected to small electric field. In addition, the possibility of fabricated nanostructure electrode can indicate the potential utilize as a single cellular activities without cell invasion.

Keywords: Neuron, SH-SY5Y, cell differentiation, ITO electrode, electrical effect

88

Magnetic Capture Hybridization –Polymerase Chain Reaction (MCH-Pcr) for Detection of Salmonella Typhimurium Artificially Contaminated in Drinking Water and Food

Author: Goragot Supanakorn^{None}

Corresponding Author: gsupanakorn@gmail.com

Magnetic polymeric nanoparticle (MPNP) has been used widely as a solid support for biomolecules in biomedical applications. Because it is convenient to control by applying external magnetic field and easy to surface functionalize. In this work, magnetic capture hybridization –polymerase chain reaction (MCH-PCR) was developed for detection of *S. Typhimurium* contaminated in drinking water and raw chicken meat artificially. Carboxylated MPNP was covalently bound to oligonucleotide probe specific to *invA* gene of *S. Typhimurium*, which is one of the most causative agents of food poisoning syndrome in Thailand. The probes were designed and synthesized to possess amino modification and five different spacers at the 5' end of sequence to compare their sensitivity and specificity

of the assay. The probe bound MPNP was allowed to hybridize with target DNA in MCH reaction and magnetically separated to use as a template in PCR amplification. The amplified products were separated in agarose gel, stained and visualized under UV light. The advantage of this method contributes to high specific of probe-DNA hybrids leading to specificity enhancement of PCR assay. In addition, the MPNP facilitate separation of the target DNA easily from the food matrix.

Falcon 1 / 89

Development of Physicochemical Properties of Pomegranate Extract using “Liponiosome” Encapsulation Technique

Author: Oraphan Phuangswai¹

¹ *National Science and Technology Development Agency*

Corresponding Author: oraphan.phu@nanotec.or.th

Pomegranate extracts have been reported as biologically active having desirable properties such as antioxidant, antifungal, anticarcinogenic and anti-inflammatory capabilities. Anthocyanins found in pomegranate fruit have higher antioxidant activity than vitamin-E (α -tocopherol), β -carotene, and ascorbic acid. Although, it shows good biological activity against a variety of target, it easily decomposes and has high acidity (pH 2.90-3.75), which is not appropriate for topical treatment on human skin (pH 3.5-5.5). It is very important to improve the properties of the pomegranate extracts to obtain desirable characteristics and properties appropriate for skin treatment. In this work, the pomegranate extracts have been encapsulated in a particle, called “liponiosome”. The liponiosome is composed of phospholipids, which are the main components in liposomes, and non-ionic surfactants, which are the main components in niosomes. The combination of these encapsulation substances, liposomes and niosomes, is referred to as “liponiosome”. This encapsulation technique provides desirable properties in terms of particles sizes (~100 nm), stability (at various conditions such as at 4°C, room temperature and 40°C for 1 month and during a heating-cooling cycle for 6 cycles) and efficacy. Moreover, this process is cheap, provides a non-toxic product and is biocompatible with the human skin.

90

Preparation of high surface area binary-CeCoO_x for VOCs catalytic oxidation

Author: Sarocha Sumrunnonasak¹

¹ *National Nanotechnology Center*

Corresponding Author: sarocha.sum@nanotec.or.th

For volatile organic compounds (VOCs) abatement, a series of high surface area cerium-cobalt mixed oxide nanocatalysts with different cerium/cobalt ratios were prepared via a surfactant assisted-templating precipitation method using cetyltrimethylammonium bromide (CTAB) as a surfactant. The obtained catalysts were characterized by different techniques including X-ray diffraction (XRD), H₂-temperature programmed reduction (H₂-TPR), N₂ physisorption, X-ray photoelectron spectroscopy (XPS) and transmission electron microscopy (TEM). The XRD and TEM results revealed highly dispersed cobalt on the surface of ceria oxide. Moreover, the incorporation of cobalt into the CeO₂ lattices to form Ce_{1-y}Co_yO_x mixed oxides at ratio of $y \leq 0.4$ increased the dispersion of the obtained catalyst as well as oxygen vacancies which leads to the enhancement of oxygen storage capacity. BET results indicated that the prepared catalysts had a mesoporous structure and a large specific surface area of 138.91 m².g⁻¹. The XPS spectra showed that both Ce⁴⁺ and Ce³⁺ were presented in the nanocatalysts with various peak shape in the different cobalt ratios and played an important role on the

oxygen vacancies in the catalysts.

Keywords: CeCoOx, catalytic oxidation, nanocatalyst, mixed oxide, oxygen vacancies

Heron 2 / 91

Deoxygenation of oleic acid to produce bio-hydrogenated diesel over molybdenum oxide catalysts on supported alumina under inert atmosphere

Author: Navapat Krobkrong¹

¹ Kasetsart university

Corresponding Author: navapat.k@hotmail.com

Deoxygenation of vegetable oil has been employed as one of important processes for highly efficient production of renewable green diesel (bio-hydrogenated diesel). Moreover, to avoiding sulfur contamination in fuel product, metal oxides, metal phosphides, and metal nitrides have become attractive. In this work, bimetal oxide catalysts over supported alumina were selected to produce diesel-like hydrocarbons via deoxygenation of oleic acid under facile condition. All catalysts were prepared by incipient wetness impregnation and characterized by XRD, SEM, TEM and BET. Furthermore, effects of reaction time and temperature were studied in a batch reactor (300 mL in size) under N₂ pressure. The results revealed that NiMo/Al₂O₃ catalyst exhibited a high conversion over 90% and the contribution of decarboxylation (DCO₂) enhanced by increasing both reaction time and temperature. In addition, saturated hydrocarbons and stearic acid were also detected. These result indicated that dehydrogenation and hydrogenation occurred during the reaction. Therefore, all active phases (MoO₃ and NiMoO₄) of Ni doped Mo oxide catalyst were deeply investigated using DFT method with ethane as a model compound. The calculations emphasized that both of metal oxide phases could produce unsaturated compounds through dehydrogenation by taking hydrogen atoms out to the surface. Interestingly, the NiMoO₄ phase contained numerous vacancies on the surface, and consumed less energy for the reaction in respect with MoO₃. As a results of that, it would be a better phase to produce unsaturated products compared to MoO₃ phase. However, the hydrogen atoms were not enough for hydrodeoxygenation(HDO) pathway because of low selectivity of C18 compared with C17 in liquid products.

Falcon 1 / 92

Characteristics of a Nanocrystalline-based, UVA-activated, 'Consume within' Indicator for Intelligent Packaging

Author: Surachai Khankaew¹

¹ Department of Packaging and Materials Technology, Faculty of Agro industry, Kasetsart University, Bangkok, Thailand

Corresponding Author: s.khankaew.rmutt@gmail.com

A 'consume within' indicator is important for the perishable foods because the oxygen is the growth factor of aerobic microorganisms in perishable foods. It follows that a useful addition in intelligent packaging technology is a capable diagnostic indicator which allows the real-time monitor of the quality or safety of the foods. A novel UVA-activated, 'consume within' indicator ink is based on TiO₂ as a nano-semiconductor photocatalyst. An anatase TiO₂ is encapsulated in CWI-ink containing remazol brilliant blue r, glycerol and hydroxyl ethyl cellulose. This study focused on characteristics of UVA-activated, CWI-ink, which utilized a nanocrystalline, TiO₂, to activate the indicator. This novel CWI-ink was applied as a thin film on a glass cover slip. The dried-ink film, originally blue color was photoactivated to yellow by UVA-light under oxygen-free condition, and recovered to

its original color when exposed to the oxygen. The result indicates that the uncovered (i.e. no O₂ barrier) and covered RBBR indicator may find a role as consume-within indicators for fresh food at 5°C (where consume-within lifetimes of 24/48 h are of relevance for fresh foods like meat and seafood).

Keywords: Anthraquinone, 'Consume within' indicator, Intelligent packaging, Oxygen indicator, Semiconductor

93

Gas adsorption on MXene surfaces: Density Functional Theory calculations

Author: Anchalee Junkaew¹

¹ *National Nanotechnology Center (NANOTEC), National Science and Technology Development Agency (NSTDA)*

Corresponding Author: nuchy96@hotmail.com

Two dimensional graphene-like materials, so-called MXenes, have been discovered recently. MXenes are layers of transition metal carbide and nitride compounds. According to their large surface area and their distinctive properties, MXenes are promising materials for many applications such as energy storage, supercapacitor, gas storage and thermoelectric applications. This work investigated gas adsorption on MXenes (i.e. Ti₂C, V₂C, Nb₂C and Mo₂C) and their oxygen-functionalized surfaces (O-MXenes) by using the periodic Density Functional Theory (DFT) calculations. The adsorbates are N₂, NO, NO₂, NH₃, CO, CO₂, O₂, H₂, H₂S, SO₂ and H₂O molecules. Both dissociative and molecular adsorption processes were observed depending on adsorption sites, types of MXene and adsorbate molecules. The functional group on the surface also plays an important role in its gas adsorption ability. On bare surfaces, the chemisorption process with high adsorption energy indicates high reactivity of MXene towards gas molecules. In the functionalized cases, O-MXenes show weaker gas adsorption strength than bare MXenes, but they are more selective to particular gas species. The results are useful for applying these materials in gas separation, gas storage and gas sensor applications. Structural and charge analysis were performed for understanding the interaction between adsorbates and substrates.

Hornbill 1 / 94

Nano Roughening of Polyethylene Surface with Acrylic acid/Benzophenone via UV irradiation for Intelligent Packaging Application

Author: Nawaporn Wannawisan¹

¹ *Department of Packaging and Materials Technology, Faculty of Agro Industry, Kasetsart University, Bangkok, Thailand; Center for Advanced Studies in Agriculture and Food (CASAF), Kasetsart University, Bangkok, Thailand*

Corresponding Author: ffsnpw@gmail.com

ABSTRACT

Surface modification methods are used in several industries as biomedical, textiles, microelectronics, bioprocessing, and food packaging. Most commercial polymers surface are inert and hydrophobic in nature, they must be modified or treated prior to covalent attachment with desired compounds on their surface. Surface modification technology as UV irradiation has been used to introduce carboxylic acid functionality and to initiate radical graft polymerization of many compounds on polymer surface to improve wettability, printability, sealability or its adhesion to other materials. Benzophenone is the most widely used as initiator for graft polymerization because of their ability to remove hydrogen and form reactive grafting sites on polymer surface. Acrylic acid is grafted

monomers which can react with different compounds and introduce functionalities on grafted surface. The objective of this work is to investigate the effect of acrylic acid and benzophenone in mixed solvent via UV irradiation technique on nano scale roughness of polyethylene surface. The grafting efficiency, surface functionalization and nano scale roughness on PE surface will be investigated using fourier transform infrared spectroscopy (FTIR), contact angle measurement, and atomic force microscope (AFM). The expected results of hydrophilicity and desired functionality possibly used to enhance immobilization of azo dye as intelligent packaging application.

Keywords: Acrylic acid, Benzophenone, Intelligent packaging, Nano roughening, UV irradiation

Heron 2 / 95

Antioxidant Activities and Properties of Quercetin Nanoparticles-Incorporated Cellulose-based Packaging Films

Author: Kanthika Nantapreecha¹

¹ Department of Packaging and Materials Technology, Faculty of Agro Industry, Kasetsart University, Bangkok, Thailand

Corresponding Author: kanthika_n@hotmail.com

As a natural-derived phenolic compound, quercetin has promisingly strong antioxidant activities. It is possible to incorporate this compound with active packaging film. However quercetin has poor water-solubility resulting in a limitation of its antioxidant efficacy. Nanotechnology is one of the innovative technologies that can increase surface area, bioactivity, and also improve the solubility of the active substance. This work aimed at investigating the antioxidant activities of quercetin nanoparticles (QC-NPs) produced by rapid expansion of a subcritical solution into liquid solvents (RESOLV) technique. The QC-NPs were incorporated into cellulose-based films, methyl cellulose (MC) with polyethylene glycol having a molecular weight of 400 (PEG-400) as a plasticizer by casting technique. The particle size of QC-NPs was evaluated by dynamics light scattering (DLS) and transmission electron microscopy (TEM). The antioxidant activities of quercetin nanoparticles were evaluated by the 2,2-diphenyl-1-picrylhydrazyl assay, 2,2'-azino-bis (3-ethylbenzthiazoline-6-sulphonic acid assay, ferric reducing antioxidant power assay, and β -carotene bleaching assay, respectively. Some properties of the QC-NPs incorporated cellulose-based films including color, thickness, tensile strength and elongation at break will also be reported. The results also indicated that the functional properties of cellulose-based films could be enhanced by an incorporation of QC-NPs.

Keywords: Active Packaging, Antioxidant Activity, Nanoparticles, Quercetin, RESOLV

Heron 1 / 96

Effect of Ammonia and Acid Concentrations on the Response of Fish Spoilage Indicator Solution Based on Coordination Compound of Transition Metal

Author: Kanokporn Pathanasriwong¹

¹ Department of Packaging and Materials Technology, Faculty of Agro-Industry, Kasetsart University, Bangkok, Thailand

Corresponding Author: k.pathanasriwong@gmail.com

Abstract

Fish products provide a vital source of essential protein and contain many minerals and vitamins in human nutrition. Unfortunately these products are extremely perishable and can be spoiled rapidly at an unsuitable storage. Diagnostic packaging plays a key role for real time monitoring quality and safety of products, by detecting volatile compounds which existed within headspace inside the package. Coordination compound of transition metal is an interesting alternative as fish spoilage indicator, having color change due to an increasing of pH caused by releasing a variety of basic volatile nitrogen compounds from fish spoilage. When iron (II) complex reacts with basic compounds, the solution is some precipitated in nanoscale that makes it noticeably different from pH-dye and clear to observe. The objective of this work is to investigate the effect of ammonia and acid concentrations on the response of fish spoilage indicator solution based on coordination compound of transition metal. The sensitivity of indicator solution and physical properties were evaluated by UV-Vis spectroscopy, spectrophotometer, pH measurement and dynamic light scattering. In order to validate an application of this system as fish spoilage detection, the tests will be conducted with fish fillets and the expected results will be reported.

Keywords: Coordination compound, Diagnostic packaging, Fish spoilage indicator, Nanoscale precipitation, Total volatile basic nitrogen, Transition metal

Heron 2 / 97

An innovative application of magnetic field for CO₂ hydrogenation reaction on Fe and Cu supported MCM-41 catalyst

Author: Sirapassorn Kiatphuengporn¹

¹ *Nanomaterials for Energy and Catalysis Laboratory, National Nanotechnology Center (NANOTEC), National Science and Technology Development Agency (NSTDA)*

Corresponding Author: sirapassorn.kia@nanotec.or.th

The external magnetic field was applied in a packed-bed reactor based on the concepts of green and sustainable production of alternative fuels through CO₂ hydrogenation reaction. Accordingly, the roles of magnetic flux density and magnetic field direction on the performance of Fe-Cu/MCM-41 catalyst with intrinsic magnetic property were investigated and compared to that of without magnetic field. It was found that magnetic field strongly affected the activity of catalyst, both CO₂ conversion and product selectivity. Over 10Cu–10Fe/MCM-41 catalyst, magnetic field remarkably promoted CO₂ conversion, especially in the north-to-south (N-S) direction (1.8 times higher than that of without magnetic field at 260°C). With increasing magnetic flux density, CO₂ conversion was increased followed the order of 27.7 mT > 20.8 mT > 0 mT in each magnetic field direction. Moreover, under the magnetic field conditions which gave the highest CO₂ conversion, it was more favorable for CH₃OH formation. CH₃OH space time yield with magnetic field was 1.5 times higher than that of without magnetic field. The improvement of catalytic activity by the magnetic field application was described by mean of the reduction of apparent activation energy (E_a). With magnetic field, the apparent activation energy was decreased for approximately 1.18 times compared to that of without magnetic field. This outstanding performance was attributed to the fact that magnetic field could facilitate the adsorption ability of reactant gases on magnetized catalyst surfaces, leading to the increase of catalytic CO₂ hydrogenation and selective conversion to CH₃OH, and lowering of the activation energy.

98

Impact of an integrated in vivo-in vitro approach for evaluating the hazardous pulmonary effects of nanomaterials and the underlying mechanisms

Author: Liying Wang¹

¹ National Institute for Occupational Safety and Health, Morgantown, WV, USA

Corresponding Author: lmw6@cdc.gov

With the promising benefit of nanotechnology and the rapid rise of engineered nanomaterial production, potential human exposure to nano-scaled respirable particles has become a major concern. Animal exposure studies have shown that pulmonary exposure to nanoparticles, such as carbon nanotubes (CNTs) and nano-scaled cerium oxide (nCeO₂), can deposit the particles deep in lung tissues and cause adverse health effects. Unique physicochemical properties of the nanoparticles greatly influence their adverse effects. With the identification of the specifically affected lung cells at the site of particle accumulation, we have developed multiple in vitro models to assess the cytotoxic, fibrogenic, and carcinogenic potential of nanomaterials using relevant human cell culture models. All in vitro doses were physiologically relevant and based on in vivo doses that induced significant pulmonary disorders in animal models. Acute (days), sub-chronic (weeks), and long-term (several months) exposures to CNTs, nCeO₂, and nFe₂O₃ were shown to cause dose- and time-dependent cytotoxic (cell damage) and fibrogenic (collagen production) effects, as well as neoplastic and/or malignant transformation (anchorage-independent growth, apoptosis evasion, increased migration, invasion, angiogenesis, and tumor formation), consistent with the in vivo animal data. In vitro assessment tools further allow detailed mechanistic investigations of key signaling pathways and mediators involved in the pathological processes (e.g. p53, transforming growth factors, and matrix metalloproteinases), which may serve as predictive biomarkers for the in vivo responses. Impact of the integrated in vivo-in vitro approach also includes that it supports the utility of the in vitro models as rapid screening tools for risk assessment of nanomaterial-induced pathologies.

Heron 2 / 99

Antimicrobial and Antioxidant Activity of Caffeic Acid Phenethyl Ester Nanoparticles

Author: Suparak Saelo¹

¹ Department of Packaging and Materials Technology, Faculty of Agro Industry, Kasetsart University, Bangkok, Thailand

Corresponding Author: suparak_num@hotmail.com

Caffeic acid phenethyl ester was successfully prepared by rapid expansion of supercritical solutions into liquid solvent. An average size of these CAPE nanoparticles was characterized by TEM and DLS techniques. They were found that diameters CAPE-NPs were ~40 to ~400 nm. The minimum inhibitory concentrations (MICs) and the minimum bactericidal concentration (MBCs) of CAPE nanoparticles were compared to CAPE particles using the plate count method against *Bacillus cereus*, *Staphylococcus aureus*, *Listeria monocytogenes*, *Escherichia coli* and *Vibrio parahaemolyticus*. The antioxidant activities determined by the 2,2-diphenyl-1-picrylhydrazyl assay, ferric reducing antioxidant power assay and total phenolic content, respectively. MICs and MBCs of Gram-positive bacteria and Gram-negative bacteria were 350, 700 µg/mL and 1400 µg/mL. CAPE-NPs presented antioxidant activities similar to CAPE dissolved in 40 % ethanol but higher activities than that of CAPE in water. Antimicrobial and antioxidant properties of CAPE can be improved by a particle-size reduction in the ranges of nano-scale. In addition, the results should be generally applicable to nanoparticles fabrication to improve their bioavailability. As a powerful antimicrobial and antioxidant activities, CAPE nanoparticles could be a potentially promising application for active food packaging.

Keywords: Active packaging, Antimicrobial, Antioxidant, Caffeic acid phenethyl ester, Nanoparticles

Magnetic properties and chemical state of nickel doped CuFeO₂ delafossite oxide powders prepared by sol-gel method

Author: Teerakorn Kongkaew¹

¹ *Materials Science and Engineering Program, Faculty of Science, Mahidol University, 273 Rama VI Road, Phayathai, Bangkok 10400 Thailand*

Corresponding Author: teerakorn.kk@gmail.com

Nickel doped CuFeO₂ were synthesized by using sol-gel method and then heat annealing was performed into two steps. The first annealing was executed at 500°C in air to transform the dried gels into spinel oxide phases and the second one was done at 800°C in argon for the formation of delafossite oxide phase. The chemical and crystal structure and morphology of dried gels and annealed powders were characterized by FT-IR, XRD and XRF while the morphology of nanostructure of annealed delafossite oxide was observed by SEM image. Magnetic properties were measured by vibrating sample magnetometer. The CuFe_{1-x}Ni_xO₂ (x = 0.01-0.05) samples exhibited a weak ferromagnetic behavior and a linear paramagnetic behavior upon hysteresis was observed. The undoped powder cannot be observed the magnetic hysteresis however small kink can be observed. In addition, chemical state of delafossite oxide was also studied from the modification of valence states near Cu, Fe and Ni k-edges.

Keyword: Sol-gel method, magnetic properties, XAS, delafossite oxides

101

TiO₂-doped WO₃ coated on charcoal activated with increases photocatalytic and antibacterial properties synthesized by microwave-assisted sol-gel method

Author: Weerachai Sangchay¹

¹ *Songkhla Rajabhat University*

Corresponding Author: weerachai.sang@yahoo.com

TiO₂-doped WO₃ coated on CA were prepared by microwave-assisted sol-gel method. The calcined at the temperature of 500 °C for 2 h with a heating rate of 10 °C/min were characterized by XRD, EDS and SEM. The photocatalytic and an antibacterial activity of TiO₂-doped WO₃ coated on CA were investigated by means of degradation of a MB solution and against the bacteria E.coli respectively. The effects of WO₃ concentration were discussed. The 1mol%WO₃-doped TiO₂ coated on CA seems to exhibit the higher photocatalytic and an antibacterial activity than other samples. The TiO₂-doped WO₃ coated on CA are expected to be applied as a materials photocatalyst for the water purification.

102

THALIDOMIDE IMPRINTED NANOPARTICLES ON THE THIN-FILM LAYERS OF INTERDIGITATED CAPACITIVE ELECTRODE FOR SENSOR APPLICATIONS

Co-author: Roongnapa Suedee¹

¹ 1

Corresponding Author: roongnapa.s@psu.ac.th

In this study, we describe the development of thalidomide sensor for detection of the chiral drug enantiomers at low concentration in the buffer and whole blood sample based on microcontact imprinting, molecularly imprinted polymer nanoparticles (MIP) as a stamp in a film of non-conducting polymer using interdigitated capacitance electrode (IDC) and surface-enhanced Raman scattering (SERS). The characterization of the obtained MIPs with film cast and topography as well as surface properties (height, roughness, chemical function, thermodynamic) properties were studied by atomic force microscopy (AFM) and Raman-AFM image and spectra. The results revealed that the interaction between particle-particle, drug-particle and enantiomer-MIP at a molecular level. AFM image and force curve analysis provided the differences of force surface adhesion from (R)-enantiomer imprint in film-cast much higher than (S)-enantiomer MIP indicating drug-binding interaction can be used to detect enantiomers and distinguished between the two enantiomers. In addition, the thickness of AFM and surface protein matrix at dry state was different between this two MIPs. The different arrangement of the surface capture on IDC was prepared with respect to electromagnetic field lines depend on the two different functional groups cause a significant different resistance response to the analyte in buffered solution and blood compared to the control. The MIP interdigitated capacitance measurement helped to clarify the surface enhanced Raman scattering (SERS) results from the effected of both layer and the combination effect between biomolecules and polymers. Taken together with the Raman-map and IDC study revealed differentiation of exposed partially buried residues by the reactivities of drug-particle interaction with accessible surface area. The important characteristics of the small distance of thin-layer increased with the added layer of biomatrix affect the interaction between active sensor and MIP cause in the low concentration of thalidomide enantiomers induced the increase of resistance signal and/or charge transfer between enantiomers in MIPs layer and matrix.

Heron 2 / 103

Metal Phthalocyanine and Metal Oxide Modifying Multiwall Carbon Nano Tube Paste Sensors for Classification of Sweet Taste

Author: Theerasak Juagwon¹

Co-author: Arthit Jityen¹

¹ *Materials Science and Engineering Program, and Capability Building Unit of Nanoscience and Nanotechnology, Faculty of Science, Mahidol University*

Corresponding Authors: j.arthit89@gmail.com, oobth_1@hotmail.com

In this work, high efficient sensor array for sweet taste classification was demonstrated for electronic tongue application. The sensor array was fabricated by electrochemical sensors based on multiwall carbon nanotube (MWCNT) paste blending with modify electroactive species including either nickel oxide (NiO), copper oxide (CuO), cobalt phthalocyanine (CoPC) or iron phthalocyanine (FePC). The sensor arrays was design to response to varieties of sweet. Samples used for sweet taste classification had the same sweetness level with different kinds of sweeteners including of glucose, fructose, maltose, sucrose and honey. Cyclic voltammogram (CV) of the modified MWCNT paste sensor was performed in the sweet taste solutions in the range of 0 to 1 V. The CV feature of the metal phthalocyanines and metal oxides can be modified due to dominant oxidation and reduction of sugar molecule catalyzed by the blended materials. To classify sweet taste, input variables of principal component analysis (PCA) were extracted from the measured CV. The PCA results were clearly separated indicating that the sweet samples can be clearly classified by this modified sensor array. The relative positions of the data clusters can approximately relate to molecular weight of sugars, i.e. monosaccharide sugars (glucose and fructose) and disaccharide sugar (maltose and sucrose). The data group of honey presented at area between the area of mono- and di-saccharide sugar because this sweetener composed of both types of sugars. The PCA results also showed that the input parameters from CuO modified sensor had the strongest influence on the first principle component.

Heron 1 / 104

Observing Chitooligosaccharide Traveling through a Biological Nanopore of *Escherichia coli*

Author: H. Sasimali M. Soysa¹

¹ *School of Chemistry, Institute of Science, Suranaree University of Technology*

Corresponding Author: sasimalisoysa@gmail.com

Observing Chitooligosaccharide Traveling through a Biological Nanopore of *Escherichia coli*
H. Sasimali M. Soysa¹, 2 and Wipa Suginta^{*1, 2}

¹Biochemistry-Electrochemistry Research Unit, Suranaree University of Technology, Nakhon Ratchasima, Thailand

²School of Chemistry, Institute of Science, Suranaree University of Technology, Nakhon Ratchasima, Thailand

Tel: +66-44226187; E-mail: wipa@sut.ac.th

Porins assembled inside the outer membrane of Gram-negative bacteria typically serve as molecular filters, allowing hydrophilic compounds to pass through by either general diffusion or facilitated diffusion process. Porins are composed of β -strands that lie in an antiparallel fashion and form a cylindrical tube, called a β -barrel, with overall dimension of 1-3 nm in diameter and 5 nm in height. In this report, we describe the identification and characterization of chitoporin, namely EcChiP, from *Escherichia coli*. Using black lipid membrane reconstitution (BLM) technique, we prove that EcChiP could readily form a stable nanopore in artificial phospholipid membranes, permitting an ion flow of average conductance of 0.55 ± 0.01 nS. Together with bulk permeation study by liposome swelling assays, we demonstrate that EcChiP is a sugar-specific transporter, with pronounced specificity towards long-chain chitooligosaccharides. From physiological point of view, this study provides the first evidence that non-chitinolytic bacteria (here is *E. coli*) can exploit chitin degradation products as alternative energy supply to thrive under glucose-deficient conditions by expressing chitoporin as a molecular gateway for nutrient uptake.

Keywords: Biological nanopore; chitooligosaccharides; single channel conductance; sugar transporter

Supported by Suranaree University of Technology and the Thailand Research Fund.

105

Silica Nanoparticle Synthesis and Characterization with Dynamic Light Scattering Method: Solution Stability

Author: Shadmani Shamim¹

¹ *Asian Institute of Technology*

Corresponding Author: st118190@ait.asia

Dynamic light scattering (DLS) offers a quick and convenient nondestructive means of particle size and zeta potential determination. However, reliability and repeatability of readings is oftentimes dependent on the type of DLS instrument, analytical procedures and solution conditions (and aging). 1. Changes in sizes of particles, e.g. by agglomeration or adsorption, in suspension in particular, can and do result in changes in particle diffusion and velocity and hence, light intensity. Scattering angle and solution viscosity are also known to influence particle size readings by DLS [3]. Alternative techniques like atomic force microscopy (AFM) can yield values significantly different from those obtained by DLS [2]. Here we measure particle size by DLS and study with statistical analysis how

solution ageing and solution conditions impact particle size. Results are compared to transmission electron microscope (TEM) analysis.

1 H. Kato, M. Suzuki, K. Fujita, M. Horie, S. Endoh, Y. Yoshida, H. Iwahashi, K.

Takahashi, A. Nakamura and S. Kinugass; Reliable size determination of nanoparticles using dynamic light scattering method for in vitro toxicology assessment, *Toxicology in Vitro*, 23(5), 927-934 (2009)

[2] B.G. Zanett-Ramos, M.B. Fritzen-Garcia, C.S. de Oliveira, A.A. Pasa, V. Soldi, R.

Borsali, T.B. Creczynski-Pasa; Dynamic light scattering and atomic force microscopy techniques for size determination of polyurethane nanoparticles, *Materials and Science Engineering: C*, 29(2), 638-640 (2009)

[3] C. Xu, X. Cai, J. Zhang and L. Liu; Fast nanoparticle sizing by dynamic light scattering; *Particle*, 19, 82-85 (2015)

106

Quantitative analysis of aqueous methanol solution using hyperspectral imaging

Author: Itthi Chatnuntawe¹

¹ *National Nanotechnology Center, Thailand*

Corresponding Author: itthi.cha@nanotec.or.th

Hyperspectral imaging is a spatio-spectral imaging technique that is capable of acquiring the electromagnetic spectrum at each spatial location in an imaging field of view. Since certain objects leave unique spectral profiles in the electromagnetic spectrum, hyperspectral imaging has gained in importance in a wide range of applications including material detection and identification. This work investigates the feasibility problem of estimating the methanol concentration of an aqueous methanol solution using hyperspectral imaging. Instead of adopting conventional techniques that are labor-intensive and typically require skilled staffs, we propose a real-time semi-automated method for methanol concentration estimation based on hyperspectral imaging. In particular, we image an aqueous methanol solution in the near-infrared region of the electromagnetic spectrum using a hyperspectral imaging system. The methanol concentration is then estimated from the acquired hyperspectral data by solving a constrained convex optimization problem. We demonstrated the feasibility of the proposed method using several sets of aqueous methanol solutions, each with five different concentrations. The methanol concentrations estimated using the proposed method were in good agreement with the expected concentrations.

107

Rapid VOC sensors based on electrolytically exfoliated graphene-loaded flame-made La-doped SnO₂ composite films

Author: nantikan tammanoon¹

¹ *Chaing mai University*

Corresponding Author: cherrynantikan@gmail.com

In this work, flame-made SnO₂ nanoparticles were systematically studied by doping with 0.1–2 wt % lanthanum (La) and loading with 0.1–10 wt% electrolytically exfoliated graphene for low detection of VOCs gases including acetone (C₃H₆O) and ethanol (C₂H₅OH) gases occurred in human breathe. The sensing films were prepared by a spin-coating technique on Au/Al₂O₃ substrates and evaluated to 6–400 ppm acetone and 3–200 ppm ethanol at working temperatures ranging from 150 to 350°C

in dry air. Structural characterizations by electron microscopy, X-ray analysis and raman spectrometry further demonstrated that La doped SnO₂ nanostructures had a spheriodal morphology with a polycrystalline tetragonal SnO₂ phase, and La was confirmed to form a solid solution with SnO₂ lattice while graphene in the sensing film after annealing and testing still retained its high-quality nonoxidized form. Gas-sensing results evidently showed that SnO₂ sensing film with optimal 0.5 wt% La-doping concentration exhibited high response of ~1200 toward 400 ppm acetone and ~700 toward 200 ppm ethanol with ultra-high detection speed with very short response time within a few seconds at 350°C. The additional loading of graphene at 0.1wt % into 0.5wt% La-doped SnO₂ led to a drastic response enhancement to ~4100 toward 400 ppm acetone at 350°C and ~1700 toward 200 ppm ethanol at 300°C with shorted response time. The superior gas sensing performances of La-doped SnO₂ nanoparticles loaded with graphene may be attributed to the large specific surface area of the composite structure, specifically the high interaction rate between acetone and/or ethanol vapor and graphene–La-doped SnO₂ nanoparticles interfaces and high electronic conductivity of graphene. Therefore, the 0.1wt% graphene loaded 0.5 wt % La-doped SnO₂ sensor is a promising candidate for fast, sensitive and selective detection of VOCs. Furthermore, the sensors displayed very high VOCs selectivity against SO₂, H₂S, NH₃, C₂H₄, C₂H₄O, CH₄ and H₂. Therefore, the graphene loaded La-doped SnO₂ sensor are potential for responsive and selective detections of VOCs at a threshold limit value (TLV) of permissible legal limit of acetone and ethanol concentration in human's breath which may be essential for drunken driving detection and biomedical applications.

108

Colloidal properties of montelukast sodium nasal spray

Author: Thunyaporn Jullaphant¹

¹ 1

Corresponding Author: thunya.new387@gmail.com

Montelukast sodium (MTL) is leukotriene receptor antagonist indicated for prophylaxis and treatment of asthma and is widely used treatment for systemic and local diseases of the upper respiratory tract. However, MTL has many adverse effects including cough, fever, bronchitis, agitation, aggression, anxiousness, hallucinations, depression, insomnia, restlessness, suicidal ideation and liver dysfunction. Therefore administration of MTL locally can result in significant reduction in dose and possibly avoid systemic side effects. In this study, we reported MTL nasal spray formulation prepared as a colloid solution using hydroxypropyl cellulose (HPC) and Carbomer 934 (C934) as a mucoadhesive agent. Colloidal systems are dispersed systems which the size of dispersed phase is less than 1 µm. MTL nasal sprays were formulated by dissolving the polymers i.e., HPC from 0.01% to 0.5% w/v and C934 from 0.005% –0.15% w/v with MTL to form a colloidal system followed by the adjustment of pH. The colloidal system can enhance binding between the drug and the receptor at the nasal epithelial cell. The dose of MTL was calculated to be 240 ng for single administration. The prepared formulations were evaluated for colloidal properties using zetasizer. Other properties including pH, viscosity, particle size and droplet size were also determined. The MTL formulations containing HPC was clear whereas the formulations with C934 was clear to cloudy which depended on the polymer concentration. The particle size and polydispersity index was found to be 167 nm and 0.34, respectively for MTL solutions. The particle size of the MTL with C934 was 800 –2,500 nm with the size being related directly to the concentration of the polymer. On the other hand, the particle size of the formulations with HPC was 80 –400 nm showing an inverse relation with the concentration of HPC. The particle size of all formulations was larger than the pore size of the nasal epithelial tight junction (20 Å). It is unlikely that the particles will enter the blood circulation via paracellular pathway and avoid systemic side effects. The particle charge of all formulations was negative. The zeta potential of the formulations with HPC was in the range 1 –6 mV whereas it was 40 –60 mV for formulations with C934. Due to the higher value of zeta potential of C934 formulations as compared to HPC formulations, the formulations with C934 would be more stable than formulations with HPC with less chances of particle aggregation. pH of all formulations was in the range of 7 to 8. The viscosity of the formulations with C934 was found to be 2 –5 cPs which was suitable for sprays whereas in case of HPC, it was 2 –80 cPs which was found to depend on the concentration. The formulations with HPC at concentrations 0.3 and 0.5% w/v were unsuitable for efficient spray formulation.

The average droplet size of the formulations with C934 was in the range of 50–80 μm that is suitable for nasal spray whereas the droplet size of the formulations with HPC was in the range 40–400 μm . The HPC concentrations at 0.1–0.5 % w/v produced the droplet size larger than 100 μm indicating that the concentration was influenced by the droplet size. Overall physicochemical properties of all formulations met the requirement for optimum nasal drug delivery. However, the stability of the formulations need to be evaluated further in a long term basis.

Key words: montelukast sodium, hydroxypropyl cellulose, Carbomer 934, colloidal

Heron 2 / 109

Selective Permeability of Antimicrobial Agents through the Protein Nanopore of the Highly-Drug Resistant Melioidosis Bacterium *Burkholderia pseudomallei*

Author: Anuwat Aunkham¹

¹ School of chemistry, Suranaree university of technology

Corresponding Author: terklor@hotmail.com

Selective Permeability of Antimicrobial Agents through the Protein Nanopore of the Highly-Drug Resistant Melioidosis Bacterium *Burkholderia pseudomallei*
Anuwat Aunkhum, 2 and Wipa Suginta*^{1,2}

1Biochemistry-Electrochemistry Research Unit, Suranaree University of Technology, Nakhon Ratchasima, Thailand

2School of Chemistry, Institute of Science, Suranaree University of Technology, Nakhon Ratchasima, Thailand

Tel: +66-44226187; E-mail: wipa@sut.ac.th

BpsOmp38 is a trimeric β -barrel protein abundantly located on the outer membrane of the ultra-drug resistant Melioidosis bacterium *Burkholderia pseudomallei*. Each barrel of BpsOmp38 has a diameter of about 1.2 to 1.5 nm and contains 16 β -strands connected with each other in an antiparallel fashion. This biological nanopore acts a molecular entry, allowing small, hydrophilic molecules, such as monosaccharides, amino acids, and antimicrobial agents, to pass through the bacterial membranes by passive diffusion. In our study, we determined the rates of sugar permeation, using liposome swelling assays and found that the permeability rates decreased as the molecular sizes of sugar increased. The permeation rates of the selected neutral sugars were in the order: L-arabinose (Mr 150) > D-galactose = D-glucose = D-mannose (Mr 180) > D-GlcNAc (Mr 221) > D-sucrose (Mr 342). Slight permeation of D-melezitose (Mr 522) or D-raffinose (Mr 504) was observed, suggesting the size exclusion limit of the molecules to pass through the BpsOmp38 nanopores to be < 500 kDa. The permeability of antimicrobial agents through the BpsOmp38 channel was further investigated and found to be barely correlated with molecular sizes, since most antimicrobial compounds carried net charge(s) that affected their relative mobility. For example, ceftazidime and cefoxitin with a net charge of -1 showed significantly higher permeating rates than the rates for meropenem and imipenem with a net charge of 0. The results emphasized the importance of ionizable groups lying inside the pore interior in controlling the molecular passage of BspOmp38. The data provide an implication for the strategic drug design that may help to improve the susceptibility of this highly drug resistant pathogen towards new drug molecules.

Keywords: Biological nanopore, outer membrane protein; melioidosis, antimicrobial resistance, *Burkholderia pseudomallei*

Supported by Suranaree University of Technology and the Thailand Research Fund.

Structural and electronic properties of the organic semiconductor ZnPc

Author: Witoon Nuleg¹

¹ *College of Nanotechnology, KMITL*

Corresponding Author: witoon_nuleg@hotmail.com

The structural and electronic properties of zinc phthalocyanine (ZnPc) monolayer were investigated using first-principles calculations. The calculated bond lengths and bond angles were found to be in good agreement with the previous works. The spin-polarized density of state (DOS) for ZnPc monolayer was presented. Furthermore, the effects of Sn intercalation on structural and electronic properties of ZnPc monolayer were also investigated. The change of bond lengths and bond angles nearby the intercalated Sn atom were analyzed. It was found that the obtained DOS is significantly changed by the intercalated Sn atom. The details of these behaviors were presented and discussed.

Heron 1 / 111

Investigation the role of Co²⁺ in LiFePO₄ cathode material during batteries operation by In-situ XANES technique

Author: Patcharapohn Chantarasuwan¹

¹ *Materials Science and Nanotechnology Program, Faculty of Science, KhonKaen University, KhonKaen, 40002, Thailand*

Corresponding Author: pp.chantra@gmail.com

Rechargeable lithium ion batteries are amongst the most advanced electrical energy storage system available today. Many families of compounds have been developed for use as cathode materials in Li-ion batteries such as layered oxides LiMO₂ (M = Co, Ni, Mn, or V), manganese spinel (LiMn₂O₄), and phospho-olivines LiMPO₄ (M = Fe, Mn, Co, or Ni). Lithium iron phosphate (LiFePO₄) have become the most interesting cathodes materials for lithium ion batteries because of their inexpensive, environmental friendly, high theoretical capacity (170 mAh/g) and long cycle life and high safety. However, LiFePO₄ inherently show poor electronic conductivity causing low rate performance. Many approaches have been used to improve conductivity of this material, e.g. carbon coating and nano-sizing. These also include isovalent doping which significantly increasing conductivity of the material.[1-3] Co is an element widely chosen as dopant due to the increasing of rate capability. However, there is not clearly evident showing mechanism of Co²⁺ incorporating with the improving rate capability during batteries operation. Here, we study the electronic structure change of Co²⁺-doped LiFePO₄ materials during battery operation by in-situ X-ray absorption near edge structure (XANES). The materials were synthesized by the solid-state reaction. The single phase of LiFePO₄ was confirmed by X-ray diffraction. The in-situ Co and Fe K edge XANES were measured during charge-discharge to observe the oxidation state of Co²⁺. The XANES result indicate that the oxidation state of Co²⁺ do not incorporate in phase transition during batteries operation. It only provides the improvement in conductivity of LiFePO₄ material.

1. Chung, S.Y., J.T. Bloking, and Y.M. Chiang, Electronically conductive phospho-olivines as lithium storage electrodes. *Nat Mater*, 2002. 1(2): p. 123-8.
2. Xu, G., et al., First-principles study of structural, electronic and Li-ion diffusion properties of N-doped LiFePO₄ (010) surface. *Solid State Ionics*, 2015. 281: p. 1-5.
3. Takahashi, M., et al., Reaction behavior of LiFePO₄ as a cathode material for rechargeable lithium batteries. *Solid State Ionics*, 2002. 148(3): p. 283-289.

112

The novel preparation of encapsulated Thai herbal extract-Alginate complex against bacteria caused periodontal diseases

Author: Jariya Romsaiyud¹

¹ *Department of Chemistry and Center of Excellence for Innovation in Chemistry, Faculty of Science, Ramkhamhaeng University, Bangkok 10240, Thailand*

Corresponding Author: jromsaiyud@gmail.com

Periodontal disease is an infection of polymicrobial around tooth-supporting tissues. The aim of this study is to assess recent therapeutic strategies in which biocompatible nanoparticles are used. The active compounds were extracted from Thai herbal and entrapped in calcium alginate beads prepared with sodium alginate by the ionotropic gelation method using calcium chloride as a crosslinking agent. The beads were evaluated for particle size and surface morphology using optical microscopy and SEM, respectively. In vitro studies against bacterial caused periodontal disease that have investigated the biocompatibility or efficacy of certain nanoparticle formulations are presented. Future directions in the application of nanoencapsulation techniques in periodontal therapies are discussed.

113

Preparation and Evaluation of Nanosuspension-based Sildenafil Pressurized Metered-dose Inhalers for Treatment of Pulmonary Arterial Hypertension Using Poloxamer 188 as a Stabilizer

Author: Charisopon Chunhachaichana¹

¹ *DDSEC, Faculty of Pharmaceutical Sciences, Prince of Songkla University*

Corresponding Author: ch.chari.21@gmail.com

Sildenafil is a phosphodiesterase-5 (PDE5) inhibitor approved for the treatment of pulmonary arterial hypertension; commercially available in oral and intravenous forms. The major obstacles in developing a new dosage form of sildenafil are its limited solubility and stability. To develop an alternative, pulmonary dosage form, these problems must be overcome. The objectives of this study are to formulate the nanosuspension-based sildenafil pressurized metered-dose inhalers using poloxamer 188 (P188) as a stabilizer and to evaluate their physical and chemical stability, delivered dose uniformity, in vitro aerosol performance, hydrodynamic particle size, and cytotoxicity. Twelve formulations of nanosuspension-based sildenafil pMDIs were prepared by the bottom-up process and pressure filling method. The formulations consisted of nano spray-dried sildenafil citrate, P188, sorbitan monooleate, ethanol, and HFA134a. Sildenafil content and delivered dose uniformity were evaluated using in-house sampling technique and high-performance liquid chromatography. In vitro aerosol performance was evaluated using a Next Generation Impactor. The dose uniformity of sildenafil content in formulation #5-12 was displayed throughout their lifespan (82.21-95.07 %). The results of aerosol performance including, emitted dose (ED), fine particle fraction (FPF), and mass median aerodynamic diameter (MMAD) of formulation #5-12 varied from 77.49-87.55 %, 51.55-62.61 %, and 1.26-1.81 μm , respectively, and the geometric standard deviation (GSD) of the results were approximately 2, which indicates a good distribution of data. Formulation #7 was selected by MODDE software as an optimal formulation based on specified criteria. The analysis of the aerosol parameters displayed the effect of ethanol content on ED and FPF, and P188 content on MMAD. The selected formulation was chemically and physically stable throughout 6 months. The hydrodynamic particle sizes of selected formulation in dichloromethane and milli-Q water obtained at month 1 were 243.8 ± 13.5 nm and 466.6 ± 138.0 nm, respectively, and the results obtained at month 6 were 255.6 ± 16.5 nm and 481.0 ± 97.6 nm, respectively, with the polydispersity indices (PDI) less than 1. The zeta potentials of the selected formulation obtained at month 1 and month 6 were -44.6 ± 2.5 and -43.4 ± 0.4 mV, respectively, which indicated a good stability. No cytotoxicity was found. This study has successfully formulated stable nanosuspension-based sildenafil pMDI using P188 as a stabilizer. The

delivered dose uniformity and aerosol parameters were within the appropriate ranges; thus, P188 displayed a promising use in the pulmonary delivery system.

114

Biosensing with allosteric nano-biocatalysts: A reductase subunit of a bacterial hydroxylase as molecular example

Author: Somjai Theanponkrang¹

¹ School of chemistry Suranaree University of Technology

Corresponding Author: mamshopping@hotmail.com

Biosensing with allosteric nano-biocatalysts:
A reductase subunit of a bacterial hydroxylase as molecular example

Somjai Theanponkrang,¹ Jeerus Sucharitakul,² Pimchai Chaiyen,³ Wipa Suginta¹ and Albert Schulte¹

¹Biochemistry –Electrochemistry Research Unit & Center of Excellence in Advanced Functional Materials

School of Chemistry, Suranaree University of Technology, Nakhon Ratchasima, Thailand

²Department of Biochemistry, Chulalongkorn University, Bangkok, Thailand

³Department of Biochemistry, Mahidol University, Bangkok, Thailand

E-mail: schulte@sut.ac.th

Abstract

p-Hydroxyphenylacetate (HPA) hydroxylase (HPAH) from *Acinetobacter baumannii* is a distinct double-subunit enzyme that capably exploits functional cooperation between its reductase (C1) and oxygenase (C2) segments for biocatalytic conversion of substrate HPA into product 3,4-dihydroxyphenylacetate. Earlier biochemical studies¹ had shown that isolated C1 on its own is a potent converter of NADH into NAD⁺, with dissolved molecular oxygen (O₂) used as partner for required enzyme redox recycling. Hydrogen peroxide (H₂O₂) is a well assessable by-product of cyclic C1/NADH/O₂ interaction, which by allosteric stimulation is much intensified through HPA effector bonding to a matching C1 affinity site.

Reported here will be exploitation of H₂O₂ electroanalysis as novel non-biochemical assay for thorough inspection of favourable C1 allostery. The most common electrochemical H₂O₂ screen, namely anodic analyte detection at carbon or noble metal working electrodes with high enough positive polarization, was impractical here as variations in the electrolyte levels of C1 substrate NADH and C1 effector HPA produced H₂O₂ signal-interfering oxidation currents. Low-potential cathodic H₂O₂ detection at Prussian blue modified screen printed carbon electrodes could, on the other hand, measure H₂O₂ in suitable HPA/NADH interference free manner. When pre-dissolved C1 was challenged in electrolyte with NADH additions cathodic H₂O₂ amperometry was indeed sensitive enough to recognize the onset of substrate conversion activity of the nano-biocatalyst almost instantly and follow the enzymatic process until total NADH depletion with truthful current traces. Comparative amperometric trials in solutions without and with different levels of HPA verified electrochemically very well the pronounced concentration dependence of the allosteric acceleration of C1-driven NADH-to-NAD⁺ turnover due to an affinity capture of the stimulating phenolic compound. Accomplishment of the highly efficient electroanalysis of C1 allostery allowed further explorations as novel competitive analytical practice for trace NADH or HPA quantification. The potential of the latter compound as a urinary biomarker of, for instance, intestinal microbial overgrowth² ('Dysbiosis') or brain defects such as Major Depressive Disorder and Parkinson Disease³ in mind, amperometric HPA valuation has advantages. Facilitation of the analytical assay by the nanoscopic biological machinery of allosteric enzyme catalysis bestows applicants with an exceptional analyte specificity while the simplicity and low prize of involved electrochemical apparatus is encouraging routine use of the methodology in country-wide communal clinical lab facilities.

Keywords: Nano-biocatalyst; enzyme allostery; cathodic H₂O₂ detection; amperometry

1J. Sucharitakul, P. Chaiyen, B. Entsch, D. P. Ballou. The reductase of p-hydroxy-phenylacetate 3-hydroxylase from *Acinetobacter baumannii* requires p-hydroxyphenyl-acetate for effective catalysis,

Biochemistry, 44 (2005) 10434. 2R. S. Lord, J. A. Bralley. Clinical Applications of Urinary Organic Acids. Part 2. Dysbiosis Markers. Alternative Medicine Review, 13 (2008) 292. 3M. An, Y. Gao. Urinary Biomarkers of Brain Diseases. Genomics, Proteomics & Bioinformatics, 13 (2015) 345.

115

Colloidal chitin-soaked nanoporous carbon nanotube thin films as biocompatible immobilization matrix of amperometric enzyme biosensors with long life-time

Author: Waraporn Rernglit¹

¹ School of Chemistry, Suranaree University of Technology

Corresponding Author: kob8883@gmail.com

Colloidal chitin-soaked nanoporous carbon nanotube thin films as biocompatible immobilization matrix of amperometric enzyme biosensors with long life-time

Waraporn Rernglit, Wipa Suginta and Albert Schulte

Biochemistry –Electrochemistry Research Unit & Center of Excellence in Advanced Functional Materials

School of Chemistry, Suranaree University of Technology, Nakhon Ratchasima, Thailand

*E-mail: schulte@sut.ac.th or wipa@sut.ac.th

Abstract

Well-working amperometric enzyme biosensors are ideal tools in the (bio-) analytical chemistry sector as they offer the superb selectivity of biological recognition elements together with the simplicity and sensitivity of modern electrochemical equipment. 1 Key factor for successful electrochemical enzyme biosensor manufacture is a gentle but leak-protected biocatalyst fixation ('immobilization') on the electrode surface that translates substrate conversion into signal.

Here, a carbon nanotube (CNT)/chitin electrode layer is introduced as nanoporous composite enzyme immobilization matrix, for glucose oxidase (GOx) as model protein and platinum or gold disk electrodes as physicochemical transducers. Motivation behind an integration of the marine biopolymer chitin into the desired biosensor architecture was a gain of matrix biocompatibility and, as a consequence, a good GOx survival and related analytical response stability. The target biosensor design was actually realized via simple drop/dry coating steps, namely via serial load of the electrode disks with μL droplets of (1) a water suspension of CNT, (2) a water solution of GOx and (3) an aqueous colloidal chitin suspension, with solvent evaporation allowed after droplet placement. Optionally, a thin epoxy-based polymeric top-coat was placed as extra barrier against enzyme loss; it was obtained via application of commercial cathodic electrodeposition paint (EDP).

Repeated conventional amperometric calibration runs confirmed for the CNT/GOx/Chitin/EDP glucose biosensors a linear range that extended competitively wide up to a few tens of mM and, with sensors in between trials stored in phosphate buffersolutions of pH 7.0 and at 4°C, signal stability was observed for periods up to weeks. Successful with close to ideal recovery rates were quantitative assessments of spiked model samples and continuous biosensor use in a flow-based three-electrode electrochemical cell with scheduled on-line glucose calibration measurements during uninterrupted flow cell operation. Apparently, electrode surface-immobilized GOx entities were in the CNT/chitin environment kept healthily in place and thus able to maintain their pronounced bio-catalytic activity for long. Possible was as a result an electrochemical biosensing service on an extended time scale for glucose quantifications, with adequate analytical figures of merit for analyte quantifications.

Keywords: Biosensors, amperometry, carbon nanotubes, chitin, enzyme immobilization

References: 1G. Rocchita et al. Enzyme biosensors for biomedical applications: Strategies for safeguarding analytical performances in biological fluids. Sensors, 16 (2016) article no. 780. 2E, Y. Jomma, S.-N. Ding. Recent advances on electrochemical enzyme biosensors. Current Analytical Chemistry, 12 (2016) 5. 3J. Wang. Electrochemical glucose biosensors. Chemical Reviews, 108 (2008) 814.

Falcon 1 / 116

Electrospun nanofibers of polylactide (PLLA)/ polyglutamic acid (γ -PGA) blends and their use as ammonia detecting kits in intelligent meat packaging

Author: Soksreymeng Sdok¹

¹ *Sirindhorn International Institute of Technology*

Corresponding Author: mengsd@hotmail.com

Freshness of products is a key factor for food industry to monitor to ensure high quality products and retain customers' satisfactory. Integrity package is capable of pointing out the quality of the products, based on the reaction between indicator and metabolites of spoilage microorganisms. In these regards, detection of volatile compounds such as ammonia gas is one of effective approaches in monitoring meat freshness. Functionalized nano-sensors, such as nanofibers with high surface areas and light weight, are attractive candidates for use in these applications by embedding in package headspace. This can lead to enhancement in detection efficiency of the devices. In this work, nanofibers of blends of biodegradable and biocompatible polylactide (PLLA) and hydrophilic polyglutamic acid (γ -PGA) are prepared by electrospinning. This leads to a combination of carboxylic acid functional groups on supporting PLLA matrix nanofibers. The nanofibers are prepared at 4 PLLA/ γ -PGA ratios (100/0, 95/5, 85/15 and 75/25). To restrain the presence of γ -PGA, the blended fibers are cross-linked by employing reaction of their carboxylic acid and hydroxyl groups of glycerol (G) and ethylene glycol (EG). FTIR and SEM results suggest that the γ -PGA component is released from the original (untreated) PLLA/ γ -PGA fibers when submerged in water, while those cured by EG and G can retain high amount of γ -PGA on the fibers. Comparing the efficiency of cross-linkers, EG exhibits high value of retaining γ -PGA due to its higher the reactivity. The ammonia absorption activity of the materials are examined. The results clearly depict that the fibers can absorb ammonia molecules by using the reaction of carboxylic acid groups on γ -PGA. The materials have high potential for use as test kits for monitoring meat freshness or in extending shelf life of the products.

117

Characterization of carbon fibers from Thai horse manure via hydrothermal carbonization

Author: Apiluck Eid-ua¹

¹ *College of Nanotechnology, King Mongkut's Institute of Technology*

Corresponding Author: apiluck.ei@kmitl.ac.th

Carbon fibers from biomass have been successfully prepared via hydrothermal-carbonization and activated in air atmosphere for catalyst supporter. In this research, we study the effect of temperature (160 -200 °C) and residence time (4-24 h) to pretreat the initial carbon precursor in terms of chemical properties (i.e. carbon content, surface functional group) including the physical properties such as porosity and total surface areas. Afterwards, carbonization was obtained at the temperature of 300 °C for 2h for developing the porosity and even removing the contaminants of hydrothermal char to reach the carbon fiber. Nevertheless, carbon fiber was characterized. Scanning electron microscopy (SEM) and Functional Transform Infrared spectroscopy (FTIR) were employed to characterize physical morphology and functional group on the surface, respectively.

Falcon 1 / 118

Effect of F incorporation on physical, electrical and optical properties of hydrothermally grown ZnO nanorods

Author: Wuttichai Sinornate¹

¹ *College of Nanotechnology, King Mongkut's Institute of Technology Ladkrabang, Thailand*

Corresponding Author: kan1479@gmail.com

F-doped ZnO nanorod were synthesized via hydrothermal process with variation of processing temperature and Fluorine doping contents (0-10%) starting from zinc oxide thin film as a seeding layer for nanorod growth. The zinc oxide seeding thin film was prepared by sol-gel spin coating at 2000 rpm on glass substrate using zinc acetate precursor with annealing at 500 °C in air for 2 h. Ammonium fluoride (NH₄F) was used as F doping precursor. The properties of F-doped ZnO nanorods were characterized by field emission electron microscope (FESEM), X-ray diffraction (XRD), energy-dispersive X-ray spectroscopy (EDX), Four-point probe technique and UV-Visible spectrophotometer. Corresponding results indicated that growth of ZnO:F nanorod with good crystallinity and grown in (002) plane. The influence of F dopant incorporated into ZnO nanorods has been extensively investigated and discussed.

119

Nanoparticulate Copper Oxide, Manganese Oxide, and Cobalt Oxide Synthesized by Solution Combustion Technique for Glucose Detection

Author: Oratai JONGPRATEEP¹

¹ *Department of Material Engineering Kasetsart University*

Corresponding Author: fengotj@ku.ac.th

Enzymeless glucose detectors offer advantages in terms of temperature and humidity stability, as well as elimination of toxic chemicals usage. Various metal oxide materials are capable of exhibiting glucose catalysis activities. This research, therefore, aimed at developing nanoparticulate oxides for enzymeless glucose sensor applications. Copper oxide (CuO), manganese oxide (Mn₂O₃) and cobalt oxide (Co₃O₄) powders with sizes ranging from 30 to 90 nanometers were successfully synthesized by solution combustion technique and embedded into multi-walled carbon nanotubes (MWCNT). Electrocatalytic activities of the metal oxides/MWCNT in glucose solutions with concentration ranging from 0.1 to 10 mM were examined by cyclic voltammetry technique. Electrical signals with sensitivity in the range of 10-2 A/ (mM cm²) were observed. The results suggested potential implementation of CuO, Mn₂O₃ and Co₃O₄ in enzymeless glucose sensor applications.

120

Ultra-sensitive and highly selective H₂ sensors based on FSP-made Rh-substituted SnO₂ sensing films

Author: Chaikarn Liewhiran¹

¹ *Department of Physics and Materials Science, Faculty of Science, Chiang Mai University, Chiang Mai 50202, Thailand*

Corresponding Author: chaikarn_l@yahoo.com

In this research, SnO₂ nanoparticles doped with 0.1-2 wt% rhodium (Rh) were synthesized by flame spray pyrolysis (FSP) and systematically investigated for H₂-sensing applications. From X-ray and

electron microscopic characterizations, SnO₂ nanostructures exhibited spheroidal morphology with polycrystalline tetragonal SnO₂ phase and Rh might form solid solution with SnO₂ lattice. The sensing films were prepared by spin coating technique and their gas sensing performances were studied at the operating temperatures ranging from 100-350°C in dry air. Gas-sensing measurements showed that SnO₂ sensing films with the optimal Rh doping level of 0.2 wt% exhibited an ultra-high response of ~22,170, which was more than three orders of magnitude higher than that of undoped one, and a short response time of 6 s towards 30,000 ppm H₂ at an optimum operating temperature of 300°C. In addition, the optimal Rh-doped SnO₂ sensor displayed high H₂ selectivity against NO₂, SO₂, C₂H₄, C₃H₆O, CH₄, H₂S and CO. Thus, Rh-doped SnO₂ nanoparticulate films are promising candidates for hydrogen-sensing applications.

121

Characterization of bacterial cellulose produced from agricultural by-product by *Gluconacetobacter* strains

Author: Wichai Soemphol¹

¹ Faculty of Applied Science and Engineering, Khon Kaen University, Nong Khai Campus, Muang Nong Khai, Thailand, 43000

Corresponding Author: wichso@kku.ac.th

Bacterial cellulose (BC) is well known as natural biomaterial exhibiting a broad applications. In this study, in order to obtain the BC with low-cost production, isolation and characterization the newly isolates from the fermented products was carried out by using non-detoxified crude glycerol derived from biodiesel processing as sole carbon source. Based on 16S rRNA, *Gluconaceter xylinum* NKC19 was isolated and identified with the highest BC production of 12.31 g/l of dried weight BC by using 1% (w/v) of crude glycerol. Increasing of crude glycerol led the production decreased suggesting that the impurities in crude glycerol might affect the cell activity. The optimal BC production was found at acidic pH and yeast extract was favorable nitrogen source. Addition of pineapple peel extract by hot water into crude glycerol without any supplementation could improve BC production. The structural and morphological properties analyzed by X-ray diffraction (XRD) and scanning electron microscope (SEM) showed similar to that of produced from the other commercial sugars, glucose and glycerol as carbon source. This study demonstrated that utilization of the by-products from biodiesel industry and agriculture could be used as the sole source of nutrient for production of BC, being a potential biomaterial and applicable to other materials.

Keywords: bacterial cellulose, crude glycerol, biodiesel, agricultural by-product

Heron 2 / 122

Nanotechnology and Health

Author: Teerapol Srichana¹

¹ Prince of Songkla University

Corresponding Author: teerapol.s@psu.ac.th

Nanotechnology and Health
Teerapol Srichana

NANOTEC-PSU Excellence Centre on Drug Delivery System, Department of Pharmaceutical Technology, Faculty of Pharmaceutical Sciences, Prince of Songkla University, Hat-Yai, Songkla 90112, Thailand

Email address: teerapol.s@psu.ac.th

Nanomedicine and nanotechnology provides an early detection and prevention of diseases resulting in improved diagnosis, proper follow-up and treatment. Nowadays biological testings can be performed quickly and become more sensitive and reliable. Potential impact of nanoscience on healthy care is summarized and given in this presentation. Electronic networks with semiconductors interface nerve cells can be applied in brain research and neurocomputation. Quantum dots (nanometer-sized crystals) contain free electrons and emit photons when submitted to UV light have been introduced into early tumor detection and could locate as few as 10 to 100 cancer cells.

Nanoparticles are used for site specific drug delivery. This technique required drug dose is lowered therefore side-effects are lowered significantly as the active agent is deposited in that region only. This highly selective approach can reduce costs and pain to the patients. Various nanoparticles such as liposomes, liquid crystals, micelles find an application. Liquid crystal and micelles synthesized in house are used for drug encapsulation. Nanodelivery system together with drug targeting to the organ can deliver drug molecules to the desired location. A targeted medicine reduces the drug dose and side effects.

Nanomedicines may improve drug bioavailability both at specific places in the body and over a specified period of time. The molecules are targeted and delivered to precised cells.

Unique nanostructures were designed for controllable regulation of proliferation and differentiation of stem cells by designing unique nanostructures. This will lead to stem cell-based therapeutics for the prevention, diagnosis and treatment of human diseases. Nanofibers help heart muscle grow in the lab. Viruses are prevented to infect human by nanocoatings over proteins on viruses that could stop viruses from binding to cells. Nanorobots of nanosized delivery systems could break apart kidney stones, clear plaque from blood vessels, carry drugs to tumor cells. In the new era of personalized medicine we can have in vitro diagnostics, in vivo diagnostics, nanotherapeutics and theranostics. Current and future health care challenges are in the area of infectious diseases, cancer, genetic disorders, aging, obesity and addiction. Gene Therapy may be a solution in several diseases by employing electrostatic gene condensation, efficient cellular entry, non-toxicity and high gene expression/silencing.

Bioimaging has been employed together with new technology in confocal laser scanning microscope, quantum dots, fluorescence microscope. Advanced flow cytometry is capable to detect cells, infected cells and cell endocytosis and even the antibacterial activities from live and death cells.

Thus nanoparticles are promising tools for drug delivery advancement, as diagnostic sensors and bioimaging. The biodistribution of nanoparticles is still under investigated due to the difficulty in targeting specific organs. Efforts are made to optimize and understand the potential and limitations of nanoparticulate systems. It is expected that the benefits will be gained from nanotechnology including lower drug toxicity, improved bioavailability, reduced cost of treatment and extended economic life of proprietary drugs.

Some examples of drug delivery systems are examples of research work in the NANOTEC-PSU on amphotericin B and rifampicin in liquid crystals systems were demonstrated the successful stories of nanotechnology. We can use the liquid crystal as nanocubic and nanovesicle to encapsulate the drugs into the system to give more effectiveness with less toxicity to the cells

Key words: drug delivery stem, cells, bioimaging

Heron 1 / 123

Electrical Properties of Co-Doped LiFePO₄ Nanomaterial by Impedance Spectroscopy Technique

Author: Phongsit Krbao¹

¹ *Department of Physics, Faculty of Science, Khon Kaen University, Khon Kaen*

Corresponding Author: phongsit28338_@hotmail.com

Keywords: Impedance spectroscopy; Lithium iron phosphate; Electronic conductivity;

The ever-growing public and now commercial sentiment supporting the widespread adoption of low and zero-emission vehicles, it is unsurprising those Li-ion batteries which currently assume

the bulk of the cost of electrified vehicles. The main challenge is obtaining cathode material with high energy density, high safety, low cost, environment friendly and long cycle life. Lithium iron phosphate (LiFePO₄, LFP) has proved itself to meet these requirements. However, the key limitation has been extremely low electronic conductivity, until now believed to be intrinsic to this family of compounds. Cation doping is one of the most promising methods in improving conductivity of this material. Here, we study the electrical properties of Co-doped LFP samples synthesized by solid state reaction. The phase composition was identified by X-ray diffraction confirming the single phase of LFP. The unit cell volume of LFP obtained by Rietveld refinement method shows that it decreases with increasing Co contents. The electric properties of the samples were measured as a function of temperature and doping content by Impedance spectroscopy technique. The conductivity of LFP sample is dependent on Co doping level.

Acknowledge: PK acknowledges the financial support from the Thailand Research Fund and Human Resource Development in Science Project (Science Achievement Scholarship of Thailand, SAST)

Heron 1 / 124

Synthesis and identification of silica and activated carbon nanocomposite from rice husks for energy storage

Author: Yutthanakon Kanaphan¹

¹ *Materials Science and Nanotechnology Program, Faculty of Science, Khon Kaen University, Khon Kaen, 40002, Thailand.*

Corresponding Author: yutthanakon25994@gmail.com

The rapidly growing demand for renewable energy storages, there has been growing the interest in nanomaterials from biomass waste. One of the key to improve performance of the nanomaterial depends on the structure of materials. The rice husks (RHs) are the most agricultural biomass waste found in Thailand. They are source of SiO₂ and carbon nanostructure. Nano-silica (SiO₂) and activated carbon (AC) can be extracted from RHs employing a simple procedure without any destruction the nanostructures, which can provide high surface area and high electrical conductivity. In this work, SiO₂/AC nanocomposites were synthesized by calcination under Argon atmosphere at temperatures between 400 and 1,200 °C. The chemical and crystal structure of SiO₂/AC nanocomposites were identified by SEM, TEM, XRD and FTIR techniques, respectively. The XRD results show crystalline and amorphous phases of silica and carbon at different calcination temperature. The FTIR results show the intensity of the major chemical groups of SiO₂ and the aromatic hydrocarbons peak of AC. Moreover, the results also show the relationship between carbon allotropes and calcination temperature. The electrochemical properties of SiO₂/AC nanocomposites in lithium ion batteries depend on chemical groups of SiO₂ and the aromatic hydrocarbons of AC.

Acknowledgements: YK acknowledges the financial support from Young Scientist and Technologist Programme, NSTDA (YSTP: SCA-CO-2559-2446-TH)

Keywords: Rice husks; Silica; Activated carbon; energy storage.

125

Electrical properties of semi-conductive yarns based polyaniline for wearable ammonia detection

Author: Naraporn Indarit¹

¹ *Thammasat University*

Corresponding Author: narap.indarit@hotmail.com

Semi-conductive yarns have been developed for wearable gas sensor applications. Three types of semi-conductive yarns based polyester, rayon and cotton fiber are prepared by dip coating process in polyaniline solutions. The structure and surface morphology of semi-conductive yarns are analyzed by fourier transformed infrared spectroscopy and scanning electron microscope. The results showed that polyaniline is highly adsorbed onto cotton yarn compared with rayon and polyester. The electrical resistivity of cotton and rayon yarns coated polyaniline are found to be 0.299 ± 0.121 M Ω /cm and 0.794 ± 0.437 M Ω /cm, respectively, while polyesters exhibited very high resistivity. For the gas sensing properties, the semi-conductive cotton yarns are sawed onto the fabric and tested under ammonia gas environment. The results exhibited that their electrical resistivity is strongly depended on the ammonia gas concentrations operable at room temperature.

Heron 2 / 126

Production of Nanocellulose from Lime Residues Using Chemical-free Technology

Author: Saranya Jongaroontaprangsee¹

¹ King Mongkut's University of Technology Thonburi

Corresponding Author: saranyajong@hotmail.com

The feasibility of using lime residues after juice extraction as a raw material to produce nanocellulose was determined in this study. Different processing schemes were applied by varying the pretreatment and defibrillation methods and conditions. Autoclaving at 110-130 °C was performed as a pretreatment to remove hemicellulose and pectin from the native fiber. The fiber images obtained from transmission electron microscopy (TEM) technique revealed that the multiple homogenizing steps could effectively disintegrate the pretreated fiber into nanometer scale. X-ray diffraction (XRD) results showed that the prepared nanocellulose possessed much higher crystallinity index (CI) comparing to that of the native fiber; it was noted that the degree of CI was dependent on the processing conditions. The results suggested that there is a potential to produce nanocellulose from citrus by-products via the application of the developed chemical-free technology, which is safely to be used for food applications.

Keywords: Lime residues; Nanocellulose; Hydrothermal

Heron 1 / 127

Simulation of single quantum well solar cells

Author: Maetee Kunrugsa¹

¹ Department of Electrical Technology Education, Faculty of Industrial Education and Technology, King Mongkut's University of Technology Thonburi, Bangkok 10140, Thailand

Corresponding Author: k.maetee@gmail.com

III-V solar cells have been extensively studied in both theoretical and experimental aspects. The efficiency of the solar cells can be enhanced by the insertion of quantum structures as a result of the quantized energy levels at which photons with energy lower than the host material can be absorbed. A window layer made of a wide band gap material increases the absorption of high energy photons but is transparent to photons absorbed by the next layers. The window layer also decreases the surface recombination. AlGaAs is one of the material used as a window layer and exhibits good optical absorption properties. Furthermore, AlGaAs has a lattice constant nearly matched to GaAs

which is a well-known substrate, meaning that AlGaAs can be grown on GaAs with very low defect density. To design and optimize the solar cell structure, numerical simulation is very crucial as the fundamental phenomena of solar cell operation can be visualized prior to the implementation of real devices. In this work, a solar cell consisting of a single AlGaAs/GaAs quantum well with an AlGaAs window layer is simulated to gain the understanding in the influence of the quantum structure and the window layer on the solar cell performance. Other important parameters such as layer thickness and doping concentration are also varied to examine their effects.

128

Comparative Study on the Catalytic Activity and Stability between Pt-Decorated Ru surfaces and Ru-Decorated Pt Surfaces Catalysts for Methanol Electrooxidation

Author: karaked tedsree¹

¹ *Burapha University*

Corresponding Author: karaked@go.buu.ac.th

PtRu bimetallic nanocatalyst has been accepted as an effective catalyst for methanol fuel cells. However, there has been a constant effort for their commercial development. This work, the correlation between the surface structure of PtRu bimetallic nanocatalyst and their methanol electro-oxidation activity was studied. Pt-decorated Ru core-shell nanocatalyst ($Pt@Ru$) and Ru-decorated Pt core-shell nanocatalyst ($Ru@Pt$) were prepared by successive reduction. Firstly, the Pt^0 or Ru^0 particles were prepared by polyol process. Then, the reaction involved the reduction of the metal salts into atoms and decoration on the core particles. Different ratios of the core to shell were controlled synthesis by controlling the reaction conditions. The particle size shape and morphology of the obtained core-shell nanoparticles were analyzed by TEM. The crystal structure and surface structure of the samples were characterized by XRD and CO adsorption probe technique, respectively. The methanol electro-oxidation performance of the bimetallic catalysts was determined by cyclic voltammetry. The maximum activity of the $Pt@Ru$ core-shell sample was obtained with Pt to Ru ratio of 3:1 while of 1:2 for $Ru@Pt$ core-shell. The stability of $Ru@Pt$ core-shell catalyst determined by chronoamperometry was found higher than $Ru@Pt$ core-shell catalyst.

129

Highly sensitive room-temperature acetone gas sensor based Ag-loaded ZnO nanoflowers

Author: Rawat Jaisutti¹

¹ *Thammasat University*

Corresponding Author: rawat_phytu@hotmail.com

Highly-sensitive room-temperature operable gas sensors based on photocatalytic activity of Ag-loaded ZnO nanostructures are demonstrated as a possible candidate for sub-ppm acetone detection. Characterizations indicate that Ag nanoparticles are well deposited on the surface of hierarchical flowerlike ZnO nanostructures. To utilize the room-temperature operable gas sensor, Ag-loaded ZnO nanoflowers based chemiresistive-type structure is activated by an ultraviolet (UV) light illumination. The gas sensors show high sensitivity and excellent stability toward 100 ppm acetone gas at the optimized operating UV intensity of 5 mW/cm², which are approximately 5 times higher than that of pure ZnO. Moreover, sub-ppm detection of acetone with low-level of 200 ppb is possible realized by Ag-loaded ZnO nanoflower. These results make it a potential candidate material for developing as an excellent acetone gas sensing element of diabetes monitoring system.

130

A Controlled Release Formulation of Medicinal Plant Extract Decrease Inflammation in Human Vascular Endothelial Cells: A Preliminary for Diabetic Adjunctive Treatment

Authors: Amornpun Sereemasun¹; Kriangsak Khownum²

Co-author: Jariya Romsaiyud³

¹ *Nanobiomedicine Laboratory, Faculty of Medicine, Chulalongkorn University, Rama 4 road, Patumwan district, Bangkok, Thailand*

² *Excellent Center for Drug Discovery Faculty of Science, Mahidol University 272 Rama VI Rd., Ratchathewi, Bangkok 10400, THAILAND*

³ *Department of Chemistry and Center of Excellence for Innovation in Chemistry, Faculty of Science, Ramkhamhaeng University, Bangkok 10240, Thailand*

Corresponding Authors: jariyar@ru.ac.th, kkhownium@gmail.com, amornpun.s@gmail.com

Currently, 230 million people worldwide have been affected by diabetes and approximately 366 million people are expected to get diabetes by 2030. Diabetes mellitus is a disease characterized by altered glucose homeostasis, persistent hyperglycemia, chronic inflammation of circulatory system, leading to many complications. The injurious effects of hyperglycemia are separated into macrovascular complications (coronary artery disease, peripheral arterial disease, and stroke) and microvascular complications (diabetic nephropathy, neuropathy, and retinopathy). Previous study revealed that medicinal extracts from Amla, goji berry, and raspberry contain high antioxidant potency which are beneficial to cardiovascular system and lipid profiles. In this study, a time release formulation of amla extract, goji berry extract and raspberry powder was developed. The sustained release performance of the beads was investigated by measuring their disintegration and dissolution properties. In a pH=1 aqueous solution the beads developed a protective gel within one hour, maintain their integrity for more than ten hours; the beads, however, had completely disintegrated by the eleventh hour. In deionized water (pH=7), a thick gel formed and persisted for an entire eleven-hour period at the end of which time the beads were still visible. In the inflammation model of human vascular endothelial cells, this formulation significantly decreased inflammation markers, as well as reactive oxygen species. These findings suggest the potential use of this medicinal formulation for treatment and prevention of microvascular complication in diabetic mellitus.

131

Hydrophilic and Photocatalytic properties of Dip-coated Synthetic Rutile-based Thin Films Derived from Minerals Ores

Author: Thanaphon Kansaard¹

¹ *King Mongkut's Institute of Technology Ladkrabang*

Corresponding Author: tkansaard@gmail.com

This article focuses on the investigation of hydrophilic property and photocatalytic activity of synthetic rutile-based thin films prepared by conventional dip coating method. The synthetic rutile was prepared by chloride leaching process for purification of synthetic rutile from mineral ores and was coated on glass substrate with binder for several times to reach designated thickness. UV-Visible spectroscopy technique was employed to study relevant optical properties meanwhile the crystalline structure of synthetic rutile-based thin films was characterized by X-ray diffraction. Surface morphologies of the coated films was monitored by scanning electron microscoped while hydrophilic property was observed by contact angle measurement. Photocatalytic activity was evaluated by mean of the degradation of organic dye Rhodamine B under ultraviolet light and visible light. Further details of results and discussion will be represented.

Keywords: hydrophilic, photocatalytic, synthetic rutile and minerals ores.

Falcon 1 / 132

Anatase/Rutile composite thin films prepared via dip coating technique and their hydrophilicity, stability and photocatalytic activity

Author: AMMAR IBRAHIM^{None}

Co-author: Wanichaya Mekprasart¹

¹ King Mongkut's Institute of Technology Ladkrabang

Corresponding Authors: nano_phy@hotmail.com, wani.mek@gmail.com

In this work, Titanium dioxide (TiO₂) mix phase powders with specific mixing ratio were prepared by sonochemical process in combination with calcination at different temperature in range of 400oC to 1000oC. The as-prepared powders were dispersed with tetraethyl orthosilicate (TEOS) as supported matrix of TiO₂ for homogeneous colloid and used as starting precursor for thin film coating. The designated thin films were deposited onto glass substrates by dip coating process. X-ray diffraction technique was employed to evaluate TiO₂ phase ratio meanwhile the film morphologies and hydrophilicity were investigated using scanning electron microscope and water contact angle, respectively. UV-Vis spectrophotometer was used to analyse the optical properties of the film. Photocatalytic activity of the prepared film was performed by mean of the decolorization of Rhodamine B dye solution under solar irradiation. The photocatalytic performance of assigned films were investigated and correlated mechanisms responsible for the activity are discussed.

Poster session / 133

DFT+U Study of CuO Surfaces and Vacancy Formation for CuO Nanowires-CNTs Hybrid Electrode in Supercapacitors

Author: Mayuree Phonyiem¹

¹ College of Nanotechnology, King Mongkut's Institute of Technology Ladkrabang

Corresponding Author: mayuree.ph@kmitl.ac.th

Supercapacitors are attracting considerable interest for clean energy storage applications due to their high specific capacitance, fast charging-discharging, long cycle life and non-toxicity. Many attempts have been made to increase performance of electrode materials, one of them is to combined both preferred properties of carbon based nanomaterials which provided high specific surface area and pore volume lead to high specific capacitance such as carbon nanotube (CNT) and the various metal oxides with obtained high energy density such as copper oxide nanowires (CuO NWs) as a so-called hybrid electrode materials. Although many synthesis methods have been investigated for example, thermal oxidation process and CVD method have been used to growth CuO NWs/CNT nanocomposites but it is still lack information corresponding to their good properties of electrode materials especially at the atomic level. Here, the structural and electrochemical properties of CuO NWs are investigated using density functional theory with Hubbard U corrections (DFT+U), followed by the investigation of a number of different low index CuO surfaces. The stabilities, electronic structure and electrochemical properties are presented. CuO (111) and ($\bar{1}$ 11) were found to have the lowest surface energies which is good agreement with the XRD pattern of CuO NWs. We consider the pathways for growing of CuO NWs by studied the oxygen vacancies formation and oxygen molecule adsorption on two most exposed CuO surfaces will be discussed.

134

Preparation of ZnO Nanorods by Hydrothermal Method

Author: Suchada Worasawat¹

¹ *Research Institute of Electronics, Shizuoka University, 3-5-1 Johoku Naka-ku Hamamatsu 432-8011 Japan*

Corresponding Author: swoswat@gmail.com

The demands of a renewable energy source have been of wide interest. Hydrogen is attractive as a clean fuel source. A photoelectrochemical (PEC) cell is a promising hydrogen generation technology through the photoelectrolysis of water using solar energy. ZnO material is applied to PEC cells because ZnO has a favorable band edge position that straddles the redox potential of photoelectrolysis in water splitting. We will present the preparation of ZnO nanorods by hydrothermal method. The seed layer were prepared on a quartz substrate by dip-coating in the solution of zinc nitrate dehydrate, ethanol and diethanolamine. After the seeding process the samples were annealed at 100 or 150 °C for various times. The ZnO seed layer coated substrates were kept inside a teflon-lined autoclave which contained zinc nitrate hexahydrate, hexamethylenetetramine and DI water. Afterward, the autoclave was sealed and heated in a hot air oven at different temperature for 1 h. Then the obtained film was washed with DI water to remove the contamination for solution and then heated in hot air at 100 °C for 15 min. We obtained vertically grown ZnO nanorods at the annealing temperature of the seed layer of 150 °C for 2 h and growth temperature of 120 °C for 1 h. At the seed layer solvent concentration of 0.2 M, the morphology of ZnO nanorods was needle-like. At 0.9 M, hexagonal ZnO nanorods were obtained. We have successfully prepared hexagonal ZnO nanorods. The details of the characteristics will be presented.

135

Fabrication and preparation of Mg-reducing 12CaO•7Al₂O₃ cement for enhancing of electrical and optical properties

Author: Chalernpol Rudradawong¹

¹ *Department of Physics, Faculty of Science, King Mongkut's Institute of Technology Ladkrabang, Chalokkrung Road, Ladkrabang, Bangkok, 10520, Thailand*

Corresponding Author: c.rudradawong@gmail.com

Polycrystalline Ca₁₂Al₁₄O₃₃ (C12A7: O⁻) was synthesized by conventional solid state reaction method and was calcined/sintered at 1300 °C. The Mg powder was used to reduce oxygen inside of nano-cage to form free electron in the cage for enhancing the electrical and optical properties of C12A7 cement compound. The crystal structure of the C12A7:O⁻ and Mg-reducing C12A7 were characterized by X-ray diffraction, morphology and element composition were investigated with scanning electron microscope. In addition, Optical properties were measured by UV-VIS-NIR spectrophotometer that shown transition of absorption because the samples change from white to green powder. Finally, the sample was measured electrical conductivity and carrier concentration by the Hall Effect which can be confirmed existence of electron in the structure and the enhancing properties will be reported.

Keyword: Ca₁₂Al₁₄O₃₃, Mg reducing agents

136

I-V, C-V-f and G-V-f Characteristics of Nanocrystalline n-Type FeSi₂/p-Type Si Heterojunctions Fabricated Using Pulsed Laser Deposition

Author: Adison Nopparuchikun¹

¹ *King Mongkut's Institute of Technology Ladkrabang*

Corresponding Author: adisonnopparachikun@gmail.com

In the present study, nanocrystalline n-type FeSi₂/p-type Si heterojunctions were fabricated by using pulsed laser deposition technique at room temperature. Their dark current density-voltage (J-V) curves were measured at room temperature. The possible carrier transportation mechanisms were investigated by analyzing the forward J-V curves. The present heterojunctions showed good rectifying behavior with the ideality factor value of 1.45 at the applied bias voltage of less than 0.2 V. This suggested that a recombination process was dominant. At the applied bias voltage of higher than 0.2V, the possible mechanism of carrier transportation was a space-charge-limited current process. Both capacitance-voltage (C-V) and conductance-voltage (G-V) curves were measured and analyzed as a function of frequency (f) ranging from 50 kHz to 2 MHz at room temperature. The density of interface state (N_{ss}) of the heterojunctions was estimated by using the Hill-Coleman method. The value of N_{ss} was $2.72 \times 10^{13} \text{ cm}^{-2}\text{eV}^{-1}$ at 50 kHz and it decreased to $2.38 \times 10^{12} \text{ cm}^{-2}\text{eV}^{-1}$ at 2 MHz. This result demonstrated the existence of a large amount of N_{ss} for our heterojunctions, which should be the cause of a large leakage current and small response under illumination for near-infrared light.

137

Fabrication and Nanostructure study of Hydroxyapatite Bioceramic from Cockle shells

Author: Tiwasawat Sirisoam^{None}

Corresponding Author: t.sirisoam@gmail.com

Hydroxyapatite (HA) powder was prepared from cockle shells by co-precipitated with phosphate solution at Ca/P ratio 1.67. Green bodies were formed to disk shape (0.5 cm high x1.5 cm diameter) by dry pressing method with hydraulic machine, sintered at temperature of 1200, 1250 and 1300 °C for 2 h in electric furnace and sintering process was carried out by setting a heating ramp rate of 120 °C/h up to 1200, 1250 and 1300 °C with a soaking time 2 h and cooled down to room temperature with ramp rate 240 °C/h. Mineralogical and chemical properties of the fabricated HA from cockle shells were analyzed by X-ray Diffraction (XRD), X-ray fluorescence (XRF) and fourier transform infrared spectroscopy (FTIR). Nanostructures of samples were studied by scanning electron microscopy (SEM).

138

Optical Extinction Spectra of Pure Noble Metal Nanorod and Silica Shell Coated Gold Nanorod Embedded in Organic Medium

Author: Thananchai Dasri¹

¹ Faculty of Applied Science and Engineering, Nong Khai Campus, Khon Kaen University, Nong Khai, 43000, Thailand

Corresponding Author: thananchai_dasri@hotmail.com

Metal nanoparticles, especially Au and Ag nanoparticles, have well known that exhibit the localized surface plasmon resonances (LSPR). This article presents the optical property named extinction spectra of pure noble metal (gold and silver) nanorods and silica shell coated gold nanorod embedded in organic medium with fixed dielectric constant were simulated using the quasi-static approximation method. The influences of the respect ratio and shell thickness of silica-coated gold nanorod on the optical extinction spectrum were investigated. The calculated extinction spectra shown that there are two localized surface plasmons resonances (LSPR) peaks corresponding with the transverse and longitudinal modes. The position resonances peaks are slightly shifted when aspect ratio is altered. Pure gold and silver nanorods, the position resonances peak of longitudinal mode is slightly shifted

to the longer wavelength, while transverse mode it is shifted to the shorter wavelength. The equations relation between the position resonances peak and aspect ratio is also presented. In addition for silica shell coated gold nanorod, the difference of shell thicknesses plays an important role in determining the position of resonance peak. As the shell thickness was increased the position resonance peak, both transverse and longitudinal modes, slightly shift to the shorter wavelength.

139

Theoretical Calculation of Optical and Magneto Optical Properties of Magnetite Nanorods

Author: Sukhontip Thaomola¹

Co-author: Thanachai Dasri²

¹ Faculty of Science and Arts, Chanthaburi Campus, Burapha University, Chanthaburi, 22170, Thailand

² Faculty of Applied Science and Engineering, Nong Khai Campus, Khon Kaen University, NongKhai, 43000, Thailand.

Corresponding Authors: thananchai_dasri@hotmail.com, suky_2547@yahoo.com

The optical and magneto-optical called Faraday rotation of composites containing isolated Fe₃O₄ (magnetite) nanorod particles are presented in the wavelength range from 300 –700 nm. The results were obtained by using the discrete dipole approximation (DDA) method. The composite materials are constructed by combining Fe₃O₄ nanorod particles and the material with fixed dielectric constant of 2.25. The Fe₃O₄ nanorod of different aspect ratio (AR), varied from 3 to 7, was used to embed in the host material. The influence of the orientation of Fe₃O₄ nanorod comparing with the incident light and number particles on the Faraday rotation spectrum were also presented. The absorption cross-section spectra of Fe₃O₄ nanorods were able to be observed only when the main axis was aligned parallel to the polarization direction and perpendicular with the direction propagation of excited light. All samples were found that the Faraday rotation spectrum show two distinct regions of negative rotation at shorter wavelength and positive rotation at both shorter and longer wavelengths. Moreover, qualitative results of Faraday rotation spectra suggest that the shifts in spectral peak position depend on aspect ratio, the relative orientation of the nanorod in the incident electromagnetic field and number of particles.

Keywords: faraday rotation; magnetite nanorod; Discrete Dipole approximation

140

Characterization of Junction Parameters in n-Type Nanocrystalline Iron Disilicide/Intrinsic Ultrananocrystalline Diamond/Amorphous Carbon Composite/p-Type Silicon Heterojunctions

Author: Phongsaphak Sittimart¹

Co-author: Adison Nopparuchikun

¹ King Mongkut's Institute of Technology Ladkrabang

Corresponding Authors: adisonnopparuchikun@gmail.com, psittimart@gmail.com

n-Type nanocrystalline (NC) iron disilicide (FeSi₂)/intrinsic (i) ultrananocrystalline diamond/amorphous carbon composite (UNCD/a-C)/p-type Si heterojunctions were successfully prepared by employing pulsed laser deposition (PLD) and coaxial arc plasma deposition (CAPD). Their dark current density-voltage (J-V) curves were measured and analyzed at low temperatures ranging from 300 K to 80 K in order to estimate the junction parameters by using thermionic emission theory (TE), Chuang's, and Norde's methods. According to the estimation by TE theory, the ideality factor (n) were 1.12 at

300 K and 5.44 at 80 K. The barrier height was 0.69 eV at 300 K and it decreased to 0.20 eV at 80 K. These parameters are in agreement with those estimated by using Chueng's and Norde's methods. The series resistance (R_s) estimated by Chueng's method were 300.88 Ω at 300 K and 4.29 M Ω at 80 K. These R_s values are equal to those estimated by using Norde's method.

Heron 1 / 141

The porous carbon derived from the KOH activation of agro-waste char for supercapacitor electrode

Author: Jedsada Sodtipinta¹

¹ Faculty of Applied Science and Engineering, Khon Kaen University, Nong Khai Campus

Corresponding Author: s_jedsada@hotmail.com

By using KOH as the chemical activating agent to prepared activated carbon from pineapple leaf fiber waste as the carbon source. The structure, morphology and the surface functional groups of the as-prepared activated carbon were investigated by X-ray diffraction (XRD), field emission scanning electron microscope equipped with energy dispersive X-ray spectroscopy (FESEM-EDX), X-ray photoelectron spectroscopy (XPS), respectively. The electrochemical behavior and performance of the as-synthesized activated carbon electrode were measured by the cyclic voltammetry (CV) and the electrochemical impedance spectroscopy (EIS) in 1 M Na₂SO₄ electrolyte solution by using the three electrode setup. The activated carbon electrode exhibited the specific capacitance of 131.3 F g⁻¹ (5 mV s⁻¹) with excellent cycling stability. The capacitance retention after 1,000 cycles was about 97% of the initial capacitance at a scan rate of 30 mV s⁻¹. Given good electrochemical properties along with the simple accessibility make this activated carbon electrode a promising candidate in future large-scale production of the electrochemical capacitors (ECs).

Keywords: Electrochemical capacitors, Biochar, Activated carbon, Pineapple leaf fiber, Agro-waste base materials

Heron 1 / 142

Gas Response of Tin Oxide Film Sensor to Varying Methane Gas Concentration

Author: Emmanuel Florido^{None}

Corresponding Author: eaflorido@up.edu.ph

This study was aimed to determine the effect of methane gas concentration on the voltage response of tin oxide (SnO) film. The sensing circuit of the tin oxide film was interfaced to a laptop computer through an arduino microcontroller for data acquisition. Real time data table and graph can be visualized on the laptop screen during the gas sensing process.

The sensor was enclosed in an airtight plastic jar container connected to a gas source and a water trap that maintained atmospheric pressure in the chamber. A mixture of 1% methane in helium was introduced into the chamber at a rate of 2 liters per minute (LPM) using a mass flow controller. The gas mixture was introduced intermittently at several stages. Each stage was followed by a standby stage during which there was no gas flow and the sensor was allowed to equilibrate with the gas mixture. It was observed that during the introduction of gas at each stage the voltage output of the sensor was increasing. During the standby stage there was no observed change in the voltage output as indicated by a flat response in the graph of voltage output versus time. The added quantity of gas can be computed from the flow rate and time duration of each stage. The incremental concentration of gas was also computed after each succeeding stage.

The computed concentration in parts per million (ppm) was plotted with the measured voltage output per stage. Results showed a linear relationship between gas concentration and voltage output in the range of 3.75 to 7.8 ppm with a linearity of 0.99 and sensor sensitivity of 140 mV/1000 ppm. The sensitivity and linearity were 161 mV/1000 ppm and 0.98, respectively in the range 1000 to 9000 ppm. It is recommended to conduct more trials at different concentration ranges, different methane input mixture percentages, and different flow rates.

Keywords: tin oxide, sensor, methane, gas concentration, gas response, sensitivity

143

Colorimetric Determination of Arsenic in Natural Waters by Nanomaterial-Based Test Strips

Author: Ratchaneegorn Prasertsom¹

¹ AIT

Corresponding Author: preaw.zimmy@gmail.com

A novel colorimetric method based on a nanocomposite test strip has been developed to detect arsenic (Asv) in natural waters. The method employs a simple vacuum-driven filtration process in which water samples are filtered through a supporting cellulose membrane doped with MoO₄²⁻ (or molybdenum blue) in NR3+ nano-dispersion. The nanocomposite membrane was capable of detecting Asv species at concentration levels as low as 10 ppb. The intensity of blue color on the test strip at this level of detection was visible to the naked eye. A non-linear calibration curve for Asv analysis as determined by colorimetry yielded correlation of 0.995, and the detection limit (at three standard deviations, 3σ) was determined to be 5.54 ppb. The standard deviation of the Asv detection procedure at the 100 ppb level for 10 samples was determined to be ±3.71ppb that indicated good precision. Uniformity of prepared membranes, effect of pH, and the reliability of using the molybdate/latex doped membranes will be discussed.

144

Low Cost and Reliable Surface Plasmon Resonance-Based Detection System for Liquid Propane Gas

Author: Saima Amjad¹

¹ Student

Corresponding Author: st116387@ait.asia

Low Cost and Reliable Surface Plasmon Resonance-Based Detection System for Liquid Propane Gas

1 Saima Amjad, 1 G. Louis Hornyak and 2,3 Waleed S. Mohammed

1 Center of Excellence in Nanotechnology (COEN), Asian Institute of Technology, Pathumthani 12120 Thailand

2 Bangkok University Center of research in Optoelectronics, Communications and Control Systems (CROCCS), Bangkok University, Pathumthani 12120 Thailand

3 Corresponding Author: Waleed.m@bu.ac.th

ABSTRACT

The development and performance of a liquid propane gas sensor based on surface plasmon resonance (SPR) procedure is presented. The development of a sensor for propane and natural gas used in homes and industries is of paramount importance for the reasons of health, safety and protection of property. However, a reliable and inexpensive gas sensor is not widely available on the marketplace. The application of SPR using a nanoscale film of gold coated with special polymeric materials, in this case poly(methylmethacrylate, PMMA) or poly(3-hexylthiophene-2,5-diyl, P3HT), as the sensing media is described. The measurand is expressed as the change in the surface plasmon resonance as a function of the effective refractive index of the gold nanoparticle film-composite due to the presence of the analytical gas.

References:

S. Banerji, W. Peng, Y.-C. Kim, N. Menegazzo and K.S. Booksh; Evaluation of polymer coatings for ammonia vapor sensing with surface plasmon resonance spectroscopy, *Sensors and Actuators B: Chemical*, 147(1) 255-262 (2010)

U. Lange, N.V. Roznyatovskaya and V.M. Mirsky; Conducting polymers in chemical sensor arrays, *Analytica Chimica Acta*, 614(1), 1-26 (2008)

H. Bai and G. Shi; Gas sensors based on conducting polymers, *Sensors*, 7, 267-307 (2007)

Falcon 1 / 145

Highly dispersed Ni and Cu nanoparticles supported SBA-15 for hydrogenation of methyl levulinate to γ -valerolactone

Author: Cheng Fang^{None}

Co-author: Kajornsak Faungnawakij¹

¹ *Nanomaterials for Energy and Catalysis Laboratory, National Nanotechnology Center (NANOTEC), National Science and Technology Development Agency (NSTDA), Khlong Luang, Pathum Thani 12120, Thailand*

Corresponding Authors: kajornsak@nanotec.or.th, fclovezuizui@gmail.com

Highly dispersed Ni and Cu nanoparticles on SBA-15 were successfully prepared by a modified impregnation route and evaluated in hydrogenation of methyl levulinate to γ -valerolactone (GVL). This catalyst was mainly characterized by such techniques as high resolution transmission electron microscopy, X-ray diffraction, N₂ adsorption-desorption analysis, H₂ temperature-programmed reduction. It was found that Ni and Cu nanoparticles were highly dispersed and anchored into the well-ordered mesoporous channels of SBA-15. As compared with conventional impregnated catalyst, the catalyst exhibits higher conversion of methyl levulinate and better yield of GVL at 200 °C in 3 h with 2-propanol as both solvent and H-donor. The superior catalytic performance can be attributed to the confinement effect deriving from the mesoporous channels of SBA-15, as well as the synergy of highly dispersed Ni and Cu nanoparticles.

146

Influence of adhesive rheology for various dispensing systems to achieve very small dot size

Author: Supichaya Kalapak¹

¹ *Mahidol University*

Corresponding Author: supichaya.klp@gmail.com

Several adhesives with different rheology behavior were used to investigate the viscosity effect on time-pressure and microdot-valve dispensing systems. For time-pressure dispensing system, epoxy adhesive with viscosity of 400,000 cps showed linearly increase of dot volume as increasing pressure between 4 to 7 bar. In this operating region, the dot size increases as increasing needle diameter from 100 to 150 μm and decreasing needle length from 18.64 to 7 mm. This variation can be described by normal flow fluid. However at lower pressure of 2–4 bar, the dot size does not depend on the needle size neither needle diameter nor length. In addition, at this low pressure the dispensing dot volume does not systematically depend on the pressure and time. This was investigated more by relative low viscosity fluid of acrylate adhesive with viscosity of 60,000 and 100,000 cps. The dot volume of these low viscosity dispensing shows the strongly depend on needle size for the whole entire pressure range of 2–7 bar. In order to achieve the small dot size of diameter about 200 μm with small variation, the microdot-valve dispensing system was also examined and found that the dot size from this dispensing system strongly depended on the stoke adjustment and depended on the needle size for the whole entire set parameters for three types of adhesive.

147

Thermal analysis of dual cure epoxy adhesive with very small dot size at extremely low and high heating temperature

Author: Waefatimah Waenawae¹

¹ Mahidol University

Corresponding Author: waefatimah.w@hotmail.com

Thermal analysis was used to study epoxy crosslink occurring during the curing process by observing lower thermal energy amount required for phase change which can be determined by differential scanning calorimetry (DSC). Dual cured epoxy adhesive was done by firstly UV light exposure then heat at about transition temperature. The DSC results indicated that epoxy adhesive exhibited curing reaction with exothermic peak at around 120 °C and decomposing endothermic peak at about 270 °C. In this work, the thermal analysis was examined at both temperature edges of this exothermic peak i.e. at 90 °C and 150 °C. The curing processes at these extreme temperatures both very relative low and high temperatures can enable different feature dependence of the curing process. The DSC peak area for heat cure at 120 °C indicates exponential decrease and is needed more curing time than that of only UV cure. However the degree of cure for heating at low temperature curing of 90 °C indicated linearly increase. For dual cure with initial exposure by 0.71 W/cm² of UV light for 0.3 sec, heating time at temperatures of 90 °C and 120 °C can be reduced from single curing process of 40 to 6 minutes and 1 to 0.5 minutes, respectively. While the high temperature cure at 150 °C exhibit very much faster curing process approximately few minutes.

Falcon 1 / 148

Atomic structures of graphene like nanomaterials including SiC and BP

Author: Taweessin Rerkhajornnamkul¹

¹ Nanoscience and Nanotechnology Center, Mahidol University

Corresponding Author: rtpoppap@gmail.com

Atomic structures of graphene like nanomaterials including SiC and BP

Taweessin Rerkhajornnamkul, Tanakorn Osotchan

Materials Science and Engineering Program, and Nanoscience and Nanotechnology Center, Faculty of Science, Mahidol University, Rama VI Road, Phyathai, Bangkok 10400

Abstract:

Honeycomb sheet, graphene like, structure has been interested and the planar structures of silicon carbide (SiC), boron phosphide (BP) and mixed of both materials $\text{h}-(\text{SiC})_{1-x}(\text{BP})_x$ were investigated with x values of 0.00, 0.25, 0.50, 0.75 and 1.00. The 2 atoms per unit cell of hexagonal and 4, 8 and 16 atoms per unit cell of orthorhombic configurations were used in atomic structure calculation with 1.5 nm space distance between layers of graphene like structure. The calculation is set for 500 eV energy cutoff, using local density approximation (LDA) exchange-correlation functional, 200 Ry mesh cutoff. The lattice constant was varied to evaluate the stable atomic structures together with the bond length. Then, the band structures including energy band gap, used to determine electronic property, was calculated to guide the utilization of novel electronic device for new millennium.

149

Coating of molybdenum oxide on anodized aluminium plate apply for ultracapacitor electrodes

Author: Rujira chaisen¹

¹ *Department of Physics and Materials Science, Faculty of Science, Chiangmai University 239 Huay Keaw Road, Muang Chiangmai 50200*

Corresponding Author: ningchaisen@gmail.com

This research was studied about coating of molybdenum oxide on anodized aluminium plate via electrochemical plating technique apply for ultracapacitor electrodes. Preparation of the samples, aluminium plates with the size of 1X1 cm were anodized at voltage of 6, 12 and 24 volt with the constant electric current at 6 amperes for 10, 20 and 30 minute, respectively. The plate samples were then coated with molybdenum oxide by electrochemical plating technique. Thereafter, the samples were examined using SEM and EDX techniques. Besides, the increased surface area and conductivity of the plate samples were determined and applied for ultracapacitor electrodes.

Falcon 1 / 150

Optical and Luminescence from Ln³⁺ doped glasses and their applications

Author: Jakrapong Kaewkhao¹

¹ *Center of Excellence in Glass Technology and Materials Science (CEGM), Nakhon Pathom Rajabhat University, Nakhon Pathom 73000, Thailand*

Corresponding Author: mink110@hotmail.com

Glasses are source of material have properties like low cost, easy to prepare, high transparency at room temperature, hardness along with sufficient strength, excellent electrical resistance, absence of the grain boundaries and continuously variable composition for the optical applications. Glasses doped with Lanthanide ions (Ln³⁺) can be well developed as luminescence materials because of high emission efficiencies, corresponding to 4f-4f and 4f-5d electronic transitions in the Ln³⁺. The 4f-4f transition gives an especially sharp fluorescence patterns from the ultraviolet to the infrared region, because of shielding effects of the outer 5s and 5p orbitals on the 4f electrons. Investigation of the optical and luminescence properties of the Ln³⁺ doped into various glasses have been found great attention due to their feasible properties, (including intense emissions in the visible and near infrared region) and vast applications in the field of lasers, scintillators, sensors, light converters, hole burning high-density memories, optical fibers, amplifiers, and three dimensional display devices. In this work, optical and luminescence from Ln³⁺ doped glasses and their applications have been explained and the effect of some nano-particles on luminescence properties have been discussed.

151

Optical and Luminescence from Ln³⁺ doped glasses and their applications

Author: Yotsakit Ruangtaweep^{None}

Corresponding Author: djone313@gmail.com

The enhancement of luminescence properties of Sm³⁺ in tellurite glasses containing silver nanoparticles (AgNPs) have been investigated. The glass samples with chemical composition of (53.5-x)(TeO₂ : 10ZnO : 35BaO : 1.5Sm₂O₃ : xAgNPs (where x= 0.00, 0.01, 0.02, 0.03, 0.04, and 0.05 % by mol) were prepared by the conventional melt quenching technique. The results show that the density and molar volume of glass are not depend on AgNPs concentration. The absorption bands in NIR region are observed and located at 946, 1082, 1235, 1382, 1488, 1540, 1593 and 1959 nm. The luminescence spectra of the Sm³⁺ doped in glasses are observed at 563 (green), 600 (orange), 645 (red) and 707 (red) nm which are attributed to 4G_{5/2} → 6H_{5/2}, 4G_{5/2} → 6H_{7/2}, 4G_{5/2} → 6H_{9/2} and 4G_{5/2} → 6H_{11/2} transitions, respectively. Moreover, the luminescence intensity of all the emission bands is increased with AgNPs concentration up to 0.01 % mol. The effect of AgNPs concentration on luminescence intensity and decay time of glasses are also discussed.

Hornbill 1 / 152

Optical diffraction of binary-nanoparticle film prepared by convective deposition with vibration assistance

Author: Nonthanan Sitpathom¹

¹ Faculty of Science, Mahidol university

Corresponding Author: sitpathom@gmail.com

Self-assembly nanoparticle films from convective deposition using assistance of vibrated substrate can show optical diffraction in reflected mode, due to uniform high order surface structure. In this work, we investigated the optical diffraction from binary-nanoparticle films which were coated by two types of nanoparticle with different diameter i.e. 100 and 1000 nm of polystyrene and silicon dioxide nanoparticle, respectively. The mixed suspension was prepared by 7 and 20% of polystyrene and silicon dioxide nanoparticles, respectively. The assembled films from binary nanoparticles were deposited with horizontal vibration frequency of 40-60 Hz and at room temperature. The first and second orders of light reflection from film's surface can be observed by detecting light wavelength from various angles of reflection at each incident angle. The films coated with two sizes of particle had the shift of an diffraction angle. This is due to nanoparticles are assemble among the microparticles then the closed packing is differ from the monosize nanoparticle deposition. The angles of reflection from binary sizes were larger than those of single-size coating.

Falcon 1 / 153

Fabrication and Electrochemical properties of CNF/MFe₂O₄: (M = Mn, CuMn) Composite Nanofiber for Electrochemical capacitors

Author: Sukanya Nilmoung¹

¹ Department of Applied Physics, Faculty of Sciences and Liberal Arts, Rajamangala University of Technology Isan, Nakhon Ratchasima 30000, Thailand

Corresponding Author: nilmoung@yahoo.com

Carbon nanofibers composite with manganese or copper manganese ferrite (CNF/MFe₂O₄: M = Mn, CuMn) have been successfully fabricated by a combination of electrospinning and heat treatment process. The structure and morphology of prepared samples were characterized by means of TGA, XRD, SEM, BET, XAS and XPS. The potential application of the prepared samples as an electrode material for supercapacitor was studied using CV, GCD and EIS techniques. The specific capacitance of about 122, 219, and 344 F/g were observed for CNF/MnFe₂O₄ carbonized at 500, 600 and 700 °C, respectively. The improvement is due to increasing of surface area with increased carbonization temperature. In this work, the ACNF/Cu_xMn_{1-x}Fe₂O₄ (x=0.2, 0.4, 0.6, and 0.8) were also prepared due to the activated carbon and copper doping in manganese ferrite are two of the effective approaches to enhance the energy storage in supercapacitors. It was found from the result that, Cu content has a significant effect on the electrochemical performance of ACNF/Cu_xMn_{1-x}Fe₂O₄ electrodes. ACNF/Cu_{0.2}Mn_{0.8}Fe₂O₄ shows the best specific capacitance of 384 F/g compared to the other three samples. This might be largely attributed to the phase transition and anti-sites defects of spinel crystal cell resulting from the Cu substitution for Mn. By comparing the capacity of CNF/MnFe₂O₄ and ACNF/CuMnFe₂O₄ carbonized at 600 °C, the ACNF/CuMnFe₂O₄ electrode exhibited a maximum specific capacitance of 384 F/g, where as non-activated CNF/MnFe₂O₄ showed the specific capacitance of about 220 F/g. The superior electrochemical performance of ACNF/CuMnFe₂O₄ may due to large surface area from activation process and high conductivity from copper doping. Moreover, the combination of the pseudocapacitance behavior of MFe₂O₄ (M = Mn, CuMn) and the electric double layer capacitance of CNF (or ACNF) well supported the enhancement of specific capacitance.

Heron 2 / 154

The effect of green synthesized gold nanoparticles on rice germination and roots

Author: Nji Tsi¹

¹ Suranaree University of Technology

Corresponding Author: nj27tnd@ymail.com

In this paper, gold nanoparticles were synthesized by means of a green approach with *T. triandra* leaf extracts under different conditions. No additional reducing or capping agents were employed. The gold nanoparticles were characterized using UV-visible spectrometry, transmission electron microscope, X-ray diffraction and Fourier transform infrared spectroscopy. Gold nanoparticles that had been synthesized at temperatures of 80°C were further used to treat rice (*Oryza sativa* L.) grains at different concentrations (0, 10, 100, 500, 1000, 2000 mg/L) for one week. While germination percentages were high (95 to 98.38 %), a slight decrease in root and shoot lengths relative to the control was observed. Phytotoxicity results indicated that the plant synthesized gold nanoparticles were of minimal toxicity to rice seedlings. Increases in cell death, hydrogen peroxide formation and lipid peroxidation in roots and shoots were noted. However, these increases were not statistically significant ($p \leq 0.05$). The overall results confirmed that *T. triandra* synthesized gold nanoparticles are biocompatible and can be potentially used as nanocarriers in agriculture.

Heron 2 / 155

Evaluation of immunochromatographic-gold nanoparticle based assay efficacy in the detection of protease inhibitor in HIV-1 infected patient's plasma

Author: Weeraya Thongkum¹

¹ Division of Clinical Immunology, Department of Medical Technology, Faculty of Associated Medical Sciences, Chiang Mai University, Chiang Mai, Thailand

Corresponding Author: ph_dot@hotmail.com

Abstract

By the use of nanotechnology in the development of bioassay kit, the ideal goals that inevitable are rapid, convenience and cost effective. Through our knowledge toward Human Immunodeficiency Virus-1/Acquire Immunodeficiency Disease (HIV-1/AIDS), we successfully produced a novel test kit for investigating both of HIV protease activity and HIV-1 protease inhibitors (PIs). This assay was developed using an immunochromatographic (IC) assay combined with colloidal gold tracers to establish the enzymatic activity IC strip test which can interpret result with the naked eye. In this present study we evaluated the efficacy of strip test by comparing the result of the strip test with the quantity of level of PI in HIV-infected patients detected by the High Performance Liquid Chromatography (HPLC) method. Various parameters including relative accuracy, relative sensitivity, relative specificity, and Kappa co-efficiency (k) of test kit were analyzed. The results revealed that the relative accuracy, relative sensitivity and relative specificity of IC strip were 97.8, 100%, and 96.8 % respectively. The Kappa co-efficiency (k) value was 0.95 showing the high strength of agreement of PI strip with the gold standard, HPLC method ($p < 0.05$). Suggesting that IC strip test has suitable efficacy to determine the PI in plasma samples from human immunodeficiency virus-infected patients.

Keywords: HIV-1 protease, HIV-1 protease, Immunochromatographic strip test, gold nanoparticle

Falcon 1 / 156

Effect of dc bias effect on the dielectric properties and nonlinear electrical behaviors of Bi_{1-x}BaxFeO₃ ceramics

Author: Benjaporn Yotburut¹

Co-author: Santi Maensiri²

¹ School of Physics, Institute of Science, Suranaree University of Technology, Nakhon Ratchasima, 30000, Thailand

² SUT Center of Excellence on Advanced Functional Materials, Suranaree University of Technology, Nakhon Ratchasima, 30000, Thailand

Corresponding Authors: benja_yot@hotmail.com, santimaensiri@gmail.com

In this work we report the dc bias effect on dielectric properties and nonlinear current-voltage behaviors of Bi_{1-x}BaxFeO₃ (where $x = 0, 0.05, 0.1, 0.2$, and 0.3) ceramics synthesized by a co-precipitate process. Structural studies using X-ray diffraction (XRD) show the formation of small amount of second phase (Bi₂Fe₄O₉). Ba-doped samples show the Rhombohedral (R3c) and Orthorhombic (Pbam) distorted structure mixed phase. SEM images indicate the average grain size decreases with the increase of Ba content and the average grain size of Ba-doped samples is about 6.48-3.28 μ m. The dielectric constant and loss tangent of the Ba-doped pellets were measured between 100 Hz –1 MHz under an applied dc bias voltage. Interestingly, it is observed that the dielectric constant gradually increases with increasing dc bias voltage for all of Ba-doped samples at low frequency region (<104 Hz). The grain boundary activation energy has been investigated using impedance microscopy. The leakage current density behavior is significantly enhanced with increase of Ba doping concentration. The relationship between J-E reveal that all of samples exhibits nonlinear characteristic, which is similar to that reported in Ba-doped CCTO ceramics [1]. The non-Ohmic property is described by the existence of Schottky-type barrier in the samples.

Keywords: Bismuth ferrite; Dielectric property; Nonlinear behavior; Impedance analysis

1. P. Thongbai, S. Vangchangyia, E. Swatsitang, V. Amornkitbamrung, T. Yamwong, & S. Maensiri. 2013. Non-Ohmic and dielectric properties of Ba-doped CaCu₃Ti₄O₁₂ ceramics. Journal of Materials Science: Materials in Electronics, 24, 875-883.

Falcon 1 / 157

Fabrication, structure and magnetic properties of Ce_{1-x}Fe_xO₂ nanostructures

Author: Somchai Sonsupap¹

Co-author: Santi Maensiri²

¹ School of Physics, Suranaree University of Technology, Nakhon Ratchasima, Thailand

² School of Physics, Suranaree University of Technology, Nakhon Ratchasima. NANOTEC-SUT Center of Excellence on Advanced Functional Nanomaterials, Suranaree University of Technology, Nakhon Ratchasima, Thailand.

Corresponding Authors: somchaisonsupap@gmail.com, santimaensiri@gmail.com

Ce_{1-x}Fe_xO₂ nanofibers (NFs) and nanoparticles (NPs) ($x=0, 0.08$ and 0.10) were prepared by electrospinning and the simple solution process, respectively. Each of sample was calcined at 500, 600, 700, and 800 °C. The calcined samples were characterized by X-ray diffraction (XRD), Transmission Electron Microscopy (TEM), Scanning Electron Microscopy (SEM), X-ray Photoelectron Spectroscopy (XPS), X-ray Absorption Spectroscopy (XAS) and Vibrating Sample Magnetometer (VSM). Both of XRD and TEM with Selected Electron Diffraction (SEAD) analysis indicated that the Ce_{1-x}Fe_xO₂ nanostructures have a cubic structure without any secondary phase. TEM was shown nanofibers of ~30-60 nm while SEM was shown nanoparticles of ~9-40 nm. The as-spun samples were exhibited a diamagnetic behavior, whereas the calcined of Ce_{0.90}Fe_{0.10}O₂ nanofibers samples exhibited ferromagnetic behavior with the specific magnetizations of 0.04 –0.32 emu/g at 10 kOe. XAS spectra was showed the valent state of mixed Fe³⁺ and Fe²⁺ in the Ce_{1-x}Fe_xO₂ samples indicating oxygen vacancies in the nanostructures. Similarly, XPS spectra confirmed that there are oxygen vacancies in the nanostructures. These oxygen vacancies play an important role to induce room temperature ferromagnetism (RT-FM) in the calcined of Ce_{1-x}Fe_xO₂ nanostructures. Our results indicated that the ferromagnetic properties of Ce_{1-x}Fe_xO₂ system is intrinsic and is not a result of any secondary magnetic phase or cluster formation.

158

The Dc bias voltage effect on dielectric properties of Ni-doped TNTs prepared by hydrothermal route

Author: Pristanuch Kasian¹

¹ School of Physics, Institute of Science Suranaree University of Technology

Corresponding Author: pristanuch@hotmail.com

Ni-doped TNTs with a nominal composition of Ni_xTi_{3-x}O₇ (Na_{0.96}H_{1.04}·3.42H₂O) (where $x = 0, 0.05$ and 0.1) were synthesized by hydrothermal route at temperature of 130 °C for 24 h. The synthesized samples were characterized by X-ray diffraction (XRD), transmission electron microscopy (SEM), UV-vis spectroscopy and vibrating sample magnetometry (VSM). Magnetic measurements by VSM indicate that undoped-TNTs sample is diamagnetic. The dielectric properties of Ni-doped TNTs samples were measured by using an Keysight E4990A Precision LCR Meter over wide ranges of frequency (100 Hz - 1 MHz) and temperature (-60 –200 °C) with the oscillation voltage of 0.5 V. The Ni-doped TNTs samples exhibited giant dielectric behavior with dielectric constant of 104 at 100 Hz at room temperature. The dc bias voltage effect on dielectric properties of the prepared TNTs were also investigated. It was found that the dielectric constant of the sample decreased with increasing dc bias voltage due to the decrease of the total resistance, resulting from the internal interface between grains. Moreover, the effect of Ni doping on the structure and electrical properties of TNTs was studied and discussed.

Fabrication, Characterization, and Electrochemical Properties of Electrospun MnCo₂O₄ Nanofibers

Author: Ornuma Kalawa¹

¹ *School of Physics, Suranaree University of Technology*

Corresponding Author: ornuma_kalawa@hotmail.co.th

Manganese cobalt spinel oxide (MnCo₂O₄) nanofibers were fabricated by electrospinning technique using polyacrylonitrile (PAN) as a polymer source and Mn and Co nitrates as metal sources. TGA-DSC was used to study the thermal property of the as-spun. The as-spun and calcined MnCo₂O₄ samples were characterized by X-ray diffraction (XRD) and transmission electron microscopy (TEM). After calcination of the as-spun MnCo₂O₄ nanofibers (fiber size of 986±12 nm in diameter) at 700, 800, and 900 °C in air for 3h, the MnCo₂O₄ nanofibers with spinel structure were successfully obtained. The MnCo₂O₄ nanofibers have fiber size of 274±8, 254±8, and 239±7 nm in diameter for the sample calcined at 700, 800, and 900 °C, respectively. The electrochemical performance was investigated by using a three-electrode cell system in 6.0 M KOH. The results show that the specific capacitance was determined to be 44.30, 31.79, and 25.27 F/g at a scan rate of 2 mV/s, and 66.78, 57.12, and 51.12 F/g at a current density of 1.0 A/g for the samples calcined at 700, 800, and 900 °C, respectively. The best capacitance retention over 70% after 1000 cycles was observed for an electrode prepared from 700°C-calcined MnCo₂O₄, indicating its long term cycling stability.

Heron 1 / 160

Synthesis, characterization and electrochemical properties of KFeO₂ nanoparticles prepared by sol-gel method

Author: Thongsuk Sichumsaeng¹

¹ *School of Physics, Institute of Science, Suranaree university of Technology, Nakhon Ratchasima, 30000, Thailand*

Corresponding Author: mo_sichumsang@hotmail.com

In this work, we report the electrochemical properties of the KFeO₂ nanoparticles synthesized by a sol-gel method. The synthesized KFeO₂ nanoparticles were calcined in air at the different temperatures from 500 to 800°C for 2 h. The X-ray diffraction (XRD) pattern confirms the phase formation of KFeO₂ with the average crystallite sizes ranging of 20-50 nm. With increasing calcination temperature, the crystallite size of the calcined samples decreased. SEM and TEM images revealed the calcination temperature affect to the morphology of the calcined samples, causing the formation of nanoparticles different in sizes. Moreover, the formation of KFeO₂ phase of the calcined samples was also confirmed by energy dispersive spectroscopy (EDS) and selected area electron diffraction (SAED) techniques. The electrochemical performances were studied by cyclic voltammetry (CV), galvanostatic charge/discharge (G-CD), and electrochemical impedance spectroscopy (EIS). The CV results show that the highest specific capacitance (CS) was calculated to be 175.03 F/g at scan rate of 2mV/s in the sample calcined at 700°C. For the G-CD results, the highest CS was determined to be 263.18 F/g at current density of 1A/g in the sample calcined at 800°C. Ragone plots of power density versus energy density show that the calcined samples are supercapacitors. In addition, the EIS analysis of the results is also discussed.

Heron 1 / 161

Improved Electrochemical Properties of Activated Biomass/FeO_x/MnO_x Composite Prepared by Hydrothermal method for Supercapacitor Electrode Materials

Author: Unchista Wongpratrat¹

¹ *School of Physics, Institute of Science, Suranaree University of Technology, Nakhon Ratchasima, 30000, Thailand.*

Corresponding Author: unchista_w@hotmail.com

Activated biomass carbon from coconut shell was composited with FeOx and MnOx by hydrothermal method at 160 °C for 18 h. The phase structure, morphology and chemical composition of samples were characterized by X-ray diffraction (XRD), Scanning electron microscopy (SEM), Transmission electron microscopy (TEM) and Energy dispersive X-ray spectroscopy (EDX). The electrochemical properties of samples were studied by cyclic voltammetry (CV) and galvanostatic charge-discharge (GCD) technique in a three-electrode electrochemical cell with 6 M of KOH electrolyte solution at different scan rates (2-200 mV/s) and constant current densities (1-30 A/g), respectively. The activated biomass composite with FeOx show the highest specific capacitances of 141.8 F/g at 2 mV/s scan rate while the activated biomass composite with FeOx and MnOx show the highest specific capacitances of 146.3 F/g at 1 A/g current density. These results show that the specific capacitances of activated biomass electrode can be improved by composite with FeOx and MnOx. Moreover, all samples also exhibit charge-discharge reversibility efficiency more than 87% after 500 cycles.

Falcon 1 / 162

Hydrothermal synthesis in egg white solution and magnetic properties of magnetite (Fe₃O₄) nanoparticles

Author: Santi Phumying¹

Co-author: Santi Maensiri²

¹ *School of Physics, Institute of Science, Suranaree University of Technology, Nakhon Ratchasima, 30000, Thailand*

² *SUT CoE on Advanced Functional Materials (SUT-AFM), Suranaree University of Technology, NakhonRatchasima, 30000, Thailand*

Corresponding Authors: santiphumying@gmail.com, santimaensiri@gmail.com

The magnetite Fe₃O₄ nanoparticles have been synthesized successfully by hydrothermal method in the egg white solution. The egg white solution was used as a surfactant and it can also reduce impurity phase in samples. This work aims to study the influence of different reaction temperatures (160-220 °C) on the structure and magnetic properties of the synthesized Fe₃O₄ nanoparticles. The results of X-ray diffraction (XRD) and selected area electron diffraction (SAED) indicate that the synthesized Fe₃O₄ nanoparticles have the inverse cubic spinel structure without the presence of any other phase. The particle sizes of samples are in the range of ~10–50 nm as revealed by transmission electron microscopy (TEM). X-ray absorption near edge structure (XANES) spectra show the oxidation state of Fe³⁺ and Fe²⁺ in the samples. The hysteresis loops of the Fe₃O₄ nanoparticles exhibit superparamagnetic behavior at room temperature for all conditions. The saturation magnetization increases with increasing reaction temperature except at 220 °C.

Falcon 1 / 163

Titanate nanotubes-AgO nanocomposites: Synthesis, characterization, and dielectric properties

Author: Kwunta Siwawongkasem¹

Co-authors: Pristanuch Kasian¹; Santi Maensiri¹

¹ *School of Physics Institute of Science Suranaree University of Technology, Nakhornratchasima, 30000, Thailand*

Corresponding Authors: wong.kwantar@gmail.com, santimaensiri@gmail.com, pristanuch@hotmail.com

The titanate nanotubes (TNTs) were synthesized by hydrothermal method and were composited with silver oxide nanoparticles (AgO) in various 1, 5, 10 wt.%. The prepared samples were characterized by X-ray diffraction (XRD), scanning electron microscopy (SEM), transmission electron microscopy (TEM), energy dispersive X-ray microscopy (EDX), and ultraviolet-visible spectroscopy (UV-vis). The phases of TNTs and TNTs-Ag nanocomposites were confirmed by XRD and EDX results. The dielectric properties of TNTs-AgO were studied at different temperatures (-50 °C to 100 °C) in the wide ranges of frequency (100 Hz to 1 MHz). The TNTs-AgO exhibited dielectric constant in the range of $10 - 10^4$ at frequency 1 kHz and 30 °C. Moreover, the dielectric constants of TNTs significantly decrease with increasing Ag composition due to the increase in the conductivity in the sample causing the reduction of the dielectric properties of TNTs.

Falcon 1 / 164

Magnetic properties of Co-doped BiFeO₃ nanoparticles

Author: Jessada Khajonrit¹

¹ School of Physics, Institute of Science, Suranaree University of Technology, Nakhon Ratchasima, 30000, Thailand

Corresponding Author: ex_phys@hotmail.com

In this study, we report the magnetic properties of BiFe_{1-x}Co_xO₃ nanoparticles (with $x = 0.05, 0.1, 0.2, 0.3$) synthesized by a simple solution method. The prepared samples were characterized by means of X-ray diffraction (XRD), scanning electron microscopy (SEM), and X-ray absorption spectroscopy (XAS). The crystallite size calculated by using the Debye-Scherrer equation decreases with increasing Co doping content. The magnetic properties of the nanoparticles were measured by a vibrating sample magnetometer (VSM). The M-H loops of all BiFe_{1-x}Co_xO₃ nanoparticles exhibited ferromagnetic behavior at room temperature. The saturation magnetization (M_s) increased to be from 1.08 emu/g for BiFe_{0.95}Co_{0.05}O₃ to 8.26 emu/g for BiFe_{0.7}Co_{0.3}O₃. Co-doped BiFeO₃ nanoparticles with smaller crystallite size also caused to the enhancement of the coercivity (H_c) and squareness (M_r/M_s). The effect of Co doping on the structure and magnetic properties of BiFeO₃ nanoparticles is discussed.

Hornbill 1 / 165

A simple electrospinning system for fabrication of core-shell nanofibers

Author: Chaturon Nettong¹

¹ School of Physics, Institute of Science, Suranaree University of Technology, Nakhon Ratchasima, 30000, Thailand.

Corresponding Author: eac-ph@live.com

A simple electrospinning system for fabrication of core-shell nanofibers

Chaturong Nettonglang¹ and Santi Maensiri^{1,2,3}

¹School of Physics, Institute of Science, Suranaree University of Technology, Nakhon Ratchasima, 30000, Thailand.

²SUT CoE on Advanced Functional Materials (SUT-AFM), Suranaree University of Technology, Nakhon-Ratchasima, 30000, Thailand

³SUT-NANOTEC CoE on Advanced Functional Nanoaterials, Suranaree University of Technology, NakhonRatchasima, 30000, Thailand

Abstract

In this work, a simple electrospinning system for fabrication of core-shell nanofibers has been developed. The electrospinning set up as well as experimental procedure are described in detail. The fabrications of metal oxide and composite nanofibers with core-shell structures and other nanostructures are demonstrated. The prepared nanostructures are characterized by various techniques including thermal analysis, X-ray diffraction, Fourier transform infrared spectroscopy, scanning electron microscopy, transmission electron microscopy, and X-ray absorption spectroscopy. This simple electrospinning system can be used to fabricate core-shell nanofibers for many innovative applications including ultrafiltration, fuel cells, membranes, tissue engineering, catalysis and drug delivery or release and nanofluidics and hydrogen storage.

Heron 1 / 166

Molecular Structure and Formation of Melatonin in the Bulk Water and at the Water–Air Interface: A Molecular Dynamics Simulation Study

Author: Aksornnarong Ritwiset¹

Co-author: Tachgiss Jampreecha¹

¹ School of Physics, Institute of Science, Suranaree University of Technology, Nakhon Ratchasima, 30000 Thailand.

Corresponding Authors: parmphy@hotmail.com, tachgiss_off@hotmail.com

Melatonin (N-acetyl-5-methoxytryptamine) is a natural hormone produced by the pineal gland, located behind the third ventricle in the brain that it is used to control the human sleep cycle. Consequently, it has been widely used as a drug for the treatment of the sleep disorder. Melatonin encapsulated niosome particle is an important key for drug delivery application. It is well-known that the melatonin has hydrophilic and lipophilic properties which enable it to pass easily into any cell, fluid or compartment within the body. In this study we report the molecular structure and dynamical properties of the melatonin molecules in the bulk water and at the water–air interface. Molecular dynamics simulations were performed at the temperature of 298 K and the pressure of 1 bar was simulated until it reaches to equilibrium. Afterward the structural and dynamical properties of the melatonin which are randomly distributed in the bulk water and at the water–air interfaces were calculated and compared with the previous studies. In the case of the melatonin in the bulk water, the simulation indicates that the melatonin molecules favor to form aggregation by separated from the bulk water, which is quite obvious. This implies that the melatonin exhibits more solubility in lipid phase than the water phase. In the case of the melatonin randomly distributed on the water–air interface, the simulation reveals that the melatonin molecules favor to form the monolayer film at the interface. The melatonin tailgroups favor to adsorb on the water surface while their headgroups point to the air phase. For the two systems, the self-diffusion coefficient of the water was calculated, and finding it decreasing ~ 36.1 % from the pure water simulation. Such characteristics shows that the self-diffusion coefficient of the water is reduced due to obstruction effects in which are similarities to that reported for surfactant self-assembly formation in solvent. In addition, we also find that the probability for hydrogen bond formation between the melatonin–water molecules of the two systems are occurred as follows: Carbonyl Oxygen(acceptors)–HW(donors), Indole NH(donors)–OW(acceptors), Amide NH(donors)–OW(acceptors), and Methoxy Oxygen(acceptors)–HW(donors), respectively. While, the melatonin–melatonin molecules of the two systems are occurred as follows: Indole NH(donors)–Carbonyl Oxygen(acceptors), Amide NH(donors)–Carbonyl Oxygen(acceptors), Indole NH(donors)–Methoxy Oxygen(acceptors), and Amide NH(donors)–Methoxy Oxygen(acceptors), respectively. Fortunately, this model can be good reproduced the quantum chemistry calculation that reported previously for the hydrogen bond formation.

Theoretical Study of Ethanol Interaction with Pristine and P-doped

Single-Walled Carbon Nanotubes

Author: Phongnared Boontueng¹

¹ *Department of Physics, Faculty of Sciences, Ubon Ratchatani University, Thailand.*

Corresponding Author: p.boontueng@gmail.com

Feasible interactions between metallic single-walled carbon nanotubes (SWCNTs) and ethanol gases were carried out via using theory of first principles based on DFT. Also, the vdW correction and spin polarized were included in this account. The equilibrium position, adsorption energy, charge transfer, density of states, and electronic band structure of ethanol rearranged inside and outside pristine also with P-doped nanotubes were calculated to estimate the responses of P-SWCNT. It was found that the ethanol preferred to absorb inside than outside the tube at diameter of 8.19 Å. Conversely, for nanotubes diameters with more 13.63 Å, the ethanol equivalently forms both inside and outside carbon nanotubes. The investigations on electronic properties have been shown that ethanol performed as electron-withdrawing group because of hydroxyl group attached with ethyl group. Then, the electron in SWCNTs moves toward the adsorbate thereby enhancing its conductivity. Furthermore, doping an impurity, Phosphorus, on the surface improved the absorption and the characteristic of all intermolecular interactions were types of physisorption.

168

Fabrication, Structure, Electrochemical, Ferromagnetic and Ferroelectric Properties of Cu Doped bismuth ferrite Thin Film

Author: Tachgiss Jampreecha¹

¹ *School of Physics, Institute of Science, Suranaree University of Technology, Nakhon Ratchasima, 30000, Thailand.*

Corresponding Author: tachgiss_off@hotmail.com

Cu-doped BiFeO₃ thin film was deposited on Pt/Ti/SiO₂ substrates by using simple spin coating technique. The structure, electrochemical properties and ferromagnetic/ferroelectric properties of the thin film were studied with the increase Cu-doped concentration. The prepared thin films were characterized by X-ray diffraction, Grazing incidence x-ray diffraction (GIXRD) and scanning electron microscopy (SEM). X-ray absorption spectroscopy (XAS) and x-ray photoemission spectroscopy (XPS) indicated oxidation states of Fe and Cu. The optical property and rough band gap of the BiFe_{1-x}Cu_xO₃ thin film were studied by ultraviolet visible spectroscopy. Vibration sample magnetometer (VSM) was used to study the magnetic properties of the thin film. The thin film exhibits ferromagnetism. The structure and magnetic properties of the Cu-doped BiFeO₃ thin film is discussed.

Falcon 1 / 169

Structure and magnetic properties of Mn-doped CeO₂ nanostructures prepared by egg-white solution route

Author: Panwit Sangkhaoartyon¹

¹ *School of Physics, Institute of Science, Suranaree University of Technology, Nakhon Ratchasima, 30000, Thailand.*

Corresponding Author: a.sangkhaoartyon@gmail.com

Ce_{1-x}Mn_xO₂ (x = 0.05, 0.075 and 0.1) nanoparticles were synthesized by simple solution method using cerium(III) nitrate hexahydrate manganese (II) nitrate hydrate (Mn(NO₃)₂·H₂O) and freshly extract egg white (ovalbumin) in an aqueous medium. The precursors were calcined at 600 °C for

2 h in air. The nanoparticles were characterized by X-ray diffraction (XRD), scanning electron microscopy (SEM), transmission electron microscopy (TEM) and X-ray absorption near edge structure (XANES) techniques. The XRD results indicated the presence of a cubic structure of $\text{Ce}_{1-x}\text{Mn}_x\text{O}_2$ in all samples. The SEM and TEM images showed thin platelike clusters with the particle sizes \approx 20-40 nm. The oxidation states of Mn and Ce K-edge in samples were confirmed by X-ray absorption near edge structure (XANES) technique. The magnetic properties were studied by a vibrating sample magnetometer (VSM). All samples exhibit superparamagnetism behavior. The saturation magnetization (MS) of $\text{Ce}_{1-x}\text{Mn}_x\text{O}_2$ ($x = 0.05, 0.075$ and 0.1) nanoparticles increase from 0.00003 to 0.00035 emu/g with increasing Mn content. The origin of the magnetic properties observed in the prepared $\text{Ce}_{1-x}\text{Mn}_x\text{O}_2$ nanoparticles is discussed.

Heron 2 / 170

Nanocatalysts for Biorefinery and Advanced Biofuel Applications

Author: Kajornsak Faungnawakij¹

¹ *National Nanotechnology Center (NANOTEC), National Science and Technology Development Agency*

Corresponding Author: kajornsak@nanotec.or.th

Nanocatalysts have played an important role in biorefinery and advanced biofuel applications. The conversion of cellulosic biomass feedstocks to platform biochemicals, such as organic acids and furans, is one of the key steps in biorefining. In our research group, metal phosphate catalysts have been developed for production of 5-hydroxymethylfurfural from C6 sugar. Incorporating metal species in phosphate networks provides suitable active sites and phases for the reaction. In addition, non-crystalline mesoporous aluminosilicate catalysts with combination of strong and weak acid sites have been developed for conversion of C5 sugar to levulinic acid in one-step without any solvent and H_2 addition. The proposed processes proceed efficiently in hot water media, making it highly effective and friendly to the environment.

As for biofuel application, the conversion of vegetable oil and animal fat feedstocks to transportation fuels over heterogeneous catalysts is of interest for new biofuel industry. Such process is not only leading to lesser amount of imported petroleum and higher energy security of Thailand, but it is also valorizing byproducts from the country agricultural sector. We have developed the catalysts for the production of green diesel, a synthetic alkane, known to be one of the candidates for future energy. The process can be accomplished via deoxygenation over $\text{NiMoS}_2/\text{Al}_2\text{O}_3$, $\text{Ni}/\text{Al}_2\text{O}_3$, and $\text{Co}/\text{Al}_2\text{O}_3$ catalysts with high product yield at above 95%. Hydrogen, which is an important chemical for the deoxygenation, can effectively be achieved from steam reforming of oxy-hydrocarbons over Cu- and Ni-based spinel nanocatalysts. The integration of all processes mentioned above would lead to new technologies for biorefinery and biofuel industries of Thailand.

Heron 1 / 171

DESIGNING MOLECULAR STRUCTURES OF D- π -A TYPE ORGANIC DYES FOR HIGH EFFICIENCY DYE-SENSITIZED SOLAR CELLS

Author: Vinich Promarak¹

¹ *School of Molecular Science and Engineering, Vidyasirimedhi Institute of Science and Technology (VISTEC)*

Corresponding Author: vinich.p@vistec.ac.th

Dye-sensitized solar cell (DSSC) has emerged as one of the most attractive photovoltaic devices because it offers the possibility of low-cost conversion of photoenergy. Ruthenium complex dyes are currently the most efficient dyes. These dyes, however, are costly and hard to prepare in high

yields, which have led to the evolution of metal-free organic dyes. Organic dyes exhibit not only higher extinction coefficient, but simple preparation, structure modification and purification procedure with a low cost. In this talk, an improvement of the performance of the organic dyes as sensitizers for DSSC by fine tuning the dye chemical structures will be presented. A series of organic dipolar compounds forming D-D- π -A type of dyads bearing carbazole-carbazole, carbazole-diphenylamine, carbazole-phenothiazine and carbazole dendrons as D-D moieties were designed, synthesized and investigated. The relationships between structure of these dyes and properties and cell performances will be drawn and discussed. The power conversion efficiencies of the corresponding devices surpass that of the Ru-based device measured under similar conditions, suggesting that the organic dyes based on this type of donor molecular design are promising candidates for improvement of the performance of the DSSCs.

Heron 2 / 172

Nanotechnology based delivery systems for peptides and vaccines

Author: Istvan Toth¹

¹ *The University of Queensland, School of Chemistry and Molecular Biosciences / The University of Queensland, School of Pharmacy*

Corresponding Author: i.toth@uq.edu.au

Poor oral absorption and rapid enzymatic degradation are the major hurdles in to deliver peptide drugs orally and vaccines via the mucosa. We developed stable, orally available peptide drugs through the chemical addition of specifically designed lipids and carbohydrates, creating amphiphilic compounds capable to reassemble to form nanoparticles. Fertility is controlled by decreasing the level of circulating Gonadotropin-Releasing Hormone (GnRH) or stimulating the down-regulation of GnRH receptors on gonadotrope cells. Using two independent approaches we regulated the action of GnRH on gonadotrope cells, thereby controlling fertility in mice and rat models.

We have also developed an oral vaccine delivery system to prevent infection by Group A streptococcus (GAS) by encapsulating lipid core peptide (LCP) antigens into the liposomes. We synthesised the LCP construct by attaching C-16 lipoamino acid (Toll-like receptor 2 agonist) to J-14 (B-cell epitope derived from GAS M-protein) and P25 (CD4+ T helper cell epitope). Blank liposomes were formulated and optimized for charge and lipid content using a thin film formation method. Optimized liposomes were coated with oppositely charged polyelectrolytes (positively charged trimethyl chitosan (TMC) and negatively charged sodium alginate) in a layer-by-layer approach. These formulations were subsequently characterized by dynamic light scattering (DLS) and transmission electron microscopy (TEM). Spherical-shaped liposomes surrounded by films of TMC and sodium alginate were observed by TEM. DLS analysis of coated liposomes showed monodispersed particles with a polydispersity index of 0.24, hydrodynamic diameter 230 nm and zeta potential of -40 mV. Optimized formulations will be further investigated for their efficiency of uptake by intestinal immune cells and ability to induce mucosal IgA and systemic IgG responses.

Falcon 1 / 173

Classic Perovskite Ferroelectric BaTiO₃ Ceramics Modified with Nanogold

Author: Supon Ananta¹

¹ *Department of Physics and Materials Science, Faculty of science, Chiang Mai University*

Corresponding Author: suponananta@yahoo.com

Perovskite barium titanate (BaTiO₃) BT-based ceramics have been of interest as one of the promising smart materials in commercial electrical components due to their non-toxic and variable electrical

properties for several decades. However, these BT-based ceramics suffer from high sintering temperature requirement, low dielectric constant and high dielectric loss, causing a limitation for their practical utilizations, especially for the multilayer ceramic capacitors with ultrathin layers. Therefore, several approaches have been introduced to minimize these limitations including a method of reinforcing the ferroelectric matrix with high electrical conducting phases. Apart from their environmental friendly, gold nanoparticles (AuNPs) are thought to be reasonable candidate used for shortening the electrode distance (i.e. leading to stronger effective electric field in the dielectric phase) in nanometal/BT ceramics. Hence, composites of BT and AuNPs phases are expected to synergistically combine the properties of both the ferroelectric BT and the conductive AuNPs, which could exhibit dielectric properties that are better than those of the monolithic BT ceramics. Here we demonstrate that under suitable sintering condition and AuNPs content, both densification and dielectric properties of the composites with fine-grained microstructure fabricated in this work were significantly improved, as compared to the monolithic BT ceramics.

Keywords: Barium titanate; Gold nanoparticles; Sintering

Falcon 1 / 174

Photocatalytic Activity of the Binary Composite CeO₂/SiO₂ for Degradation of Dye

Author: Sukon Phanichphant¹

¹ *Materials Science Research Center, Faculty of Science, Chiang Mai University*

Corresponding Author: sphanichphant@yahoo.com

In this study, CeO₂ photocatalyst was modified by composite with SiO₂ to increase efficiency and improve photocatalytic activity. The as-prepared SiO₂ particles have been incorporated into the precursor mixture of CeO₂ by homogeneous precipitation and subsequent calcination process. The phase compositions of CeO₂ before and after compositing with SiO₂ were identified by X-ray diffraction (XRD). The morphology and particle size of CeO₂/SiO₂ composite was analyzed by high resolution transmission electron microscopy (HRTEM) and field emission scanning electron microscopy (FESEM). The results showed SiO₂ spheres with the particle size approximately 100–120 nm, and a uniform layer of CeO₂ nanoparticles with a diameter of about 5–7 nm that were fully composite to the surfaces of SiO₂. The X-ray photoelectron spectroscopy (XPS) technique was carried out in order to characterize the change in valence state and composite characteristic by shifted peaks of binding energies. The photocatalytic activity was studied through the degradation of Rhodamine B in aqueous solution under visible light exposure. The highest photocatalytic efficiency of CeO₂/SiO₂ composite was also obtained. To explain the high photocatalytic efficiency of CeO₂/SiO₂ composite, the proposed mechanism involves the high surface properties of the CeO₂/SiO₂ composite, as measured by Brunauer–Emmett–Teller (BET) method.

Keywords: Composite materials, CeO₂, Rhodamine B, Silica, Photocatalysis

Heron 1 / 175

The mystery of high temperature superconductivity at the FeSe/STO interface

Author: Donglai Feng¹

¹ *State Key Laboratory of Surface Physics, Department of Physics, Fudan University, Shanghai, China*

Corresponding Author: dlffeng@fudan.edu.cn

Interface and surface become important playgrounds for unconventional superconductivity, since they bring broken symmetry, competing orders, charge transfer, strain and other factors into the problem. Recently, interfacial superconductivity up to 75K has been discovered in FeSe/STO and FeSe/BTO interfaces [1,2]. In this talk, I will demonstrate that the combination of angle resolved photoemission spectroscopy (ARPES), scanning tunneling microscopy (STM) and molecular beam epitaxy (MBE) is a powerful tool to study the superconductivity at interfaces and surfaces. Specifically, I will present: our recent efforts in the understanding of the pairing symmetry of FeSe/STO [3] and the anomalous phase diagram of FeSe films upon surface electron doping [4,5]. Our results suggest that the interfacial effects, particularly interfacial electron-phonon interactions, may play a critical role in the high-T_c of FeSe/STO. In line with it, I will introduce our latest findings of the surprising interfacial structure of FeSe/STO.

[1] S. Tan et al., Nature Materials 12, 634 (2013).

[2] R. Peng et al., Nature Comm. 5, 5044 (2014).

[3] Q. Fan et al., Nature Physics 11, 946–952 (2015).

[4] C.-H.-P. Wen et al., Nature Comm. 7, 10840 (2016).

[5] W. H. Zhang et al., Nano Lett. 16 (3), 1969–1973 (2016).

Falcon 1 / 176

Effect of boron addition on the structure and magnetic properties of CoPt nanoparticles

Author: Supree Pinitsoontorn¹

Co-author: Apiwat Chompoosor²

¹ Department of Physics, Khon Kaen University

² Integrated Nanotechnology Research Center, Department of Physics, Faculty of Science, Khon Kaen University / Nanotec-KKU Center of Excellence on Advanced Nanomaterials for Energy Production and Storage, Khon Kaen University

Corresponding Authors: psupree@kku.ac.th, id023@mail.com

We reported the effect of boron addition on magnetic properties and structure of CoPt nanoparticles. The CoPt-B nanoparticles were synthesized by means of the polyol process. The magnetic property measurement showed that the CoPt-B sample exhibited a much larger coercivity compared to the sample without B additive at the same annealing temperature. Transmission electron microscopy and energy dispersive X-ray spectroscopy revealed that the average particle size was about 2 nm for the as-synthesized sample with the ratio of Co and Pt was close to 1:1. After annealing, the particle sizes increased but the composition was maintained. The phase transformation of the nanoparticles versus temperature was investigated using a combination of X-ray diffraction and in-situ X-ray absorption analysis. It was shown that the phase transition temperature at which the nanoparticles change from the disordered A1 phase to the ordered L10 phase occurs at temperature of 600 °C. We concluded that boron additives could reduce the ordering temperature of CoPt of about 100 °C.

The addition of B at up to 60% promoted the formation of the L10 phase when the nanoparticles were subjected to annealing at 600 °C. If the B content is higher than 60%, the phase transition is suppressed. The evidence of B addition on the structure of CoPt nanoparticles was further supported by the magnetic measurements. The results show that the coercivity of the annealed CoPt-B nanoparticles was enhanced by the B additions from 20 to 60%, with the maximum coercivity of 12,000 Oe for the CoPt-40%B sample.

Keywords: CoPt, nanoparticles, magnetic properties, boron addition, phase transformation, recording media

Plenary talk / 177

How to Predict New Nano-structured Materials with Confidence? -Theoretical Study on Task Specific Ionic Liquid for Metal Extraction from Garbage Caused by Tsunami-

Author: Yoshiyuki Kawazoe¹

¹ *New Industry Creation Hatchery Center, Tohoku University, Sendai, Japan*

Corresponding Author: kawazoe@imr.edu

In the 50 years of the history of DFT proposed by Professor Walter Kohn in 1964, applying this formulation, a number of ab initio calculations have been performed to explain experimental observations and to predict new materials from atomic and electronic levels. Unfortunately, recent trend is to increase number of atoms to treat complex systems and to include parameters such as U for band-gap fitting or to modify Exc for van der Waals interaction, and shifting to phenomenology. By these methods, we can only explain experimental data, but not have good confidence to design new materials. In the talk, I will introduce several new methods which certify our ab initio calculations with confidence; (1) initial atomic configurations designed with mathematicians based on symmetry consideration, (2) checking necessary conditions such as virial theorem and cusp condition, and (3) checking dynamical stability by phonon calculation.

After 5 years from the big tsunami attacked Tohoku area in Japan, still there remain a large amount of garbage. They have been collected to limited areas and classified as stones, steels, woods, etc., and among them there are a large amount of electronic circuit boards, which contain expensive metals should be reused. We have been trying to extract such metals by using ionic liquid experimentally and theoretically. The ionic liquid is functionalized by attached ligands for extraction of specific metal element, and is called "task specific ionic liquids (TSIL)". Since the properties of TSIL varies strongly as a function of temperature and not easy to understand experimentally, especially temperature dependence of viscosity and hydrophobicity are difficult. We have developed a new theoretical method based on molecular dynamics and hydrodynamics to determine theoretically the viscosity in TSIL, and successfully applied to compute for several TSIL. Up to the present Rh has been the worst to be extracted efficiently from garbage in industry. We studied the properties of Rh and proposed a new TSIL, which atomic structure is shown on the right and is expected to be suitable for Rh extraction compared to existing industrial methods.

The author is thankful to the Tohoku Innovation Materials Technology Initiatives for Reconstruction for the support of this research. He also is grateful to the HPCI project for the supply of supercomputer power as the grant ID hp150076, .

178

The effects of hydroxyapatite nanoparticle on germination and seedlings of rice

Author: Ampawan Jantasee¹

¹ *School of Biology, Institute of Science, Suranaree University of Technology*

Corresponding Author: ampawan_923@hotmail.com

Although hydroxyapatite nanoparticle was reported to have potential for enhancing plant growth, its effect on rice had never been investigated. The objective of the present study was to investigate the effects of hydroxyapatite nanoparticles (HAp-NPs) at concentrations of 0, 10, 25, 50, 100, 500, 1,000 and 2,000 µg/ml on seed germination and seedlings of rice (*Oryza sativa* L.). Assessments of root and shoot growth, cell death, and electrolyte leakage at early seedling stage were made. The results showed that HAp-NPs had no apparent positive or negative effect on seed germination, although there may be some negative effect at high concentrations of 1,000 and 2,000 µg/ml. NPs distribution in seed was observed by using transmission electron microscope. Micrographs showed nanoparticles to be primarily trapped in the cell wall. The synchrotron radiation based micro-X-ray

fluorescence (micro-XRF) was used to track the presence and chemical speciation of calcium within the rice seed. It was found that seeds treated with high concentration of HAp-NPs (2,000 µg/ml) had higher amount of calcium than the control. In addition, rice in seedling stage (20-30 days) showed better growth and more chlorophyll content with increasing concentrations of hydroxyapatite nanoparticles. In summary, HAp-NPs has no effect upon exposure on short term basis, but positively affects the seedling stage on long term basis at concentrations of 500 to 2,000 µg/ml.

Keywords: Nanoparticles, Hydroxyapatite (HAp), Rice (*Oryza sativa* L.)

179

The effect of hydroxyapatite nanoparticles on rice (*Oryza sativa* L.) callus

Author: Apakorn Poonpoklang¹

¹ School of Biology, Institute of Science, Suranaree University of Technology, Nakhon Ratchasima 30000, Thailand

Corresponding Author: apakornp@gmail.com

The effect of hydroxyapatite (HAp) nanoparticles on plant growth has been studied in recent years due to the chemical composition of the material which consists of calcium and phosphate. However, little has been done with regards to the effect of nanoparticles on callus. In this study, the effects of HAp on callus induction and morphology were investigated. The production of embryogenesis callus was carried out under two conditions: culturing on inducing medium containing different concentrations of HAp nanoparticles and incubating in suspension of 50 µg/ml HAp nanoparticles on a shaker at 120 rpm for 15, 30 and 60 minutes prior to culturing on inducing medium. Calli from all treatments were harvested after 3 weeks. Callus growth was examined. Size, fresh and dry weight of callus were measured. The morphology of calli and callus cells were investigated under an optical microscope. The results showed that HAp nanoparticles were not toxic to rice calli and did not suppress growth of all the calli tested. The study of morphology showed that calli were yellow or cream in color and compact. More embryogenic calli were observed in HAp pretreated groups as characterized by their nodular and compact structure. Calli on solid medium containing HAp nanoparticles showed less embryogenic structure at the same concentration. In addition, tracheary elements were observed in all HAp exposed calli although more of such cells were found in calli pre-exposed to suspensions of HAp nanoparticles. The results suggest the potential of HAp to be used as effective embryogenesis inducing supplement in tissue culture medium.

180

Anticandidal Activity of the Spinel Ferrite CoFe₂O₄ Nanospheres

Author: Nuannoi Chudapongse¹

¹ School of Preclinical Sciences, Institute of Science, Suranaree University of Technology, Nakhon Ratchasima, 30000, Thailand

Corresponding Author: nuannoi@sut.ac.th

Cobalt ferrite nanoparticles (CoFe₂O₄-NPs) have received much interest regarding potential applications in medicine. They have potential to be used in magnetic resonance imaging (MRI), diagnostics, electronic devices, cancer treatment and drug-delivery technology due to their high permeability, coercivity, moderate magnetization, high saturation magnetization and physiochemical stability. The required sizes and shapes of the spinel ferrites nanocrystals can be achieved depending on a variety of fabrication methods and/or precipitation agents, for example sol-gel methods, the ball-milling technique, co-precipitation, the reverse micelles process, and the micro-emulsion method. Antibacterial activity of angular- and irregular-shaped cobalt ferrite nanoparticles synthesized by sol-gel

technique has been reported. Polyaniline/CoFe₂O₄ nanocomposite has also shown to inhibit the growth of *Candida albicans* by ROS production. In the present study, CoFe₂O₄ nanospheres were carried out in a solvothermal system by modified reduction reactions between FeCl₃ and ethylene glycol. SEM micrographs showed that the size of CoFe₂O₄ nanospheres was about 20-40 nm. Cobalt ferrite nanospheres (2 mg/ml) were sonicated in distilled water and supernatant was used to test antifungal activity against *Candida albicans*. Measured by dynamic light scattering, the average size of CoFe₂O₄ nanospheres dispersed in supernatant was 56.68 nm. The MIC was found at 1/2048 dilution of the supernatant which implicated that CoFe₂O₄ nanospheres obtained by solvothermal system had strong anticandidal activity.

181

Green synthesis of silver chloride nanoparticles: a comparison study in three different species of Curcuma

Author: Nuannoi Chudapongse¹

Co-author: Khairiza Lubis²

¹ School of Preclinical Sciences, Institute of Science, Suranaree University of Technology, Nakhon Ratchasima, 30000, Thailand

² School of Biology, Institute of science, Suranaree University of Technology, Nakhon Ratchasima, 30000, Thailand

Corresponding Authors: nuannoi@sut.ac.th, id030@mail.com

Green synthesis, a low cost and eco-friendly method, has received much attention as an alternative for the development of inorganic nanoparticles (NPs) such as metals, metal oxides, and metal chlorides. Several applications of silver chloride nanoparticles (AgCl-NPs) have been widely recognized, including catalytic material, ionic conductor material and antibacterial agent. A synthesis method of antimicrobial AgCl-NPs from the leaf extracts of *Prunus persica* L. has been developed and showed synergistic activity against several pathogenic microorganisms with standard drugs. Therefore, the objective of this work is to compare the potential of three different species of *Curcuma* genus to produce AgCl-NPs. UV-visible spectroscopy showed that absorption peaks of the synthesized AgCl-NPs from *C. longa*, *C. xanthorrhiza* and *C. latifolia* were 420 nm, 425 nm and 410 nm, respectively. The crystalline nature of the synthesized AgCl-NPs were confirmed by X-ray diffraction (XRD) analysis. The XRD peaks from all plants were obtained at $2\theta = 27.831, 32.244, 46.234, 54.830, 57.480, 67.473$ and 76.736 which were corresponding to the (1 1 1), (2 0 0), (2 2 0), (3 1 1), (2 2 2), (4 0 0) and (4 2 0) Bragg's reflections of the cubic structure of metallic AgCl. The data from dynamic light scattering measurement showed that the average size of AgCl-NPs synthesized from *C. xanthorrhiza*, *C. longa*, and *C. latifolia* were 48, 50 and 56 nm, respectively. Moreover, transmission electron microscopy (TEM) revealed that AgCl-NPs obtained from all plants had irregular shapes. This preliminary data suggested that all of these three species of *Curcuma* had potential to be used for green synthesis of AgCl-NPs. Since they are anticipated to have potential applications as antimicrobial agents, their antibacterial and antifungal activities will be also further investigated.

182

Synthesis of PLGA-based nanoparticles loaded with lupinifolin extracted from *Derris reticulata*

Author: Nuannoi Chudapongse¹

Co-author: Jidapa Musika¹

¹ School of Preclinical Sciences, Institute of Science, Suranaree University of Technology, Nakhon Ratchasima, 30000, Thailand

Corresponding Authors: nuannoi@sut.ac.th, id031@mail.com

Lupinifolin is a prenylated flavonoid isolated from several medicinal plants, such as *Myriopterum extensum*, *Eriosema chinense*, *Albizia myriophylla* and *Erythrina fusca*. It is also reported to be a major compound of *Derris reticulata*. There are several lines of evidence demonstrating that lupinifolin exerts antimicrobial activities. However, due to its very insoluble property, poor bioavailability of lupinifolin is anticipated. Thus, this study aims to improve oral bioavailability of lupinifolin isolated from *Derris reticulata*, by encapsulation with poly[lactic-co-glycolic acid] (PLGA), a biocompatible, biodegradable and FDA approved polymer. Lupinifolin-loaded PLGA nanoparticles (NPs) were produced by single emulsion-solvent evaporation technique with 96% encapsulation efficiency. Regarding the morphology of the NPs, TEM images showed that the lupinifolin-loaded NPs had spherical shape and the size agreed with the result from dynamic light scattering measurement (194 nm in diameter). The polydispersity index and zeta potential were 0.05 and -28.30 mV, respectively, indicating that lupinifolin-loaded NPs obtained from the present study were nearly monodispersed and moderately stable. Their releasing profile and oral bioavailability in Caco-2 permeability model will be further investigated.

183

Toxicity Test of Nano-Encapsulated Eugenol Containing Biopesticide by Brine Shrimp Lethality Test

Author: Mila Tejamaya¹

¹ *Department of Occupational Health and Safety, Faculty of Public Health, Universitas Indonesia, Depok Indonesia, 16424*

Corresponding Author: mila.tejamaya@gmail.com

Concern against short-term and long-term adverse health effect of synthetic pesticide, both to the human and environment has encouraged the development of bio-pesticide. Eugenol as major component of Clove, *Syzygium aromaticum*, has been proofed as potential biopesticide in various study (Bakkali et al. 2008; Burt 2004; Deans & Ritchie 1987). However, evaporation and photosensitive properties of eugenol limit its benefit. Thus nano-encapsulation was implemented to overcome those constraints (Cortés-Rojas et al. 2014; Donsi et al. 2011). On the other hand, the effect of nano-encapsulation into Biopesticide toxicity needs to be investigated.

This study aimed to examine the toxicity of nano-encapsulated Eugenol Containing Biopesticide (ECB) against *Artemia salina* sp by Brine Shrimp Lethality Test (BSLT). It was found that nano-encapsulation treatment has statistically increased the toxicity of ECB with a confidence level of 95%. LC50 of nano-ECB was 0.264 µg/L while LC50 of ECB-suspension was 4.445 µg/L. The amplification of ECB toxicity might be due to stability improvement as well as penetration enhancement of NPS to the exposed organism, known as "Trojan Horse Effect" (Cortés-Rojas et al. 2014; Donsi et al. 2011; Turek & Stintzing 2013; Kumari et al. 2014; Garg & Singh 2011).

Key words: eugenol, nano encapsulation, biopesticide, BSLT.

184

Rapid and portable aflatoxin sensor using screen printed graphene electrode

Author: Chanpen Karuwan¹

Co-author: A. Tuantranont¹

¹ *Thai Organic and Printed Electronics Innovation Center, National Electronics and Computer Technology Center, Klong 1, Paholyothin Rd, Pathumthani, Thailand 12120*

Corresponding Authors: ckaruwan@gmail.com, adisorn.tuantranont@nectec.or.th

In this work, we present a new electrochemical DNA biosensor using screen-printed graphene electrode and Hoechst 33258 intercalator for detection of *Aspergillus flavus* DNA that produces aflatoxin B1. The principle of detection is based on suppression of activity of redox molecules (H33258), which will be intercalated between A-T based of hybridized DNA of *Aspergillus flavus* that produces aflatoxin B1, resulting in a decrease of anodic current (ΔI). There are five processes including DNA extraction, DNA amplification, hybridization, mediator mixing and electrochemical detection. For electrochemical detection, the detected current will be converted to aflatoxin concentration within 20 s. The measured value will be shown on LED display. A good linear relationship is obtained over concentration range of 0 to 400 ppb. The developed AflaSense was applied to successfully determine aflatoxin in 52 samples.

Hornbill 1 / 185

Risk mapping and Risk management by control of release –strategies to design better materials and products

Author: Michael Riediker¹

¹ IOM (Institute of Occupational Medicine) Singapore / Nanyang Technological University (NTU), Singapore / IST, University of Lausanne, Switzerland

Corresponding Author: michael.riediker@iom-world.sg

Nanomaterials have enormous economic potential for technical and medical applications due to their new properties acquired on the nanoscale. However, given multiple exposure pathways from the raw material production to the final product and its disposal, it is necessary to understand where and how nanomaterials can be released, and how this release can lead to exposure of workers, consumers and the environment. Once we understand release and exposure, we can design and implement adequate measures to protect humans and the environment from potential exposure along these value chains. Focusing on release reduction from materials, products and during production processes is a very efficient approach to reduce risks of nanomaterials because no release means no exposure, and without exposure, even a dangerous material cannot lead to negative health effects.

The management of nanomaterial-related risks poses some special challenges, such as uncertainties related to human hazard data and exposure assessment; as well as insufficient communication of risk-relevant information along the value chain. Good management strategies need to identify adequate and cost effective solutions for such safety and health challenges. Risk mapping is a novel tool for addressing safety, health and environmental challenges in companies, from R&D over production facilities all the way to the interaction with end-consumers. Risk mapping identifies the various elements in a company and along the value chain that need to be addressed for a complete risk management, such as product development and testing, workplace assessments, facility design, and training of staff. These elements then are mapped onto the business processes to integrate the health and safety approach into the corporate management and effective company policies.

This talk will provide an overview of how risk mapping can help to successfully address nanomaterial specific challenges and what role release management by smart design can play in risk reduction.

186

Microfluidic device integrated with screen printed graphene based-electrochemical sensor for glutathione sensing

Author: Chanpen Karuwan¹

Co-authors: A. Tuantranont²; W. Pimpao²

¹ Flow Innovative Research for Science and Technology laboratories (FIRST Labs.), Department of Chemistry and Center of Excellence for Innovation in Chemistry, Faculty of Science, Mahidol University, Rama VI Rd, Bangkok 10400, Thailand / Thai Organic and Printed Electronics Innovation Center, National Electronics and Computer Technology Center, Klong 1, Paholyothin Rd, Pathumthani, Thailand 12120

² Thai Organic and Printed Electronics Innovation Center, National Electronics and Computer Technology Center, Klong 1, Paholyothin Rd, Pathumthani, Thailand 12120

Corresponding Authors: adisorn.tuantranont@nectec.or.th, ckaruwan@gmail.com, id037@mail.com

This work presents a new microfluidic device with integrated graphene-based electrochemical electrodes for in-channel amperometric detection. Graphene-based working and counter electrodes were fabricated by screen printing graphene paste on a glass substrate followed by screen printing of silver/silver chloride (Ag/AgCl) reference electrode. The screen-printed substrate was then bonded to prefabricated polydimethylsiloxane (PDMS) sheet containing microchannels via oxygen plasma treatment. The developed microfluidic device was then applied for glutathione analysis in pharmaceutical products. The method offers effective and fast glutathione detection with good analytical features including wide dynamic range (10-500 μ M) and low detection limit (3 μ M). In addition, the screen printed graphene electrode (SPGE) exhibits a good stability in microfluidic flow system and good repeatability for amperometric detection. The method has numerous advantages including low fabrication cost, high sensitivity, high throughput and satisfactory reproducibility. Thus, it holds great promise for advanced analytical applications.

Heron 2 / 189

Prof. Ruengpung Sutthent, Director, COE MU

Corresponding Author: ruengpung.sut@mahidol.ac.th

To be added

Heron 1 / 229

Fabrication of Highly Aligned CNT and P(VDF/TrFE) Nanofiber Sheets

Author: Hidenori Mimura^{None}

Co-authors: Katsunori Suzuki¹; Yoichiro Neo²; Yoku Inoue³

¹ Research and Development Division, Yamaha Corporation

² Research Institute of Electronics, Shizuoka University, Japan

³ Department of Electronics and Materials Science, Shizuoka University

Recently, nanofibers attract much interest not only in apparel industry, but also information technology, bio-medical, or environmental fields. In the presentation, I will introduce fabrication and characteristics of highly aligned carbon nanotube (CNT) nanofiber sheets [1-4]. The multiwalled CNTs (MWCNTs) were deposited by chloride-assisted chemical vapor deposition. The length of obtained MWCNTs ranges up to the millimeter scale, and they can easily be spun into yarn by hand with the naked eye. The aligned CNT sheets were formed by stacking CNT webs drawn from spinnable CNT forest. As applications of the CNT sheets I will present strain sensors [5]. In addition to the CNT

sheets, we fabricated copolymer of vinylidene fluoride and trifluoroethylene P(VDF/TrFE)(75/25 molar ratio) nanofiber sheets [6]. The highly aligned P(VDF/TrFE) nanofiber webs with high uniformity and smooth surface were obtained by electrospinning. The stretching and annealing process improved their crystallinity. I will also present their characteristics in my presentation.

Hornbill 1 / 230

Asst. Prof. Toemsak Srikhirin

To be added

Heron 1 / 233

Natural Materials for Dye Sensitized Solar Cells: Experimental and Theoretical Study

Density functional theory (DFT) and time dependent DFT (TDDFT) were used to study on electronic and photoelectrochemical properties of monascus, cochineal, lac insects and anthocyanin dyes. The low-cost dye-sensitized solar cells (DSSCs) utilized by crude and pre-concentrated anthocyanins extracted from mangosteen pericarp, roselle, red cabbage, Thai berry, black rice, blue pea and purple corn were fabricated. The ultraviolet-visible (UV-VIS) spectroscopy, Fourier transform infrared spectroscopy (FTIR), electrochemical impedance spectroscopy (EIS) and incident photo-to-current efficiency (IPCE) were employed to characterize the natural dye and the DSSCs. Nanoporous carbon microspheres from carrot juice and mesoporous honeycomb-like carbon structure from mangosteen peel were used as counter electrodes for DSSCs.

References

- 1 Chaiamornnugool, P., Tontapha, S., Phatchana, R., Ratchapolthavisin, N., Kanokmedhakul, S., Sangaroon, W., Amornkitbamrung, V., "Performance and stability of low-cost dye-sensitized solar cell based crude and pre-concentrated anthocyanins: Combined experimental and DFT/TDDFT study," *Journal of Molecular Structure*, 1127, pp. 145-155. (2017)
- [2] Phinjaturos, K., Maiaugree, W., Suriharn, B., Pimanpaeng, S., Amornkitbamrung, V., Swatsitang, K. "Dye-sensitized solar cells based on purple corn sensitizers," *Applied Surface Science*, 380, pp. 101-107. (2016)
- [3] Maiaugree, W., Lowpa, S., Towannang, M., Rutphonsan, P., Tangtrakarn, A., Pimanpang, S., Maiaugree, P., Ratchapolthavisin, N., Sang-Aroon, W., Jarernboon, W., Amornkitbamrung, V., "A dye sensitized solar cell using natural counter electrode and natural dye derived from mangosteen peel waste," *Scientific Reports*, 5, art. no. 15230, (2015)
- [4] Lowpa, S., Pimanpang, S., Maiaugree, W., Saekow, S., Uppachai, P., Mitravong, S., Amornkitbamrung, V., "Nanoporous carbon microspheres from carrot juice used as a counter electrode for a dye-sensitized solar cell," *Materials Letters*, 158, pp. 115-118. (2015)
- [5] Sang-Aroon, W., Laopha, S., Chaiamornnugool, P., Tontapha, S., Saekow, S., Amornkitbamrung, V., "DFT and TDDFT study on the electronic structure and photoelectrochemical properties of dyes derived from cochineal and lac insects as photosensitizer for dye-sensitized solar cells," *Journal of Molecular Modeling*, 19 (3), pp. 1407-1415. (2013)
- [6] Sang-Aroon, W., Saekow, S., Amornkitbamrung, V., "Density functional theory study on the electronic structure of Monascus dyes as photosensitizer for dye-sensitized solar cells," *Journal of Photochemistry and Photobiology A: Chemistry*, 236, pp. 35-40. (2012)

Heron 1 / 235

Nondestructive 3D Characterization of Materials Using Optical Coherence Tomography

Author: Panomsak Meemon¹

¹ *School of Physics, Institute of Science, Suranaree University of Technology, Nakhon Ratchasima, Thailand 30000*

Optical Coherence Tomography (OCT) is an optical imaging technology that produces cross-sectional image similar to that obtained by Ultrasound imaging but at much higher resolution, higher imaging speed, and higher sensitivity. Unlike other optical microscope, OCT utilizes low-coherence properties of the broadband light source to gate the sample's microscopic structure over depth and hence is capable of noncontact and nondestructive three dimensional (3D) mapping of sample's structure. Moreover, utilizing the principle of light interference in the frequency domain, our custom developed OCT systems is capable of imaging speed of more than 100 frames per second. This high speed imaging capability allows for three dimensional (3D) imaging in less than 10 seconds, which is useful for nondestructive monitoring of micro structures of samples in 3D and in real time. Here, we report the progress on the development of several techniques of nondestructive metrology using OCT system, such as surface topography, thickness topography, refractive index profilometry, 3D flow velocity mapping, 3D elasticity measurement, and polarization sensitive characterization. Furthermore, several approaches to push the limit of OCT for 3D characterization of nanomaterials will be presented and discussed.

Keywords: Optical tomography, 3D imaging, Thickness topography, Elastography, Birefringence map, flow analysis

Falcon 1 / 240

Electrical properties and dielectric responses in rutile-TiO₂-based ceramics

Author: pravit thongbai¹

Co-authors: A. Boonkhuang²; B. Putasaeng³; J. Boonlakhorn²; K. Meeporn⁴; N. Chanlek⁵; N. Thanamoon²; N. Thongyong²; P. Kidkhunthod⁵; P. Siriya²; S. Danwittayakul³; S. Maensiri⁶; T. Nachaithong⁴; T. Yamwong³; W. Tuichai²

¹ *Khonkaen University*

² *Integrated Nanotechnology Research Center (INRC), Department of Physics, Faculty of Science, Khon Kaen University, Khon Kaen 40002, Thailand*

³ *National Metal and Materials Technology Center, National Science and Technology Development Agency, Thailand Science Park, Pathumthani 12120, Thailand*

⁴ *Materials Science and Nanotechnology Program, Khon Kaen University, Khon Kaen 40002, Thailand*

⁵ *Synchrotron Light Research Institute (Public Organization), 111 University Avenue, Muang District, Nakhon Ratchasima 30000, Thailand*

⁶ *School of Physics, Institute of Science, Suranaree University of Technology, Nakhon Ratchasima 30000, Thailand*

Corresponding Author: pthongbai@kku.ac.th

Colossal dielectric responses in rutile-TiO₂-based ceramics were investigated. Very high dielectric performance with ultra-high dielectric permittivity ($\epsilon' \approx 10^3 - 10^6$) and very low loss tangent ($\tan(\delta) < 0.05$) over wide frequency and temperature ranges were achieved by co-doping with M³⁺ and N⁵⁺ ions. Good temperature stability of ϵ' was also obtained. Electron-pinned defect-dipoles, grain boundary response, surface-barrier layer and electrode effects have a great influence on the overall dielectric properties of rutile-TiO₂-based ceramics. X-ray photoelectron and Raman spectroscopy analyses were carried out to describe the origin(s) of the colossal permittivity. Impedance spectroscopy was used to study the electrical responses of the grains and grain boundary.

Heron 2 / 241

Synthesis and fabrication of nanomaterials for applications in food and agriculture

Author: Mongkol Sukwattanasinitt¹

¹ *Department of Chemistry, Faculty of Science, Chulalongkorn University, Bangkok 10330, Thailand*

Corresponding Author: msukwatt@gmail.com

Nanotechnology are beneficial for safe and efficient consumption of food, water and agricultural products. The NANOTEC-CU center of excellent on food and agriculture has focused the research in molecular design, synthesis and fabrication of nanomaterials for applications in the field of food and agriculture including chemical analysis and delivery systems. Various chromophores and fluorophores responsive to changes of physical environment and chemical contaminants are developed as the indicators for ensuring safety and quality of foods, drinking water and agricultural products. Molecular self-assemblies of amphiphilic molecules or large π -conjugated arrays allow facile fabrications of nano-sized materials for simple and efficient applications of sensing, storing and delivery systems. Micellar incorporation of essential oil into edible natural polymers allows effective preservation and simple usage of Thai natural herbs in foods and drinks. Graphitic nanocarbon cluster are developed as an efficient delivery vehicle for biological active compounds and genetically important agents into cells and nucleus.

Keywords: Drug delivery, Food safety, Molecular self-assembly, Sensor, Vesicle

Falcon 1 / 243

Limitation of Rheology and Curing Processes for Tiny Adhesive Dot with Various Dispensing Systems in Hard Disk Assembly Process

Author: Tanakorn Osotchan¹

¹ *Center of Nanoscience and Nanotechnology, and Physics Department, Faculty of Science, Mahidol University, Thailand*

Corresponding Author: sctos@mahidol.ac.th

In order to reduce the size of magnetic head in hard disk manufacturing, an important assemble process required to further develop is an adhesive dispensing at controllable small amount in order of nanoliter. Together with the confined tiny space during assembly, the exposure of UV light for rapid adhesive curing may not be possible thus the shadow curing with shorten period is also needed to be developed. For manufacturing process, a method to determine the percentage of cure of this tiny adhesive dot is also necessary to verify the optimum assemble process. In this work, the rheology of adhesive was studied for two dispensing systems including time-pressure and microdot valve dispensing systems. The system parameters including air pressure, dispensing time and spring force were varied to determine the limitation of parameters relative to fluctuation of dot size variation. The material parameters of adhesive especially viscosity were also modified in order to describe the type of fluid flow behavior. After forming the desired dot size, the curing process was investigated by heat cure, UV cure and dual cure. The gel fraction and differential scanning calorimeter (DSC) were used to determine the curing percentage. The amount of heat required to complete phase transition indicated in DSC cure is the reliable parameter to determine the degree of cure. Fourier transform infrared absorption is hard to apply to detect the curing process while the Raman spectroscopy has advantage potential to determine the degree of curing. The micro-Raman spectrometer can demonstrate the micro-region of different degree of cure on nanoliter adhesive dot size by the ratio of observed peak heights.

Heron 2 / 245

Highly Sensitive Nucleic Acid and Antibody Based Electrochemical Detection by Using of Nanomaterials as Signal Amplification Elements

Author: Werasak Surareungchai¹

¹ _

Corresponding Author: werasak.sur@kmutt.ac.th

Highly sensitive detection is a major goal for sensing and/or diagnosis of diseases, food-borne bacteria and biological warfare agents. High specific and sensitive detections can be achieved via labeling techniques in DNA hybridization and antibody-antigen interaction. Labels based on nanoscale materials open a new opportunity over the traditional methods - in terms of greater reporting signal per binding event. We have been able to lower the limit of detection (LOD) of < 1 fM for DNA and < 1 fg mL⁻¹ for antigens or < 5 CFU mL⁻¹, without using PCR or other methods of non-electrochemical amplification. In addition, some possibilities on high-throughput simultaneous assays have been attempted and reported. The talk will describe some our approaches engineered electrochemical labels using nanomaterials such as carbon nanotubes, graphene, and metal nanoparticles. Last, the talk will also present some real food pathogen applications.

Heron 2 / 246

Nanomedicine-based drug delivery systems for anti-cancer targeting and treatment.

Author: Teerapong Yata¹

¹ _

Corresponding Author: teerapong@nanotec.or.th

Over the last several decades, there has been tremendous amount of interest in developing novel nanoparticles for drug delivery to cancers. These nanoparticle platforms can be categorized as organic-based (e.g., lipid nanoparticles, biodegradable polymeric nanoparticles, and viral vectors), inorganic-based (e.g., metallic nanostructures, silica nanoparticles, and quantum dots), or a hybrid combination of the aforementioned.

The Nano Delivery System Laboratory group of National Nanotechnology Centre has been focusing on the use of nanotechnology for targeted delivery and controlled release of drugs, and biopharmaceuticals, in order to improve their effectiveness for the prevention and treatment of human diseases. Our group has generated a number of nanocarrier platforms and demonstrated their potential for cancer treatment. For example, we investigated the application of modified chitosan biopolymer as a potential vector for suicide gene delivery to cancers related to the reproductive system. We also engineered the bacteriophage-based nanocarrier (derived from a virus of bacteria and non-pathogenic for humans) that has promise in cancer gene therapy. Moreover, our group has reported a number of improved versions of lipid-based nanocarriers such as phospholipid-chitosan nanoliposomes, antibody-directed lipid nanoparticle platforms and mucoadhesive nanostructure lipid carrier (NLC), all of which have great potential for the delivery anti-cancer drug to various types of cancers.

Importantly, numerous nanoparticle platforms are being investigated and therefore require preclinical in vitro studies that accurately represent physiological conditions. In addition to conventional cell culture models, we have developed three dimensional (3D) tumour spheroid models as well as a flow chamber system and evaluated the possibility of using these system as a valuable device to examine efficiency of nanocarrier-mediated anticancer drug delivery and targeting specificity before moving on to animal studies.

This talk covers our current research as well as our previously reported nanocarrier platforms, their conceptual design and development, and the success of these platforms that present a breakthrough in the delivery of anti-cancer agents. This talk will also summarize the established models for in vitro

therapeutic screening that have potential to provide reliable information superior to conventional cell culture to improve and optimize drug delivery systems for an effective cancer targeting.

Heron 1 / 247

Chitosan-metal nanohybrids for microbial detection and extraction

Author: Suwabun Chirachanchai¹

¹ *Chulalongkorn University*

Corresponding Author: suwabun.c@chula.ac.th

Nowadays, environmental problems, for example, climate changes, overpopulation, and emerging and re-emerging diseases are considered as the global issues obstructing the human activities. In fact, environmental health-related problems are derived from several microbial for which an accurate and early detection and separation is a way to prevent the spread over. Therefore, specific sensors and/or effective extraction to detect the types of microbial are important. On this viewpoint, polymeric nanomaterials can be developed to obtain the materials as desired. For the past decades, our group focuses on functionalization of chitosan in water-based system for biomedical purposes. Here, we consider chitosan-metal nanoparticles so that the materials obtained are satisfied for microbial detections and extraction. The presentation covers the preparation of chitosan hybridized with metal nanoparticles, i.e. magnetic and gold nanoparticles, including the model studies on bacteria and fungi detection/extraction. The presentation also extends to the system in which we can entrap-release metal nanoparticles to isolate the metal nanoparticles which was hybridized with chitosan after use. Based on this concept, we demonstrate the way to fabricate the naturally abundant biomaterial, i.e. chitosan to be nano-biosensors which are simple, effective and practical for environmental health's purposes.

Falcon 1 / 248

Effects of Electric and Magnetic Fields on Nanoparticle Thin Films Prepared by Sparking-off Metal Tips

Author: Pisith Singjai¹

Co-authors: Stefan Ruckman ; Winai Thongpan ; Wiradej Thongsuwa

¹ *Chiangmai University*

Corresponding Author: pisith.s@cmu.ac.th

Nanomaterials have a vast range of applications in various fields due to their superior properties. There are a number of methods for nanoparticle-thin film coatings, for example spray pyrolysis, electrodeposition, spin coating and sol-gel process. However, these methods are either time consuming or require the use of toxic substances. The sparking method can be used to prepare nanoparticles and nanoparticle-thin films by applying a high voltage across any two metal wire tips. This talk will cover the effects of electric and magnetic fields on film morphology and crystalline phase formation. Preparation and characterization of ZnO, TiO₂, In₂O₃, FeN nanoparticle-thin films will be presented. It was found that the electric and magnetic fields enhanced the growth rate and uniformity of the films, whereas the magnetic field also altered the phase formation. Investigations of the sparked nanoparticles or nanoparticle-thin films as a photo-catalyst in dye-sensitized solar cells, a self-cleaning glass and a volatile organic compound sensor will be reviewed. A commercial lab-scale instrument of the sparking method from Nanogeneration Co., Ltd. as a spin-off company will be also demonstrated.

Heron 2 / 249

Smart Farm System : Case Studies in Thailand

Author: Teerakiat Kerdcharoen¹

¹ _

Corresponding Author: teerakiat.ker@mahidol.ac.th

Smell, taste, appearance and flavor are central to the value of agricultural products, especially fruits and their post-harvest spin-offs such as teas, coffees and wines. In specific, the uniqueness of a wine depends on types and ratio of such aroma molecules collected in the leaves or fruits during the growing seasons, which is related to many external factors such as soil conditions, fertilizers, irrigation, sun light and climate. Aroma management is a complex task involving various kinds of day-to-day activities that require year-long vigilant attention from the people concerned. Recently, modern technologies, for example, “precision farming”, have been introduced to plantation at the farm level. We have developed several technologies for farm management. The system features: (1) wireless sensor networks to monitor microclimate conditions such as solar energy, temperature, humidity, rain, air mass flow and pressure, soil water contents throughout the farm area; (2) plant monitoring system to monitor various parameters for proper irrigation management and analysis of plant growth; (3) web-based farm monitoring tools that farmer can access all information over the farm intranet/internet; (4) daily activities monitoring in which GPS-tracking systems follow activities of all equipments in the farm; (5) electronic nose system to monitor soil abundance, fruit growth and development of the fermented wines. This system was tested at various sites such as Gran-Monte vineyard in Nakhon Ratchasima, paddy in Kanchanaburi, HCF eggplant farm in Chiang Rai and Edamame farm in Chiang Mai. We have integrated both commercial and in-house technologies to build up such smart farm system. For wireless sensor networks, we have developed microclimate monitoring system based on IEEE 802.15.4, or the so-called ZigBee, using the mesh topology. For the monitoring of fruit and its post-harvest products, electronic nose has been demonstrated that it can be helpful tool both in the field (vineyard) and winery. By that, grape ripeness and fermentation stage can be tracked, leading to better quality control of the products.

Hornbill 1 / 250

Nano-materials Engineering and Manufacturing in Hard Disk Drives for Cloud Storage

Author: Krishnan Subramanian¹

¹ _

Corresponding Author: krishnan.subramanian@seagate.com

We are experiencing an explosion in the amount of digital content that is being generated every minute and the need to store this content has seen the demand for data storage reach unprecedented levels. This has led to the emergence of the “Cloud” as the pre-eminent paradigm for data storage and represents a marked shift from how data used to be stored just a few years ago.

This talk focuses on advances in the field of nano-materials engineering and manufacturing in order to achieve increases in storage capacities in hard disc drives to meet the growing demand for Cloud storage. Nano-engineering of the write and read elements, head-to-medium spacing, and media grains are discussed in, both conventional Perpendicular Magnetic Recording (PMR), as well as Heat-Assisted Magnetic Recording (HAMR) applications and some of the manufacturing challenges and considerations.

Finally, projections for the growth of Areal Density from the current 1Tbits/in² to 5 Tbits/in² and beyond are discussed.

Heron 2 / 251

Domain-Exchanged Antibody with Potentiated Effector Functions

Author: Florian Rucker¹

Co-authors: Gerhard Stadlmayr ; Gordana Wozniak-Knopp ; Jan Walther Perthold ; Katharina Stadlbauer

¹ _

Corresponding Author: florian.rueker@boku.ac.at

We have designed a complete-antibody-like construct where the CL and CH1 domains of trastuzumab are exchanged for a pair of CH3 domains and efficient heterodimerization of the light and the heavy chain is achieved using “Knobs-into-Holes” strategy. The construct prepared in this way expressed at a high level in HEK293 system. Rational mutagenesis of the amino acid residues located at the interface between the variable domains and the exchanged CH3 domains was applied to significantly improve thermostability and solubility of the molecule. The domain-exchanged construct was able to bind to the surface of the strongly HER2/neu positive cell line SK-BR3 within less than 2-fold the affinity of trastuzumab, but could nevertheless incite a more potent T-cell activation in an ADCC assay. This could be explained by a more than 3-fold stronger binding to the FcγRIIIa. The domain-exchanged antibody presents a novel class of engineered immunoglobulin molecules of therapeutic interest due to their potentiated engagement of the molecules that can elicit effector functions.

Hornbill 1 / 252

Tailoring Nanocapsules for Self-Healing Materials

Author: Daniel Crespy¹

¹ *Department of Materials Science and Engineering, School of Molecular Science and Engineering, Vidyasirimedhi Institute of Science and Technology, Rayong 21210, Thailand*

Corresponding Author: daniel.crespy@vistec.ac.th

Abstract

Self-healing materials are a class of materials that can repair themselves. This feature is very interesting because it allows for saving resources to build new materials, saving energy need to make new materials, and finally reducing the amount of waste that can contaminate the environment. In our research, we use the power of nanotechnology to tailor new materials that are useful for self-healing and anticorrosion properties. We show here different methods for encapsulating healing agents and corrosion inhibitors. The release of the healing agents is either trigger by mechanical damage of the capsules or triggered by the corrosion of metal. In another approach, we embedded nanocapsules in nanofibers by colloid-electrospinning. The release profile of payloads encapsulated in the nanocapsules could be controlled by the materials constituting the nanocapsules shells and the nanofibers matrix.

Keywords: Anticorrosion, Colloid-electrospinning, Nanocapsules, Nanofibers, Self-Healing Materials

References

- [1] Zhao, Y.; Fickert, J.; Landfester, K.; Crespy, D. *Small* 2012, 8, 2954
- [2] Fickert, J.; Landfester, K.; Crespy, D. *Polym. Chem.* 2016, 7, 4330
- [3] Tran, T.H.; Vimalanandan, A.; Genchev, G.; Fickert, J.; Landfester, K.; Crespy, D.; Rohwerder, M. *Adv. Mater.* 2015, 27, 3825
- [4] Lv, L.-P.; Zhao, Y.; Vilbrandt, N.; Gallei, M.; Vimalanandan, A.; Rohwerder, M.; Landfester, K.; Crespy, D. *J. Amer. Chem. Soc.* 2013, 135, 14198

[5] Vimalanandan, A.; Lv, L.-P.; Tran, T.H.; Landfester, K.; Crespy, D.; Rohwerder, M. *Adv. Mater.* 2013, 25, 6980

Heron 2 / 253

Use of nanobodies in developing a bacterial antibody production platform

Author: Mehmet Berkmen¹

¹ *Harvard University*

Corresponding Author: mehmet_berkmen@hms.harvard.edu

SHuffle is a genetically engineered E.coli strain that allows disulfide bond formation in its cytoplasm with high fidelity. Many proteins containing disulfide bonds have been successfully expressed in SHuffle. In this study, we have expressed for the first time full length human, rabbit and mouse antibodies, along with chimeric versions, including the commercial blockbuster Humira in SHuffle (*Nature Communications* (2015) Aug 27; 6:8072). In order to improve the folding and assembly of IgG, we have co-expressed a set of chaperones and other helper proteins from our newly developed pAL plasmid system. The co-expression of the pAL plasmid set increased the production of IgG in SHuffle several fold. The IgG produced in SHuffle was comparable to hybridoma produced IgG. SHuffle is an easy, fast, robust platform for antibody engineering, screening and expression.

Heron 2 / 254

Bionanomaterials for Diagnostics, Imagine and Drug delivery

Author: Uracha Ruktanonchai¹

¹ _

Corresponding Author: uracha@nanotec.or.th

To be added

Hornbill 1 / 255

Material, Device and Interfacial Engineering for High efficiency Solution Processable Organic Light Emitting Diode

Author: Kai Lin Woon¹

Co-authors: Azhar Ariffin²; Bee Kian Ong²; Calvin Yi Bin Ng³; Hideki Nakajima⁴; Keat Hoe Yeoh³; Noor Azrina Talik³; Nurul Nadiah Zakaria²; Prayoon Songsiririthigul⁵; Raimonda Griniene⁶; Ratchadaporn Supruangnet⁴; Saulius Grigalevicius⁶; Show-An Chen⁷; Thanit Saisopa⁴; Thomas J Whitcher³; Zainal A. Hasan²

¹ *University of Malaysia*

² *Department of Chemistry, University of Malaya, 50603 Kuala Lumpur, Malaysia*

³ *Low Dimensional Materials Research Center, Department of Physics, University of Malaya*

⁴ *Synchrotron Light Research Institute, Nakhon Ratchasima 30000, Thailand*

⁵ NANOTEC-SUT Center of Excellence on Advanced Functional Nanomaterials and School of Physics, Suranaree University of Technology, Nakhon Ratchasima 30000, Thailand

⁶ Department of Polymer Chemistry and Technology, Kaunas University of Technology, Radvilenu Plentas 19, LT-50254 Kaunas, Lithuania

⁷ Department of Chemical Engineering and Frontier Research Center on Fundamental and Applied Sciences of Matters, National Tsing-Hua University, 101, Section 2, Kuang-Fu Road, Hsinchu 30041, Taiwan, Republic of China

Corresponding Authors: id07@mail.com, id03@mail.com, id09@mail.com, id08@mail.com, id02@mail.com, id04@mail.com, id11@mail.com, id05@mail.com, id10@mail.com, id06@mail.com, id15@mail.com, id16@mail.com, id13@mail.com, id12@mail.com, id01@mail.com, ph7klw76@um.edu.my

Generally, Organic LEDs can be fabricated using either vacuum deposition or wet processes. It is well known that vacuum deposition can produce high efficiency Organic LEDs. Solution processable organic light emitting diode offers simpler, cheaper method of fabrication which is compatible with the roll-to-roll and inkjetting process. However, generally solution processable LED suffers from poorer efficiency and the generally lack of materials in the market. Here, we demonstrate that by simple surface engineering, the efficiency of commercial available long lifetime 'super-yellow' poly-(p-phenylenevinylene) (SY-PPV) can be almost doubled. In order to obtain high efficiency solution processable Organic LEDs, molecules of size larger than 1000 molecular weight with triplet energy higher than 2.8eV are required. Hence, we have developed an accurate computational method to predict the triplet energies of materials allowing us to screen a wide range of materials. From here, we are able to synthesize materials with high triplet energies. We also found out that intermolecular distance and non-chromophoric side group substitutions such as bulky alkyl groups and fluorine can significantly influence the triplet energy. Effective charge confinement is also important to obtain charge balance for high efficiency Organic LEDs. Here we also demonstrated fully solution processable red, green blue organic phosphorescent light emitting diodes with little deviation of CIE colour coordinate within a wide range of brightness as a result of effective excitons and charge confinement.

Heron 1 / 256

Prof. Nguyen Van Hieu

Author: Nguyen Van Hieu¹

¹ 227 Nguyen Van Cu Street, Ward 4, District 5, Ho Chi Minh City, Viet Nam

Corresponding Author: nvhieu@hcmus.edu.vn

Abstract will be added by the contribution

Heron 2 / 257

Nanomaterials for analytical detection

Author: Orawon Chailapakul¹

¹ Electrochemistry and Optical Spectroscopy Research Unit (EOSRU), Department of Chemistry, Faculty of Science, Chulalongkorn University, 254 Phayathai Road, Patumwan, Bangkok 10330, Thailand / Center for Petroleum, Petrochemicals and Advanced Materials, Chulalongkorn University, 254 Phayathai Road, Pathumwan, Bangkok 10330, Thailand

Corresponding Author: corawon@chula.ac.th

Nanomaterials have received unceasingly consideration for decades. Profuse utilizations have been afforded to raise the efficacy of research in numerous scientific fields since their discovery. This

novel supplies trigger the versatility of materials properties in which diversely expedite the applications in analytical research. Due to exceptional features derived from indigenous of particles in nanometer-size, they have received abounding attraction in environmental, food, clinical analysis. Particularly, medical detection based on nanomaterials as signal amplification has been positively subjected as crucial keys towards conceptual biomedical analytical tools because nanomaterials process biocompatible property. For these reasons, many research groups have proposed various strategies engaging nanomaterials for detection of biological targets. Our group also resembles an interest of nanomaterials use and characteristic. However, we exclusively highlight the reinforcement of excellent properties of graphene in electrochemical detection, also nanoparticles as probe for optical detection.

The outstanding physical, chemical, and electrical features compel an adaptation of graphene (G) in many means of electrode modification. Its magnificent electrons conductivity arises from layer of carbon atoms packed closely into a two-dimensional honeycomb arrangement. Consequently, our groups have adopted graphene in numerous clinical sensing applications including cholesterol and glucose. In our works, graphene was consolidated with polyaniline (PANI), a conducting polymer, on the electrodes. The integrity of geminate materials improved the sensitivity in electrochemical detection substantially. Following a thorough investigation of electrochemical properties, the composite nanomaterials were electro-sprayed onto screen-printed carbon electrode (SPCE) and applied for cholesterol detection. The results demonstrated clearly that the signal was improved and more-well defined. The limit of detection proposed in this work was as low as 1 μ M after optimization. Another work has confirmed the advantages of G-PANI by casting the working electrode in the electrochemical compact disk (eCD) platform prior detection of glucose. Wide linear dynamic range (1-10 mM) was obtained with low detection limit of 0.29 mM. Both methods were applied in real serum and blood samples showed satisfied results validating with the standard methods. In addition, recently our groups have reported methodology for detection of human papillomavirus (HPV) using SPCE surface modified with G-PANI. The signal was distinctly increased as a great function of G-PANI, while the selectivity was achieved from the PNA probe.

Nanoparticles are particles in nanometers range which dominate the extra unique properties contrasting from their bulk materials. Numerous prestige is inscribed for optical features of nanoparticles. Therefore, applications based on colorimetry and spectrophotometry of nanoparticles are extensively introduced. Our groups also developed a superior methodology for detection of metal ions in blood samples on facile and cheap paper-based analytical devices (PADs). The etching reaction between silver nanoplates (AgNPIs) and metal target was attributed to the resulting color change. From pink to colorless, the detection of copper ions (Cu^{2+}) was successfully achieved. On the other hands, nanoparticles occupied high surface area to volume ratio which benefits the electrons transferring among surface of conducting materials. A comprehension of this behavior accomplished our skilled electrochemical works on enzymatic cholesterol detection using silver nanoparticles (Ag-NPs) electroplating incorporating with cholesterol oxidase (ChOx) on boron doped diamond (BDD) electrode. The enhancement of H_2O_2 signal was obtained from AgNPs depositing on the surface of working electrode, whereas ChOx provided the selectivity for this reaction. In this works, not only the sensitivity was increased, but the cathodic peak also displayed more well-defined compared with bare electrode. This work demonstrated that cholesterol as low as 0.25 mg dL⁻¹ can be detected in real serum samples with the involvement of AgNPs.

Keywords: Graphene, Nanoparticles, Electrochemical detection, Optical detection, Paper-based analytical devices (PADs)

Falcon 1 / 258

Metal-oxide Semiconducting Nanostructures by Microwave-assisted Thermal Oxidation Technique for Sensor and Solar Cell Applications

Author: Supab Choopun¹

Co-authors: Atcharawon Gardchareon¹; Duangmanee Wongratanaphisan¹; Karakade Kaewyai¹; Meechai Thepnurat¹; Niyom Hongstith¹; Pipat Ruankham¹; Sanpet Nilphai¹; Surachet Phadungdhitidhada¹; Torranin Chairu-

angsri¹¹ *Department of Physics and Materials Science, Faculty of Science, Chiang Mai University, Chiang Mai 50200, Thailand***Corresponding Author:** supab.c@cmu.ac.th

Metal-oxide semiconducting (MOS) Nanostructures prepared by microwave assisted thermal oxidation technique are demonstrated. With this simple and fast process, MOS nanostructures with various morphologies can be synthesized such as ZnO tetrapods, interlinked ZnO tetrapod networks (ITN-ZnO), MgO nanoparticles, CuO/Cu₂O fibers. Mostly, ITN-ZnO morphology which have tetrapod-like features with leg-to-leg linking is presented here. The electrical and ethanol-sensing properties related to the morphology of ITN-ZnO compared with those of other ZnO morphologies are investigated. It is found that ITN-ZnO unexpectedly exhibits superior electrical and gas-sensing properties in terms of providing pathways for electron transport to the electrode. A UV sensor and a room-temperature gas sensor with improved performance are achieved. Therefore, ITN-ZnO is an attractive morphology of ZnO that is applicable for many new applications because of its novel properties. The novel properties of ITN-ZnO are beneficial for electronic, photonic, optoelectronic, and sensing applications. ITN-ZnO may provide a means to improve the devices based on ITN-ZnO. Moreover, MgO nanoparticles and CuO/Cu₂O fibers prepared by microwave assisted thermal oxidation technique are also demonstrated and applied for dye-sensitized solar cells.

Heron 2 / 259

Cosmeceutical based nanotechnology: the beauty from nature

Author: Mattaka Khongkow¹¹ *National Nanotechnology Centre (NANOTEC), National Science and Technology Development Agency, 130 Thailand Science Park, Paholyothin Rd., Klong Luang, Pathumthani, 12120, Thailand***Corresponding Author:** mattaka@nanotec.or.th

Cosmeceuticals from natural products or herbal cosmetics has become the most topic of interest in nowadays cosmetic trend, as they are natural, safe and free from all the harmful synthetic chemicals. Many naturally available herbs serves as active ingredients in different uses for skincare, haircare and antioxidant formulation. However, the application of phytochemical extracts in cosmeceutical products is still challenging due to their stabilities as well as their abilities for skin adsorption and penetration. To address these challenges and to overcome a skin barrier, nanotechnology have been widely applied.

In our Nano-cosmeceutical laboratory, the main focuses are based on the implication of nanotechnology and delivery system in novel cosmeceutical products, especially from Thai medicinal herbs. The expertise also includes an in vitro and cell-based assays for the investigation of bioactivities as well as cosmeceutical efficacies of the extracts for anti-oxidation, anti-ageing, anti-acne, anti-septic, anti-inflammatory, and whitening prior to technology transfer and commercialization.

This current talk gives a brief overview of importance of nanotechnology in cosmeceutical products. It also covers different types of nanoencapsulation systems and carriers in present products including the development of lipid-based nanoparticles such as liposome, noisome, and nanostructured lipid carriers (NLCs). The investigation of bioactivity, biocompatibility and cytotoxicity of these carriers using cell-based assay will be addressed. Finally, our ongoing research on applications of these carrier in cosmeceutical formulation will be also highlighted.

Falcon 1 / 260

Biodegradable nanocomposite blown films based on PLA and PBAT containing silver-loaded kaolinite: Formulation and property testing for use as smart packaging for dried longan

Author: Winita Punyodom¹

Co-authors: Patnarin Worajittiphon²; Robert Molloy¹; Sutinee Girdthep²; Thanawadee Leejarkpai³

¹ Polymer Research Laboratory, Department of Chemistry, Faculty of Science, Chiang Mai University, Chiang Mai, 50200, Thailand / Materials Science Research Center, Faculty of Science, Chiang Mai University, Chiang Mai, 50200, Thailand

² Polymer Research Laboratory, Department of Chemistry, Faculty of Science, Chiang Mai University, Chiang Mai, 50200, Thailand

³ National Metal and Materials Technology Center, National Science and Technology Development Agency, Pathumthani, 12120, Thailand

Corresponding Author: winitacmu@gmail.com

Novel biodegradable nanocomposite blown films based on compatibilized poly(lactic acid)-poly(butylene adipate-co-terephthalate) (PLA/PBAT) blends were fabricated for use as packaging for dried longan. Silver-loaded kaolinite (AgKT) dispersed in the polymer matrix as intercalated-exfoliated microdomains improved the properties of the films, in particular the moisture barrier properties. In addition, controlled silver release provided long-term antibacterial activity which can be attributed to AgKT's layered structure. The amount of released silver ions also complies with migration levels specified by the standard for food-contact plastic packaging. It was found that as little as 4 phr AgKT in the nanocomposites decreased the film's elongation at break from 213.0±5.85% to 53.8±1.81%, increased thermal stability for processing, and decreased the water vapor permeability by 41.85%. The shelf-life of dried longan as predicted experimentally by a moisture sorption isotherm and theoretically by the Peleg model were almost identical (~308 days) and were more than twice as long as for the films without AgKT under ambient conditions. Biodegradability testing for the whole life cycle was also carried out for the PLA/PBAT films both with and without AgKT and compared with PLA alone. The PLA film showed the highest rate of biodegradation followed by the PLA/PBAT blend and the PLA/PBAT/AgKT nanocomposite, respectively. Even though the presence of AgKT in the nanocomposite slowed down its rate of biodegradation, its % biodegradation of 69.94 % at the end of the test period (90 days) still conformed to the Chinese National Standard (GB/T 20197-2006) for a biodegradable plastic by being higher than 60 %. On the basis of these properties, the PLA/PBAT/AgKT nanocomposites are considered to be promising candidates for use in film packaging applications to replace non-biodegradable and petro-based plastics

Heron 1 / 261

X-ray Absorption Investigation on Cation Distribution and Magnetic Behavior of Zinc Ferrite Nanoparticles

Author: Wisanu Pecharapa¹

¹ College of Nanotechnology, King Mongkut's Institute of Technology Ladkrabang, Ladkrabang, Bangkok 10520

Corresponding Author: kpwisan@kmitl.ac.th

Zinc Ferrite (ZnFe₂O₄) nanopowders were synthesized by ball-milling technique at different milling times (0 to 24 h) starting from as-combusted powders. The XRD and SEM results ensure significant decrease in particle size of these ferrites with increasing processing time. The distribution of cations including zinc (Zn²⁺) and ferric (Fe³⁺) ions was investigated by Zn and Fe K-edge X-ray absorption near-edge structure (XANES) and extended X-ray absorption fine structure (EXAFS) spectra. Comparing to after-calcined zinc ferrite, both XANES and EXAFS spectra of milled-zinc ferrite powders obviously indicate the translocation of Zn²⁺ ions from the tetrahedral (A) sites to the octahedral (B) sites and the reverse translocation of some of Fe³⁺ ions without affecting the long-range structural order. Moreover, the analysis of Zn and Fe K-edge EXAFS spectra exhibit obviously increasing degree of inversion as the particle size decreases resulting in the difference in the magnetic properties of the powders.

Hornbill 1 / 262

Printed Graphene Electronics

Author: Adisorn Tuantranont¹

¹ *Thai Organic and Printed Electronics Innovation Center (TOPIC), National Electronics and Computer Technology Center (NECTEC), National Sciences and Technology Development Agency (NSTDA), Thailand*

Corresponding Author: adisorn.tuantranont@nectec.or.th

Graphene, emerging as a true 2-dimensional material, has received increasing attention due to its unique physicochemical properties (high surface area, excellent conductivity, high mechanical strength, and ease of functionalization and synthesis). Printed Electronic also is a new wave of large-area electronics and flexible electronics manufactured by printing technology. The fusion of these two emerging technologies created the new opportunity to invent variety of novel electronic devices with low cost including nanosensors. Recent development on printed sensors based on graphene and graphene hybrid composite at TOPIC are comprehensively presented. Printed graphene based biosensors exhibited promising properties with good reliability suitable for commercial applications such as food pathogen sensors, biomedical sensors etc. Moreover, the application of printed graphene-based electronic devices researched at TOPIC will be presented including graphene-based electroluminescent light sheet, touch switch and supercapacitors for energy storage applications.

Heron 1 / 263

Molecular Dynamics Simulations and Gaussian Network Model in Improving Protein–Protein Binding Affinity: HIV and Dengue Cases

Author: Vannajan Sanghiran Lee¹

¹ *University of Malaya*

Corresponding Author: vannajan@um.edu.my

Conformational dynamics of proteins have been suggested to play crucial roles in protein-protein binding and dissociation which are the two fundamental steps of protein–protein interactions, and determine the binding affinity. Intrinsic disorder in specific protein regions plays its role in recognition and such disordered protein regions may control the degree of motion between domains and in fact confer advantages over folded proteins in binding. Not surprisingly, a major endeavor in recent years has been to develop models and methods for simulating the dynamics of proteins, and relating the observed behavior to experimental data. Here, we demonstrate how protein dynamics dictate the binding affinity through the atomistic molecular dynamics simulations (MDs) and Gaussian Network Model (GNM), an elastic network model introduced at the amino acid residue level. A study cases for HIV and Dengue will be discussed. Comparison of both methods will be discussed. Binding free energy from longtime-scale molecular dynamics simulation under graphic processing units (GPUs) computing and mode shape analysis from GNM can be used to distinguish the higher/lower affinity protein towards the protein target.

Falcon 1 / 264

Chemical syntheses of functional nanostructures and their SERS applications

Author: Sanong Ekgasit¹

Co-authors: Apichat Pangdam ; Harnchana Katemala ; Kanet Wongravee ; Promponmg Pienpinijtham ; Supeera Nootchanat

¹ *Department of Chemistry, Faculty of Science, Chulalongkorn University, Thailand*

Corresponding Author: sanong.e@chula.ac.th

Nanomaterials is well-known for their versatile applications in electronics, medicals, chemicals, catalysts as well as environments. By tuning their size, shape, morphology, and composition, one could systematically change their chemical, physical, electrical, mechanical, and catalytic properties. In this contribution, we chemically synthesized complex gold and silver nanostructure (nanospheres, nanoplates, nanoporous, and nanostars) using hydrogen peroxide (HP) as the reducing and shape-controlling agents. The strong etchant of HP and surface passivation of chloride ion promote the dissolution of certain facets while preserving and promoting growth of other facets enables the formation of complex nanostructures. By systematically tuned the nucleation and growth environment, we could selectively fabricate desired nanostructure. We then later explore their nano-size effects and surface enhance capabilities for trace chemical analysis using surface enhanced Raman scattering (SERS), tip enhanced Raman scattering (TERS) as well as light harvesting potential using organic solar cell (OSC).

Keywords: nanostructures, SERS, TERS, selective etching, hydrogen peroxide

References:

1. S. Vantasin, W. Ji, Y. Tanaka, Y. Kitahama, M. Wang, K. Wongravee, H. Gatemala, S. Ekgasit, and Y. Ozaki, *Angewandte Chemie International Edition* 2016, 55, 8391–8395.
2. P. Pienpinijtham, S. Vantasin, Y. Kitahama, S. Ekgasit and Y. Ozaki, *J. Phys.Chem. C* 2016, 120, 14663-14668.
3. H. Gatemala, C. Thammacharoen, S. Ekgasit and P. Pienpinijtham, *CrystEngCom.* 2016, 18, 6664-6672.
4. H. Gatemala, P. Pienpinijtham, C. Thammacharoen, S. Ekgasit, *CrystEngComm*, 2015, 17, 5530-5537.
5. P. Parnklang, C. Lertvachirapaiboon, P. Pienpinijtham, K. Wongravee, C. Thammacharoen, S. Ekgasit, *RSC Advances* 2013, 3, 12886–12894.
6. P. Parnklang, B. Lamlua, H. Gatemala, C. Thammacharoen, S. Kuimalee, B. Lohwongwatana, S. Ekgasit, *Materials Chemistry and Physics* 2015, 153, 127-134.

Heron 1 / 265

Possible electric field induced indirect to direct band gap transition in MoSe₂

Author: Kim Changyoung¹

¹ *Seoul National University, Seoul, Korea*

Corresponding Author: changyoung@snu.ac.kr

Novel phenomena such as indirect to direct band gap transition, giant exciton binding energy, spin-valley-layer locking and polarization dependent valley control are attractive features of transition metal dichalcogenides (TMDs). Especially, the layer dependent indirect to direct band gap transition raised enormous interest in TMDs. There have already been many efforts to control the band gap with means other than the number of layers. Here, we report the possibility for electric field induced indirect to direct band gap transition in bulk MoSe₂ observed by using angle resolved photoemission spectroscopy (ARPES). In order to demonstrate the evolution of the electronic structure as a function of surface electron doping and/or surface electric field, we use in-situ alkali metal dosing on the surface of in situ cleaved MoSe₂. We find that the alkali metal evaporation affects the Γ and the K point electronic structure differently. The difference in binding energy between valence band maximum (VBM) at the Γ and the K points changes from 370 meV to 30 meV. Our results not only clearly show a possibility of indirect to direct band gap transition by electric field, but also show the relation between the gap size and surface electric field in this material.

Heron 1 / 266

First-principles study on two dimensional dichalcogenides for hydrogen production

Authors: Kye Yeop Kim¹; Seungwu Han¹

Co-author: Joohee Lee ¹

¹ Department of Materials Science and Engineering Seoul National University

Corresponding Authors: id01@mail.com, id02@mail.com, hansw@snu.ac.kr

Hydrogen is a promising candidate for the clean energy carrier that may replace fossil fuels. For the production of hydrogen, water splitting with efficient catalysts has been intensively studied over the past decades. Platinum, which is known to be the best catalyst for water splitting, is too expensive to be used in large-scale applications. Therefore, numerous earth-abundant materials have been investigated as a replacement of Pt. Recently, transition metal dichalcogenides (TMDs), most notably MoS₂, are receiving a great deal of attention as a novel catalyst for water splitting. Although the basal plane of TMDs are efficient as catalysts, it was found recently that the sulfur vacancy in MoS₂ can increase the catalytic activity for hydrogen evolution.

In this presentation, motivated by the previous work, we explore the detailed mechanism for hydrogen production from the sulfur vacancy in MoS₂ and calculate the activation energies along the reaction path. Furthermore, we evaluate the catalytic efficiency of vacancy sites in various TMDs and suggest TMDs that may show high catalytic effects in hydrogen evolution reaction.

Heron 1 / 268

Sustainable Innovation of Magnetic Field Application in Catalytic Co₂ Conversion

Author: Metta Chareonpanich¹

¹ _

Corresponding Author: fengmtc@ku.ac.th

To be added

Heron 1 / 269

Polymer/Metal Nanoparticle/Nanocarbon Hybrid Materials for Highly Sensitive and Selective Volatile Organic compound Detection

Author: Winadda Wongwiriyan¹

Co-authors: Chanchana Thanachayanont²; Chanoknan Rattanabut³; Jiti Nukeaw⁴; Rungroj Maolanon⁵; Sasiphapa Rodbuntum³; Supanit Porntheeraphat⁶; Visittapong Yordsri²; Win Bunjongpru⁷; Worawut Muangrat⁸

¹ College of Nanotechnology, King Mongkut's Institute of Technology Ladkrabang, Bangkok, Thailand / Nanotec-KMITL Center of Excellence on Nanoelectronic Device, Bangkok, Thailand

² National Metal and Materials Technology Center, Pathumthani, Thailand

³ College of Nanotechnology, King Mongkut's Institute of Technology Ladkrabang, Bangkok, Thailand

⁴ 1College of Nanotechnology, King Mongkut's Institute of Technology Ladkrabang, Bangkok, Thailand / Nanotec-KMITL Center of Excellence on Nanoelectronic Device, Bangkok, Thailand

⁵ *National Nanotechnology Center, Pathumthani, Thailand*

⁶ *National Electronics and Computer Technology Center, Pathumthani, Thailand*

⁷ *Thai Microelectronics Center, National Electronics and Computer Technology Center, Chachoengsao, Thailand*

⁸ *Navamindradhiraj University, Bangkok, Thailand*

Corresponding Author: winadda.wo@kmitl.ac.th

Recently, gas sensor based on the simple change in its resistance in response to the analytes, has been focused as a promising candidate for practical sensing devices. Several nanostructured materials such as carbon nanotube (CNT) and graphene, have attracted considerable attention as alternative sensing materials because of their distinctive characteristics in structural, electrical and mechanical properties. In this study, we studied on hybrid materials based on metal nanoparticle (NP) and polymer-functionalized nanocarbon materials for highly sensitive and selective volatile organic compound (VOC) detection. By taking dichloromethane (DCM) sensing as an example, we successfully demonstrated a highly sensitive detection of DCM vapor at room-temperature operation by means of functionalization of CNT with PMMA and Pt NPs. The response of hybrid sensor to DCM was 69-fold higher than that of pristine SWNT and linearly increased with increasing DCM concentration. The sensing mechanism was elucidated by polymer swelling and catalytic oxidation on the Pt NPs catalyst surface. Besides Pt/PMMA/CNT system, the sensing performance of the sensor based on polymer-coated graphene was also investigated. With the selection of coating polymer, the sensitivity and selectivity of the sensor were successfully improved. These results suggest that the integration of nanocarbon materials with polymer and nanoparticle is a promising approach for highly sensitive and selective volatile organic compound detection.

Hornbill 2 / 276

Photoemission Electron Spectroscopy (PES) at the Siam Photon Laboratory, SLRI

Author: Narong Chanlek¹

¹ *Synchrotron light research institute*

Corresponding Author: narong@slri.or.th

Photoemission electron spectroscopy (PES) is a powerful technique that provides information about chemical composition and electronic structure of a material surface. In this talk, the basic concepts and methods of PES will be introduced. The PES experiment facilities at the Siam Photon Laboratory, Synchrotron Light Research Institute (SLRI), will be overviewed. Examples for its applications will also be given and discussed to demonstrate the technique capabilities.

Hornbill 2 / 277

Classification and Application of Diamond-Like Carbon Films Using SR-Based Spectromicroscopy

Author: Sarayut Tunmee¹

¹ *Synchrotron Light Research Institute*

Corresponding Author: sarayut@slri.or.th

The attractive properties of diamond-like carbon (DLC) films consist of chemical inertness, high hardness, excellent tribological behavior, optical properties, and biocompatibility.^{1,2} These properties make them reasonable for using in a broad range of the industrial applications. For example, the DLC films are used for magnetic storage disks, automotive parts, biomedical devices, cutting tools,

and solar cells.¹⁻³ In the last decades, many research groups published the articles of 5,555 in an international journal based on Scopus database which is related to the DLC films through improved by doping with a “hetero element”.⁴ The data plays a significant role in the increment of the DLC applications and fields of studies in future. Currently, the combination of near-edge X-ray absorption fine structure (NEXAFS) and the X-ray photoemission electron microscopy (X-PEEM), so-called spectromicroscopy method at the Beamline 3.2Ua/b, enables us to make a sensitive evaluation of the surface structure together with the chemical states. It is a necessary result because it opens up the way to examine the classification of the DLC films for further understanding of chemical characteristics.

Hornbill 2 / 278

Synchrotron SAXS/WAXS for nano structural investigation

Author: Siriwat Soontaranon¹

¹ *Synchrotron Light Research Institute*

Corresponding Author: siriwat@slri.or.th

BL1.3W: SAXS/WAXS (Small/Wide angle x-ray scattering) at SLRI is a dedicated beamline for nano-structural investigation of material that has electron density fluctuation on the length scale under 100 nm. High intensity x-ray is obtained by incorporating the synchrotron radiation from a wiggler insertion device and a double multi-layers monochromator. The beam is focused by a toroidal mirror while three four blades slit systems were used for collimation purpose. Rayonix SX165 CCD detector having the diameter of 165 mm was employed as the x-ray detector.

The beamline is equipped with sample holder where the temperature of 15-200 °C can be controlled. The sample situated in air environment can be powder, solid or liquid state. A temperature controlled tensile machine is also available for in-situ study of nano structure of material under tension. The sample to detector distance can be varied from 0.1 to 4.8 m to cover the q-range of wide and small angle x-ray scattering $0.08 < q < 35 \text{ nm}^{-1}$.

SAXS can be used to study several types of material. For nano particle in colloidal system, the size, size distribution, fractal dimension can be obtained. For protein solution, SAXS offer folding/unfolding, aggregation, shape and conformation. For polymer system, orientation and period of periodic domain in block copolymer, lamellar structure of semicrystalline polymer can be extracted. The setup for WAXS measurement is also possible for the study of crystal structure such as phase identification and calculation of crystallinity.

Hornbill 2 / 279

An Application of Synchrotron-based X-ray Absorption Spectroscopy Study on Advanced Functional Materials

Author: Pinit Kidkhunthod¹

¹ *Synchrotron Light Research Institute*

Corresponding Author: pinit@slri.or.th

The investigation of the local geometric and electronic structure of probing element in bulk samples is the most extensive field of application in X-ray Absorption Spectroscopy (XAS). XAS consists of two main regions which are X-ray Absorption Near Edge Structure (XANES) and Extended X-ray Absorption Fine Structure (EXAFS). The former region is used to explain the local geometry and oxidation states of selected element in a sample whilst the latter one is used to address the local structure around probing element in samples. In my talk, the introduction of XAS, the XAS beamlines at

the Synchrotron Light Research Institute, THAILAND, and applications of synchrotron-based XAS on advanced functional materials such as carbon-ferrite composite nanofibers 1 and thermoelectric materials will be introduced in order to obtain the accuracy of their locally structural information which cause different properties in these materials.

Plenary talk / 280

Nano-needles, nano-conduits, nano-biocatalysts and nano-biopores On powerful tiny tools for atomic/molecular resolution surface inspections and effective nanoscopic facilitators of electroanaly- sis, bacterial cell survival and antibiotic design

Author: Albert Schulte¹

¹ *Biochemistry –Electrochemistry Research Unit & Center of Excellence in Advanced Functional Materials School of Chemistry, Suranaree University of Technology, Nakhon Ratchasima, Thailand*

Corresponding Author: albschulte@yahoo.com

Global work in the Nanoscience & Nanotechnology (NS & NT) section is with great enthusiasm a nonstop challenge in methodology development for high-quality visualization and controlled manipulation of surface and/or bulk matter properties on the nanometre scale. Logical further exciting endeavour in the field is obviously clever utilization of developed skills in the defined delicate tasks for miniaturized device fabrication and advanced high-tech commercial product synthesis. Introduced in this plenary session will be recent and current research work of the Biochemistry-Electrochemistry Research Unit of Suranaree University of Technology that, in a broader sense, has a relation to the distinct frame setting of the NS & NT research. Covered with a general technical background introduction and presentation of own accomplishments will be:

- Graphitic STM probe tip ('carbon nano-needle') fabrication for in situ electrochemical scanning tunnelling microscopy (EC-STM) with widened assessable electrochemical potential window.
- Carbon nanotube ('nano-conduit') utilization in enzyme biosensors with a joint of high signalling molecule collection efficiency and long response stability.
- Disease marker biosensing with allosteric enzyme ('nano-biocatalyst') facilitation.
- Bacterial outer membrane protein channel ('nano-biopore') adaptation for efficient nutrient uptake under tough environmental conditions.

Worth mentioning that the enormous level of sophistication that with no doubt has been gained in an

Hornbill 1 / 282

The progress of Taiwan nano-EHS regulations and researches

Author: Chuen Jin Tsai¹

¹ *Institute of Environmental Engineering, National Chiao Tung University No. 1001, University Road, Hsinchu, 30010, Taiwan*

Corresponding Author: cjtsai1@g2.nctu.edu.tw

Taiwan Nanotechnology Program has been launched from 2003 up to now in which nano-EHS program remains one of the main projects collaborated by many different agencies, including Taiwan MOST, EPA, ILOSH, MOHW, BSMT, universities and research institutes (ITRI, NHRI etc.). Through

inter-agency efforts, progress has been made in core facility establishment for nanomaterial characterization, certification of nanoproducts as nanoMark products, promulgation of regulations for registration of new chemicals, issuing guidances for the Assessment of Hazardous Chemicals and CCB (Chemicals Control Banding) Management of Chemicals, and the Registration of Nanomaterial-containing Food utensils, Containers and Packages...etc. It can be said that the commercialization of nanotechnology-related products is being emerged and promoted while it is being regulated at well.

To support nanoproduct commercialization and regulation, research progress has been made in the development of Nanoscale Reference Material, exposure assessment of nanotechnology workplaces, development of personal nanoparticle samplers, development of highly Raman-enhancing substrates based on silver nanoparticle arrays with tunable gaps, in-vitro studies using impedance-based Real-Time Cell Analysis detection platform, in-vivo studies using the whole body exposure chamber and efficient powder dispersion system etc. The progress in regulations and researches has been documented and archived in Taiwan Nanotechnology EHS Database (http://ehs.epa.gov.tw/Home/EN_F_Home_Index) which serves as the platform for the exchange of information and communication among different stakeholders and for the promotion of collaboration among international communities.

Heron 2 / 283

Enhanced Production and Selected Use of Nanocellulose from Fruit and Vegetable Residues: A Brief Review

Author: Sakamon Devahastin¹

Co-author: Naphaporn Chiewchan¹

¹ *Advanced Food Processing Research Laboratory, Department of Food Engineering, Faculty of Engineering, King Mongkut's University of Technology Thonburi*

Corresponding Authors: sakamon.dev@kmutt.ac.th, id01@mail.com

Nanocellulose is a cellulose-based material that possesses at least one of its dimensions in the nanometer range. Due to its unique characteristics, including its excellent mechanical properties, high degrees of thermal stability and water holding capacity, biodegradability and biocompatibility, nanocellulose is a promising naturally-derived material that can be used for various biomedical as well as agriculture and food applications. Typically, nanocellulose is produced from wood-based sources but interest in producing nanocellulose from fruit and vegetable by-products is on the rise as these residues are available in large quantity. The residues can also be more easily transformed into the desired material with less use of chemicals since the fibers of fruits and vegetables are more vulnerable than those of the woody plants. Increasing the yield of nanocellulose produced from such residues remains a challenge, however. Hydrothermal, chemical or enzymatic pretreatment methods may need to be applied to help disintegrate the inter-fibrillar hydrogen bonds of native cellulose microfibrils into nanosized fibrils to achieve such an objective. In this presentation, a brief review on how selected pretreatment methods can help enhance the defibrillation process will be mentioned. Use of nanocellulose in various food-based applications, including its use as a food additive or as a starting material for the production of edible packaging films will also be highlighted.

Hornbill 1 / 284

High throughput screening method for nanoparticles toxicity using 3D cells

Author: Seokjoo Yoon¹

¹ *Department of Predictive Toxicology, Korea Institute of Toxicology, Daejeon, South Korea*

Corresponding Author: sjyoon@kitox.re.kr

With the increase of nano-consumer using nanomaterials, the potential exposure to nanomaterials have been raised. Therefore recently the human and environmental impacts of nanomaterials have emerged as an issue. However, there are no suitable methods to evaluate the cytotoxicity of nanoparticles based on high-throughput screening method. High-throughput approaches allow the bulk of the screening analysis for manufactured nanoparticles and high volume data generation for nanoparticle toxicity. To assess the potential toxicity of manufactured or engineered nanoparticles, traditional in vitro toxicity studies have been performed using normal 2D culture system. But several problems were encountered during assay validation, ranging from particle agglomeration in biological media and optical interference with assay system. To date, there are several ISO activities on the cytotoxic effects of nanoparticle using cell viability assay and detection of ROS level. This work item is different from the others in that new assay platform such as 3D cells on pillar insert was applied to evaluate the cytotoxicity to exclude the artifacts of traditional cell-based assay such as optical absorption and reactivity with assay reagent. 3D cells based on pillar insert provide more in vivo mimicking state and to allow us to easily change cell growth media or expose 3D cells to detecting reagents by immersing the tip of the pillar insert in different reaction plates. This method allows the high-throughput screening of nanoparticle cytotoxicity by excluding the optical absorption and reactivity with assay reagent.

Hornbill 1 / 285

Teaching and Learning on Nano Safety in School

Author: Mana Intarasawang¹

¹ _

Corresponding Author: physicsmana@hotmail.com

A good form of teaching and learning approach for nanosafety related topics is the use of games and entertainment values activities. According to experts much of the way we learn today is through the use of higher order skills. Games naturally support the form of education that requires ability to think through and solve complex problems, or interact critically through language or media. Game playing is an excellent way to help wire our brains in ways that are crucial to the what, why, and how of learning needs for the 21st century.

Hornbill 1 / 286

Malaysia National Nanosafety Initiative.

Author: Mohd Helme Mohd Helan¹

¹ *National Nanotechnology Centre Ministry of Science, Technology & Innovation Malaysia.*

Corresponding Author: helme@mosti.gov.my

The National Nanotechnology Centre under the Ministry of Science, Technology and Innovation Malaysia is embarking a 5-year project on benchmarking studies for risk assessment of nano-based products. Four major activities have been outlined. First activity will look into the distribution of nano-based products in the local market and the nanomaterials involved. Data will be used to develop an inventory list to be made publicly available. Second activity targeted for nanosafety studies will assess and recognize the gaps at local infrastructure and expertise. Third activity will be to identify the relevant testing and toxicology methods, and conduct some of the studies. Life cycle assessment studies will also be carried out on some of the nano-based products. Final activity will be to establish strategic collaboration with international and smart partners. The presentation will discuss the four activities above.

Hornbill 1 / 287

Characterization of nanoparticles in photocatalytic and regular cement using an aerosolizing nanoparticle generator system

Author: Kiattisak Batsungnoen¹

¹ *Université de Lausanne*

Corresponding Author: kiattisak.batsungnoen@unil.ch

Nanotechnology has been implemented in the construction industry and one application is the use of photocatalytic cement which is Portland cement containing titanium dioxide (TiO₂) nanoparticles. Photocatalytic cement makes the surface white without the need of paint. TiO₂ acts as a biocide making the surface selfcleaning.

However, TiO₂ is a human carcinogen (Group 2B; IARC) and construction workers are exposed to airborne particles while handling cement. The deposition of inhaled particles is influenced by physical and chemical properties such as particle size and density, shape and penetrability, surface area, electrostatic charge, and hygroscopicity. Portland cement is well characterized fine powder with an aerodynamic diameter in the range of 0.05-5 µm. Photocatalytic cement has not previously been described in terms of physical characteristics and chemical composition. This cement might have a smaller aerodynamic diameter, changing the lung deposition mechanisms from that of regular cement. Nanoparticles have been shown to accumulate in the lungs, especially in the alveoli, and be translocated into blood circulation where they are transported to different target organs (lymph nodes, kidney, liver, heart, and brain). Physical parameters for cement can be obtained using an aerosolizing nanoparticle generator system. Our research aims are to (1) characterize photocatalytic cement and (2) compare the parameters to regular cement using this aerosolizing system.

Hornbill 1 / 288

Perception and Attitudes about Nanotechnology and Nano-Safety in Thailand's University Community

Author: G. Louis Hornyak¹

¹ *Asian Institute of Technology P.O. Box 4, Klong Luang Pathumthani 12120 Thailand*

Corresponding Author: glhornyak@gmail.com

A survey of 512 students from two local universities revealed that perception of nanotechnology regarding its importance to Thailand's economy and personal welfare was overall positive. Students especially 'agreed' or 'strongly agreed' with survey questions that focused on government support and regulation of nanomaterials and nano-labelling and were overwhelmingly in favor of developing a nano-safety program in Thailand. Most students believed that nanotechnology-based products would be cheaper, would improve the quality of life and aid in producing high technology jobs—even though knowledge about nanotechnology by a majority of students was still in the formative stages (not different from similar surveys done in other parts of the world and not unexpected considering the newness of nanotechnology). Demographics included gender, field of study (engineering & sciences vs. social sciences), nanotechnology experience, nanotechnology knowledge and home university.

Hornbill 1 / 289

Comparison of nano perception between Asia and Europe and its influence on nano regulation

Author: Georg Karlaganis¹

¹ *Head of the Substances, Soil & Biotech. Div.*

Corresponding Author: georg.karlaganis@wti.org

Nano information is crucial for nano safety along the life cycle of nanomaterials. Transparency on nano content offers advantages for producers, downstream users and consumers of nanoparticles. There are differences in the nano perception between different continents. Consumers in Asian countries like to buy nano products with nano particles because they appreciate the advantages of nano particles in them. In Asia many products are advertised as nano products, even if they are imitations. Thailand has introduced a certification system Nano Q which helps to distinguish between real and fake nano products.

In European countries industry often fears harm through stigmatisation, if companies have to declare nano particles in consumer goods. Many of them prefer not to label their products even if they contain nano particles. Therefore classification and labelling has only been introduced in a few regions and in a few product categories, such as in cosmetics and in biocides. The justification for such regulation is the protection of human health and the environment from hazards and risks of nanomaterials and / or the consumers' right to know if they buy products containing nano materials. There is an ongoing debate whether nano regulation including the compulsory declaration of nano particles in products is compatible with WTO law. The present article investigates nano regulations in various regions and their compliance with WTO rules.

Hornbill 1 / 290

Alternatives to animal testing in Nanotoxicology

Author: Rawiwan Maniratanachote¹

¹ *NANOTEC*

Corresponding Author: rawiwan@nanotec.or.th

Thailand is currently in the stage of moving forward in the area of humane science by reduce, refine and replacement of animals, knowing as the 3Rs principle, in research and development of consumer products. With this regard, the Thai Food and Drug Administration (FDA), Ministry of Public Health, has adopted ASEAN cosmetic directive for non-animal testing of cosmetics. Meanwhile, the use of conventional animals for toxicity testing is becoming obsolete as alternative methods are increasingly developed and validated for chemicals, which are also useful for the field of nanotoxicology. This talk will give an overview of nanosafety research at NANOTEC using in vitro models of cells, tissues, as well as microorganisms for investigating effects of nanomaterials to human health and the environment. In addition, zebrafish embryo is now increasing of interest as an alternative, since they are not considered as animal experimentation according to the EU Directive 2010/63/EU on the protection of animals used for scientific purposes. This model allows for study on embryonic development and various biomolecular endpoints.

Hornbill 1 / 291

Human studies and experimental studies for nanosafety

Author: Gaku ichihara^{None}

Corresponding Author: gak@rs.tus.ac.jp

How we learn from occupational diseases induced by exposure to conventional particles and how we prevent diseases from new materials by bridging the above with human studies and experimental

studies? Many studies focus on specific effects of particles to obtain the knowledge on safe by design, but also we should understand non-specific effects of particles. The idea of mixed-dust pneumoconiosis (MDP) tells us the existence of commonality in the effects of different types of particles. The pneumoconiosis-inducing effects of dusts are known to depend on the content of the crystal silica in them. This idea gives a basis for occupational exposure limit by Japan Society for Occupational Health. The commonality of particles in induction of fibrosis can be described histopathologically by comparison with silicosis or asbestosis. Size, surface area or charge of the particles may influence these effects. A recent pilot study also generates a hypothesis of common effect of exposure to particles on autonomic nervous system in humans. Exposure to different-sized titanium dioxide and heart rate variability (HRV) was monitored in workers. The result showed that the number of particles with diameter less than 300 nm was associated negatively with HRV parameters of parasympathetic function, although the number of bigger particles did not show such associations with the HRV parameters. Understanding the non-specific effect of particles on lung and cardiovascular/autonomic nervous system might be useful for setting exposure limit of nanomaterials.

Plenary talk / 292

What Can We Learn from the Nanotoxicology Publications?

Author: Harald Krug¹

¹ *International Research Cooperation Manager, Empa - Swiss Federal Laboratories for Materials Science and Technology and Stakeholder - NanoCASE GmbH, Switzerland*

Corresponding Author: harald.krug@empa.ch

During the last decade several literature surveys on “Nanotoxicology” have shown that most of the published data on toxicological effects of nanoparticles or nanomaterials is not useful for risk analysis or risk assessment of these materials^{1, 2}. Although the evaluated publications use buzz words such as “toxicological effects”, “risk assessment”, “toxicity” or “genotoxicity” most of them do not respect the rules of toxicological studies. As the term “nano” in the title was nearly a guarantee for project proposals to get money within the last two decades, no one claimed for the adequate quality control which should be applied for toxicological studies.

Most of the published studies contain severe weaknesses such as missing controls, no well characterized materials or they show high-dose-experiments only to observe an effect which is publishable³. Altogether this ends up in the situation that we cannot use all published data without its critical evaluation⁴.

The evaluation of nearly 6000 publications is in some respect disappointing. If one looks carefully into the details of the published studies it becomes more and more apparent that many of these publications contain shortcomings as mentioned above and often the conclusions drawn from these studies are misleading¹. Hence, it would be a great mistake if regulation would be built upon such studies. Obviously, the above described limitations offer difficulties in issuing clear statements on “Safety Aspects of Nanomaterials”. International standards and harmonization of test protocols are urgently needed and should be used in all future projects and experiments.

Nanotoxicology or better nanosafety research may be pushed back on track if the researchers will respect measurement uncertainty and other important rules for biological studies in total and specifically for toxicological studies^{5,6}. One recent example for a possible approach to achieve better quality for nanosafety studies is available online. Here a consortium build up from 6 international institutes in different countries from America, Asia and Europe carried out a study on the harmonization of a cytotoxicity assay for the measurement of nanomaterials in an interlaboratory round robin⁷. This pioneering activity is our showpiece project and may serve as a set point for future nanosafety research quality standards.

References

1. H. F. Krug, *Angew Chem Int Ed* 53, 12304 (2014).
2. D. R. Hristozov, S. Gottardo, A. Critto, and A. Marcomini, *Nanotoxicology* 6, 880 (2012).
3. D. B. Warheit and E. M. Donner, *Sci Technol Adv Mater* 16, 034603 (2015).

4. H. F. Krug and P. Wick, *Angew Chem Int Ed* 50, 1260 (2011).
5. M. Rösslein et al., *Int J Mol Sci* 14, 24320 (2013).
6. M. Rösslein et al., *Chem Res Toxicol* 28, 21 (2015).
7. J.T. Elliott et al., *ALTEX*, online first, http://www.altex.ch/resources/ALTEX_Elliott_OF_160929.pdf

Heron 1 / 293

A recent development of mixed metal oxides/polymer nanocomposites as energy storage catalysts

Authors: Pailin NGAOTRAKANWIWAT¹; Vissanu Meeyoo²

¹ _

² *Department of Chemical Engineering, Mahanakorn University of Technology, Bangkok, Thailand / Nanotec-KMUTT Center of Excellence on Hybrid Nanomaterials for Alternative Energy (HyNae)*

Corresponding Author: vissanu.meeyoo@gmail.com

Titanium dioxide (TiO₂) is a promising material for versatile applications, i.e., air-water purification, anti-fogging, anti-corrosion. However, those applications are limited to the available of the appropriate light source. To overcome this problem, modification with energy storage substances such as WO₃ [1], Phosphotungstic acid [2] and TiO₂-V₂O₅ [3] is applied. An energy storage system is composed of electron generating source (i.e., TiO₂) and energy storage substance. The mechanism of energy storage in the air states that TiO₂ generates photo-excited electrons under UV light and those electrons transfer to energy storage substance. Those stored electrons release and carry on the cathodic reactions in the dark as shown in Fig. 1. The energy storage system can be used as multi-purpose materials for many aspects i.e. anti-corrosion, pollutant decomposition, coating substances for smart window. The photocatalytic electron can subsidize the electron deficiency that metal lose to the environment [3], while coincident hydroxyl radical, which is a product from water oxidation by photo-excited holes can decompose the pollutant [4]. However, the efficiency of the system is relied on the contact between TiO₂ and an energy storage substance. The use of conduction polymer to bridge the electron generating source and the energy storage substance has proved to be effective and overcome the aforementioned problem [4]. In this presentation, we demonstrate the use of the hybrid materials as energy storage catalysts. The photocatalytic oxidations of toluene in a gas phase and methylene blue are given as examples.

294

Computational Studies of Transition-Metal Decorated Graphene Adsorbent for Air Pollutants Removal

Author: M. Kunaseth¹

Co-authors: P. Poldorn²; T. Mudchimo²

¹ *National Nanotechnology Center (NANOTEC), National Science and Technology Development Agency (NSTDA), Pathum Thani, Thailand*

² *Department of Chemistry, Faculty of Science, Ubon Ratchathani University, Ubon Ratchathani, Thailand*

Corresponding Authors: id01@mail.com, manaschai@nanotec.or.th, id02@mail.com

Coal combustion in a coal power plant is a major source causing severe environmental implication such as releasing elemental mercury (Hg⁰), toxic arsine gas (AsH₃), and volatile organic compounds (VOCs) into the atmosphere. In this work, we have investigated transition metal decorated graphene

as adsorbent for removal of these pollutants from flue gas using density functional theory calculation on three applications. In the first application, boron-doped graphene decorated with transition metal nanocluster(M-BDG) is used to study the adsorption of Hg⁰ (for M = Pd, Pt, Ru, W). The result shows that Pd₄-BDG is the most efficient adsorbent for Hg⁰ adsorption, while capacity investigation suggests that maximum of 6 Hg atoms per Pd₄ site can be adsorbed via chemisorption. In the second application, Pd nanocluster is deposited on single-vacancy graphene (SDG) for AsH₃ adsorption. The study reveals the size effect of Pd cluster on the adsorption strength of AsH₃ and its variants based dominantly on Coulomb interaction. In the third application, transition metal nanocluster decorated SDG is used to study adsorption selectivity of heterocyclic VOCs on various metal species. The result shows that organonitrogen compound adsorbed the strongest among all VOCs, especially on Pt₄ (-2.11 eV). In conclusion, computational insights from our studies provide key understandings for enhancement of graphene-based adsorbent design and synthesis.

Heron 1 / 295

Charge storage mechanisms of manganese oxide nanosheets and N-doped reduced graphene oxide aerogel for high-performance asymmetric supercapacitors

Authors: Montree Sawangphruk¹; Pawin Iamprasertkun¹

Co-authors: Atiweena Krittayavathananon²; Pinit Kidkhunthod³

¹ *Department of Chemical and Biomolecular Engineering, School of Energy Science and Engineering, Vidyasirimedhi Institute of Science and Technology, Rayong 21210, Thailand / Department of Chemical Engineering, Kasetsart University, Bangkok 10900, Thailand*

² *Department of Chemical and Biomolecular Engineering, School of Energy Science and Engineering, Vidyasirimedhi Institute of Science and Technology, Rayong 21210, Thailand*

³ *Synchrotron Light Research Institute (Public Organization), 111 University Avenue, Muang District, Nakhon Ratchasima 30000, Thailand*

Corresponding Authors: pinit@slri.or.th, id02@mail.com, nanotechnology2@googlemail.com, id01@mail.com

Although manganese oxide and graphene supercapacitors have been widely studied, their charge storage mechanisms are not yet clear. In this work, we have investigated the charge storage mechanisms of MnO₂ nanosheets and N-doped reduced graphene oxide aerogel (N-rGOae) using in situ X-ray absorption spectroscopy (XAS) and electrochemical quartz crystal microbalance (EQCM). The in situ XAS carried out together with a chronoamperometry indicates that the oxidation state of manganese in the MnO₂ electrode being charged increases from +3.01 at 0.0 V vs. SCE to +3.12 at +0.8 V vs. SCE and then returns to +3.01 for the discharge process. This is an origin why the MnO₂ nanosheets can provide excellent capacity retention. The mass changes of the N-rGOae and MnO₂-coated Au/TiO₂ quartz crystal EQCM electrodes during the charge process gradually increases to 8.15 μg cm⁻² and 10.34 μg cm⁻², respectively. A finely tuned mass ratio of MnO₂ to N-rGOae is 1.75 providing the maximum charge storage performance. A single coin-cell asymmetric supercapacitor (CR2016) of MnO₂//N-rGOae provides a maximum specific capacitance of ca. 467 F g⁻¹ at 1 A g⁻¹, a maximum specific power of 39 kW kg⁻¹ and a specific energy of 40 Wh kg⁻¹ with a wide working potential of 1.6 V at 93.2% capacity retention after 7,500 cycles. The coin-cell supercapacitor can practically supply electricity to a spinning motor with a nominal voltage of 3 V for 1.45 min. The enhancement in the specific energy and specific power of the MnO₂//N-rGOae supercapacitors can compete with the batteries in many applications.

KEYWORDS

Charge storage mechanism; Asymmetric supercapacitors; Birnessite-type potassium manganese oxide; N-doped graphene aerogel; In situ X-ray absorption spectroscopy

Plenary talk / 296

Functional and responsive core-shell nanoparticle assembly at oil and lipid interfaces

Author: Erik Reimhult¹

¹ *Department of Nanobiotechnology, University of Natural Resources and Life Sciences, Vienna, Austria*

Corresponding Author: erik.reimhult@boku.ac.at

Carefully controlled core-shell nanoparticles can be used in biomedical applications, e.g., as biomedical imaging contrast agents, for hyperthermia and in drug delivery [1, 2], as well as for biotechnological applications such as separation and purification. Unique material functions can be achieved by using nanoscale inorganic cores, such as plasmonic or superparamagnetic interactions with electromagnetic fields. However, to enable these functions in a biological environment a dense organic shell has to control colloidal interactions with biomolecules, cells and other nanoparticles [1, 3]. Control over nanoparticle physical properties through an organic shell also allows tailoring of the assembly of functional nanoparticles into supramolecular structures, such as nanoscale vesicles or nanoscale Pickering-type emulsomes. The self-assembled structures can incorporate environmentally responsive building blocks and therefore be controlled through the strong interaction of the inorganic core with externally applied electromagnetic fields.

I will describe multiple recent developments from our lab regarding the synthesis and assembly of superparamagnetic core-shell nanoparticles that illustrate this design philosophy. The combination of new organic shell grafting methods [3-7] and control over nanoscale self-assembly [8-13] has allowed us to vastly improve performance of superparamagnetic core-shell nanoparticles, perform detailed investigations of interactions of colloidal responsive nanoparticles as well as demonstrate unprecedented control over magnetically controlled nanovesicular and nanoemulsion systems for transport and release applications that could impact future directions in drug delivery and biomedical imaging.

Hornbill 1 / 299

Welcome Remarks

-

Hornbill 1 / 300

The industrial-academic network for nanoscience research in cementitious materials

Author: Sakprayut Sinthupinyo¹

¹ _

Corresponding Author: scg@mail.com

To be added

Hornbill 1 / 301

SCG Speaker

Author: SCG speaker¹

¹ _**Corresponding Author:** scg@mail.com

To be added

Heron 2 / 303

Development of Theranostic Nanoparticles for Cancers

Author: Sith Sathornsumetee¹**Co-author:** Ruengpung Sutthent²¹ NANOTEC-Mahidol University Center of Excellence in Nanotechnology for Cancer Diagnosis and Treatment and Departments of Medicine, Faculty of Medicine Siriraj Hospital, Mahidol University, Bangkok, 10700, Thailand² NANOTEC-Mahidol University Center of Excellence in Nanotechnology for Cancer Diagnosis and Treatment and Departments of Microbiology, Faculty of Medicine Siriraj Hospital, Mahidol University, Bangkok, 10700, Thailand**Corresponding Authors:** ruengpung.sut@mahidol.ac.th, sith.sat@mahidol.ac.th

Cancer is the leading cause of death in Thailand. Despite advances in cancer research during the past decades, the survival of cancer patients has only marginally improved and the cure remains unlikely. Complex genomic heterogeneity and limited drug delivery represent major obstacles for effective antineoplastic treatments. Thus, new therapeutic strategies to increase drug delivery may improve outcome for cancer patients. Among several approaches, nanoparticle conjugate is a promising modality with distinct characteristics that are favorable for cancer drug delivery. Nanoparticles can be developed not only to improve drug delivery, but also to offer diagnostic and monitoring capabilities. This emerging molecular platform is called “theranostics”. Theranostic nanoparticles include liposomes, micelles, dendrimers, nanospheres and others. These particles can protect drugs and deliver them to targets in a controlled manner. In addition, they can be decorated with “molecular antennae” such as antibodies or aptamers on their surface to allow specific interaction with targets of interest. During this presentation, current collaborative research efforts between NANOTEC and Faculty of Medicine Siriraj Hospital, Mahidol University exploiting nanoparticles to target brain, liver, colorectal, breast and gynecologic cancers will be discussed.

Heron 2 / 306

Discovery of biological self-assembling systems that have potential for incorporation into nanodevices and sensors

Author: Robert Robinson¹¹ Institute of Molecular and Cell Biology, Agency for Science, Technology and Research**Corresponding Author:** rrobinson@imcb.a-star.edu.sg

Elongating filaments systems, such as actin, are polymerizing motors that drive movement in many biological processes. The actin filament is astonishingly well conserved across a diverse set of eukaryotic species. It has essentially remained unchanged in the billion years that separate yeast, Arabidopsis and man. In contrast, bacterial actin-like proteins have diverged to the extreme, many of which are not readily identified from sequence-based homology searches. My laboratory is particularly interested in understanding how the force generated from these varied polymerization system is integrated into different biological processes. Once understood, then these machineries have potential for exploitation in nanodevices. Finally, I will describe the non-physiological, yet curious, case

the kinase domain of PAK4, which spontaneously forms crystals inside mammalian cells. We are exploiting this phenomenon to create sensors within mammalian cells.